WAVE TRANSFORMATION IN THE SURF ZONE

BY

WILLIAM RENNEKER DALLY

A DISSERTATION PRESENTED TO THE GRADUATE SCHOOL
OF THE UNIVERSITY OF FLORIDA IN
PARTIAL FULFILLMENT OF THE REQUIREMENTS
FOR THE DEGREE OF DOCTOR OF PHILOSOPHY

UNIVERSITY OF FLORIDA

1987

"Genius [research] is two percent inspiration

and ninety-eight percent perspiration."

Thomas A. Edison

Without inspiration, perspiration is just plain sweat.

W.R.D.

ACKNOWLEDGEMENTS

The author gratefully acknowledges the financial support of the Sea Grant University Program, the State of Florida Department of Natural Resources, and the Coastal and Oceanographic Engineering Department, University of Florida. He would like to thank his committee chairman and mentor, Dr. Robert G. Dean, for his interest and support over the past decade, and his committee members Drs. Joseph L. Hammack, Lawrence E. Malvern, Michel K. Ochi and Andrew J. Vince. The comments and additional calculations by Dr. Edward B. Thornton, Naval Postgraduate School, in regard to data from the Nearshore Sediment Transport Study are greatly appreciated.

A debt of gratitude is owed to his friend and colleague Marc Perlin for his valuable advice and assistance in conducting the laboratory portion of this study. Thanks are also offered to him and to friends and colleagues Kevin R. Bodge, David L. Kriebel, Claudio F. Neves, and Iordanis I. Sahinoglou for hours of discussion of coursework, coastal engineering, and life in general.

Although personal friends rarely have direct input to a Ph.D. dissertation, there is no doubt in the author's mind that this work, nor the years of study preceding it, could not have been completed without the love and support of his friends. As the author is a very rich man when it comes to friends, he could not possibly name even just the closest of them here. However, he would like to offer special thanks to his roommates and buddies Jonathan W. Lott and Michael R. Barnett for

putting up with him during some particularly stressful times, and to longtime friend Joseph E. Harris of Orlando, Florida, for giving him a place to periodically escape to when school was no longer bearable. Heartfelt gratitude is offered to Theresa Perlin for her friendship and many home-cooked meals. The author also wishes to thank his dear friends the Millicks, especially Lore, who encouraged him to return to school.

As always, the exchange of love and support with his parents William J. Dally and Louise D. Dally, and his sisters Janette, Ellen and Kathleen, is paramount. These are truly fine people, who every day show the author the difference between pride and ego.

Finally, this dissertation is especially dedicated to Debra S. Islas, a rare woman who possesses both outer and inner beauty, and wisdom beyond her years. Her patience, understanding and support during the final stages of this effort are forever appreciated.

TABLE OF CONTENTS

LIST OF TABLES

LIST OF FIGURES

Abstract of Dissertation Presented to the Graduate School
of the University of Florida in Partial Fulfillment of the
Requirements for the Degree of Doctor of Philosophy

WAVE TRANSFORMATION IN THE SURF ZONE

By

William Renneker Dally

May 1987

Chairman: Dr. Robert Dean
Major Department: Engineering Sciences

The transformation of wave height during the processes of shoaling, breaking and reformation as waves cross the nearshore region is investigated. Previous work by the author on regular breaking waves is extended to a random wave field, and two closed form solutions for the probability density function (pdf) of breaking and non-breaking wave height for a planar beach are derived. These solutions are unique in that the shape of the pdf is not assumed a priori, but is determined using an exact transformation of random variable from the initial (offshore) pdf. For more complex bottom profiles such as those containing multiple bar/trough systems, the initial pdf is discretized into a histogram and each representative wave is transformed numerically across the surf zone. The behavior of statistically representative waves can then be monitored and histograms of height are generated. The random wave model is verified to field data and good agreement is obtained for both statistically representative waves and histograms,

without additional calibration. The effect of a collinear current on the breaking process of regular waves is then investigated theoretically and experimentally. A governing equation is proposed and verified to the laboratory data with good results, except for the combination of a short-period wave and a strong opposing current. The effects of long waves such as surf beat (which can be depicted as a slowly varying current and mean water level) on the transformation of random wind-waves is investigated by incorporating the results of the regular wave/current study. If no correlation between the wind-wave group and the surf beat is assumed, only a slight (~ 4%) increase in decay of the root mean square wave height, H_{rms}, is observed. However, if the relative phase of the group and beat is such that high waves enter the surf zone when the beat opposes, a marked (~ 15%) increase in decay in H_{rms} is found. Attempts to verify the surf beat model to the field data of the Nearshore Sediment Transport Study were unsuccessful, believed due to severe low-pass-filtering of the original raw data.

CHAPTER 1

INTRODUCTION AND BACKGROUND

To an observer standing on a beach, perhaps the most conspicuous phenomenon is the breaking of incident wind-waves. Following an individual wave by eye as it travels towards shore, it first shoals, gaining height at an ever-increasing rate until it becomes so steep that it is no longer stable. From this incipient break point, the crest of the wave curls over, "white water" appears, and the wave begins to dissipate its energy and lose height, in some instances gradually (spilling breakers) and in others almost explosively (plunging breakers). Breaking may be a continuous process until the wave reaches the shoreline, or at some intermediate point breaking may stop, the wave "reforms," and the shoaling and breaking process repeats. The local height of the breaking wave and the rate at which it dissipates its energy directly affect the strength of littoral currents in both the alongshore and onshore/offshore directions, sediment mobilization and suspension, and set-up/set-down in the mean water level--in short, inducing sand transport and the resulting changes in shoreline position and bottom topography. Currents generated by the wind waves (e.g., longshore currents, undertow, and rip currents) can be seen to in turn affect the refraction, diffraction, shoaling and breaking behavior of newly arrived waves. Another readily observed feature of the wind-waves is their variability in height and period as different waves pass a particular location. The nature and spatial change of this "randomness"

is important, as waves which arrive in distinct groups can generate long waves such as surf beat and edge waves. The long waves in turn affect the transformation of the wind-waves, which see them as temporally and spatially varying currents and mean water level.

Moving from a beach to a tidal inlet, an observer can see incident waves which normally would pose no threat, shoal and break on ebb currents, causing severe navigational and safety hazards for boat traffic. On flood tide, large waves which would normally shoal and break as the water depth decreased are stretched by the assisting current either reducing energy dissipation or preventing it entirely. Thus the waves penetrate the inlet to the relatively still water of the bay, regain height, and are free to damage port and harbor facilities and affect shorelines. Finally, wave height, whether breaking or non-breaking, is the single most important parameter to determine during the design of coastal structures.

With the premier role in the coastal realm of wave height and its transformation induced by currents and varying water depth duly emphasized, it is noted that only in the non-breaking instance is the transformation process (refraction, diffraction, and shoaling) physically understood and even marginally predicted using analytical and numerical solutions to accepted governing equations. In contrast, even the physical process of wave breaking is poorly understood and no universally acknowledged governing equation(s) exist, let alone solutions to such. The "simple" breaking wave is perhaps the most difficult problem encountered in incompressible-fluid mechanics if one attempts to address the details of fluid motion in the highly turbulent, aerated white water where most of the energy is dissipated. However, some

insight and predictive capability can be gained via a macroscopic or integral approach to the problem, which treats the entire wave as a system.

To provide the reader with some background and to introduce the observed behavioral phenomena displayed by breaking waves which this research attempts to address, explain, and predict, sample results of several previous laboratory and field measurement programs are presented and briefly examined. In Figures 1.1 and 1.2, results are presented from one of the earliest and most extensive laboratory studies of regular breaking waves, conducted by Horikawa and Kuo (1966). In Figure 1.1, wave height, H, is plotted versus still water depth, h', from the point of incipient breaking, across plane slopes (m) of 1/80, 1/65, 1/30 and 1/20. Different combinations of deepwater wave height, H_o, and wave period, T (and therefore deepwater wavelength, $L_o = gT^2/2\pi$ where g is gravity), were tested. The incipient condition, γ, is defined as the ratio of wave height to local water depth at the point where breaking is imminent; i.e.,

$$\gamma = (H/h)_b \tag{1.1}$$

where the subscript b refers to incipient breaking. Increasing bottom slope and/or decreasing wave steepness, H_o/L_o, increases γ and tends to induce plunging breaking (Galvin, 1968). However, as shown in the figure, once breaking is initiated the decay in wave height does not appear to have a strong dependence on wave period, but is markedly affected by beach slope. Not only do waves on steeper slopes have greater incipient conditions, but they maintain a greater height

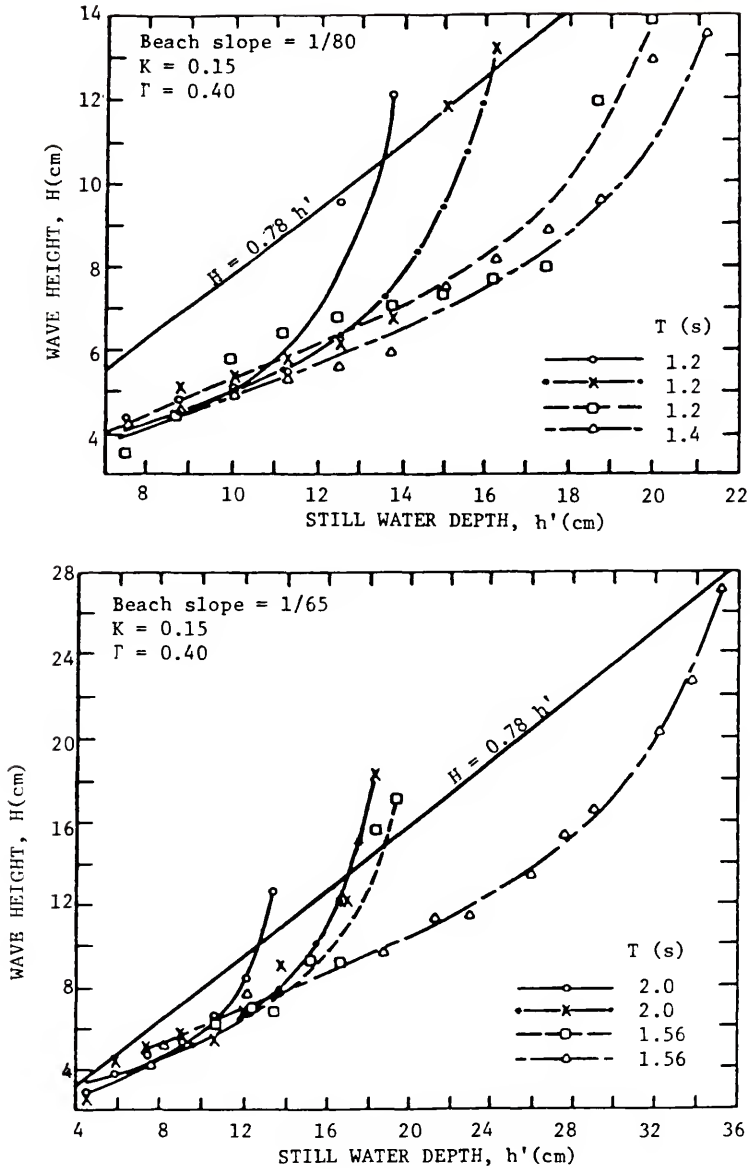

Figure 1.1 Decay of regular waves on plane slopes. Breaker model of Dally et al. (1985) (curves) and laboratory data of Horikawa and Kuo (1966).

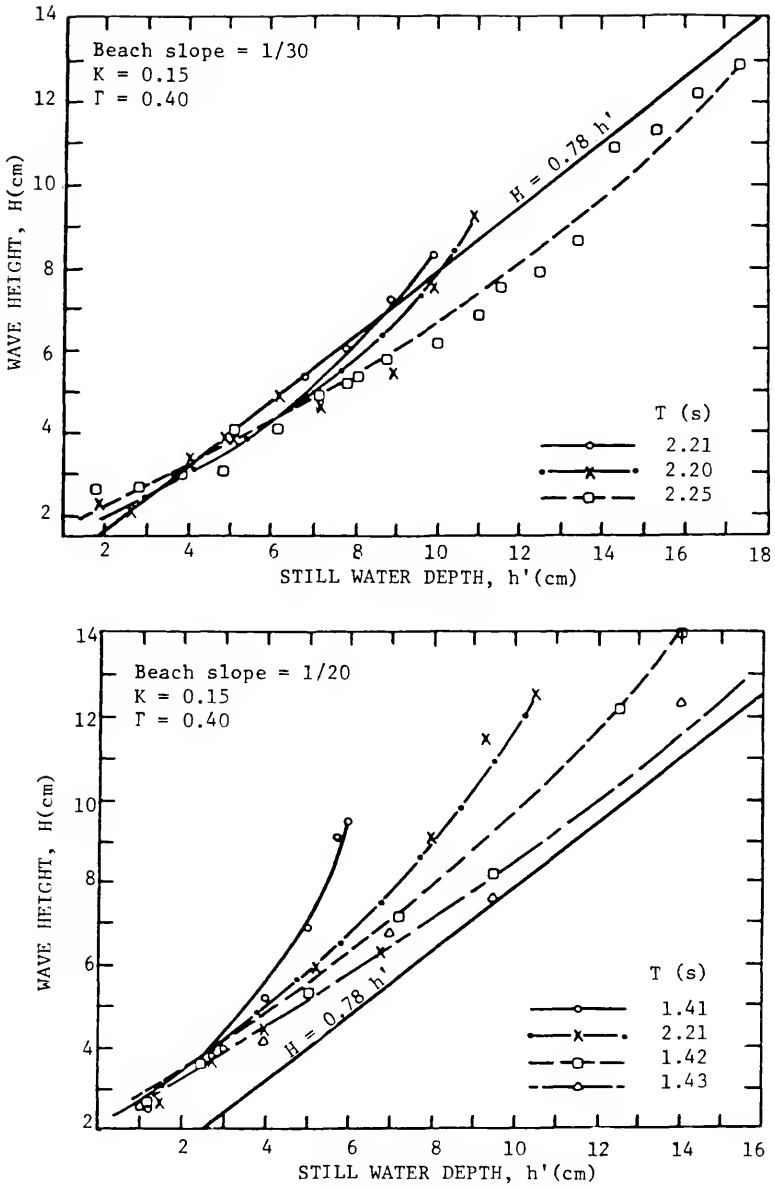

Figure 1.1 -- continued

throughout most of the surf zone. This is evident from the general shape of the decay profiles which are very concave on the 1/80 slope, but almost straight lines on the 1/20 slope. In this regard, the commonly assumed "0.78 criterion" (ratio of wave height to water depth equals 0.78) is also displayed in Figure 1.1. It is apparent that assuming the breaker height is directly proportional to water depth is an especially bad assumption on mild slopes, just where it is most often utilized for natural beaches. The 0.78 criterion appears to be at best marginally accurate on the 1/30 slope. Wave decay as predicted by a model previously developed by the author (Dally, 1980; Dally, Dean and Dalrymple, 1984, 1985) is also presented for comparison. This model is reviewed in Chapter 2.

The effects of beach slope on breaker decay can be substantially removed from the problem by examining breaking on a "shelf beach"; i.e., at some water depth the plane beach is truncated and the bottom becomes horizontal. Horikawa and Kuo also performed such an experiment, where the wave generator was tuned so that incipient breaking was attained at, or just seaward of, the beginning of the horizontal section. A portion of these results are displayed in Figure 1.2 in which wave height is plotted versus distance from the breaker line in non-dimensional form. The most important observation here is that all waves, regardless of deepwater steepness, seem to approach the same dimensionless "stable" wave height, where breaking stopped and the wave reformed. All decay profiles are concave upwards. Of course, the 0.78 criterion is especially inappropriate in this situation.

The effect of a collinear, steady current on wave breaking has received very little attention in the literature. No field studies of

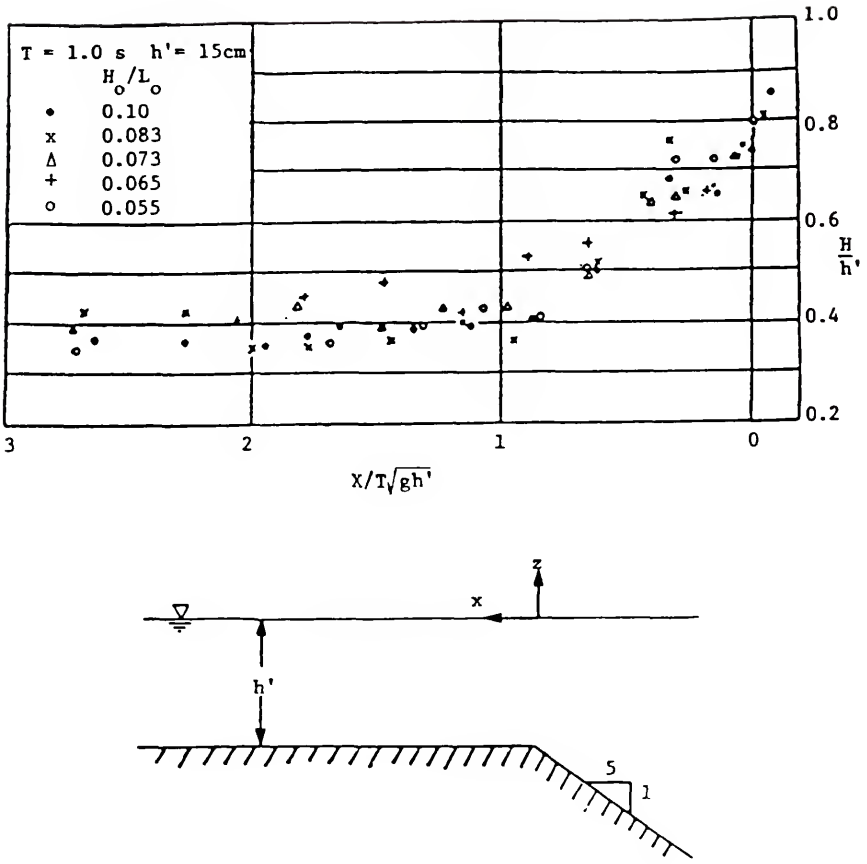

Figure 1.2 Decay of regular waves on a shelf beach (uniform depth). Laboratory data and adapted figure from Horikawa and Kuo (1966).

the problem are known to the author, and only one germane laboratory study has been found in the literature. As a result, much of the effort of this dissertation was devoted to a laboratory study of breaking waves on steady, opposing currents, which is described in Appendix B. The results of four experiments of regular wave transformation on a planar beach with a steady opposing current, reported in Sakai and Saeki (1984) are displayed in Figure 1.3. Holding the deepwater steepness nearly constant, note that increasing the discharge (q) 1) increases the rate of shoaling, 2) increases the wave height at incipient breaking, 3) pushes the incipient break point offshore, and 4) increases the rate of decay in wave height. The results of the laboratory study described in Appendix B also indicate that for a shelf beach, the point where the wave reforms is moved offshore significantly; i.e., the surf zone is compressed and moved offshore slightly.

We turn our attention now to random waves and their transformation through the surf zone. Measurements are usually presented as 1) the probability density function (pdf) of wave height at different locations on a transect across the nearshore, and/or 2) transformation of statistically representative waves, such as the average wave height ($\bar{H}$), the root mean square wave height (H_{rms}) or significant wave height ($H_{1/3}$). Figure 1.4 is taken from Goda (1975) and shows the transformation of the pdf of wave height across a steep laboratory beach of 1/10 slope. Note that in deeper water (50 cm) where no waves were breaking, the Rayleigh distribution fits the data well, but as the water becomes shallow and a greater proportion of the waves break, the pdf departs significantly from the Rayleigh form. In particular, the pdf above the mean value declines sharply as compared to the upper tail of the Rayleigh

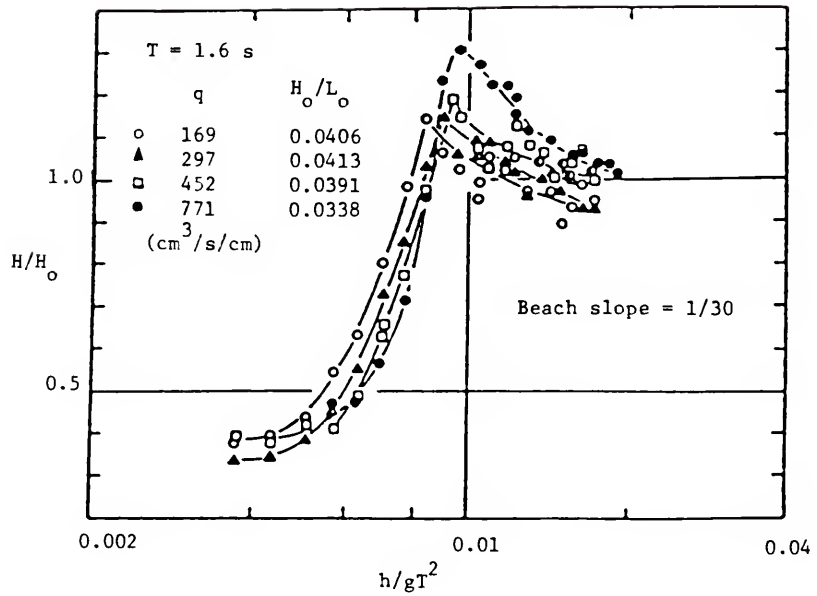

Figure 1.3 Shoaling and decay of regular waves on a plane beach with opposing currents. Laboratory data and adapted figure from Sakai and Saeki (1984).

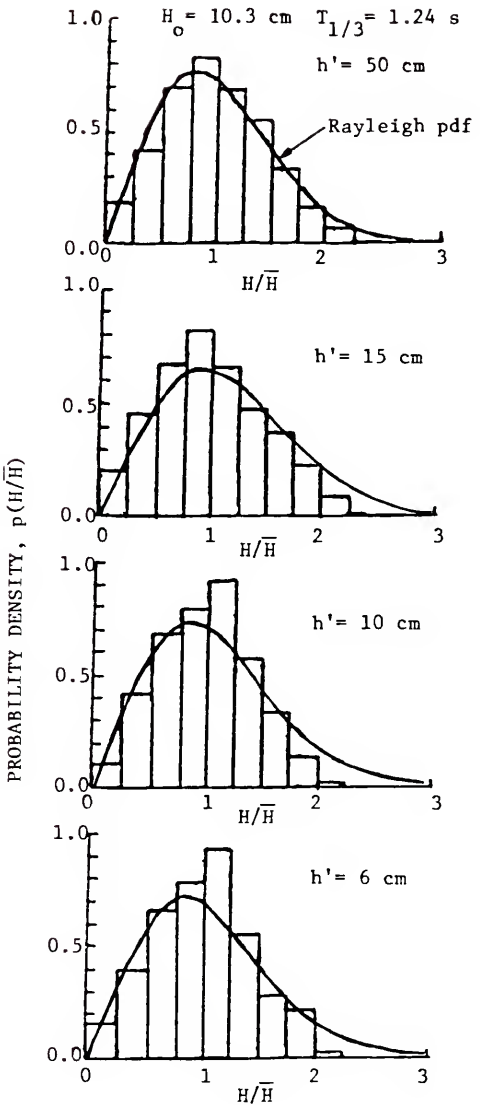

Figure 1.4 Transformation of the histogram of wave height across a plane beach (slope = 1/10). Laboratory data and adapted figure from Goda (1975).

distribution. Goda developed a model in an attempt to address this behavior, which is reviewed in Chapter 3.

Figure 1.5 displays some of the random wave results of Mase and Iwagaki (1984) for transformation of $\bar{H}$ and $H_{1/3}$ across plane laboratory beaches of 1/30 slope and shows the dependence of statistically representative wave transformation on average deepwater wave steepness, $\bar{S}_o$, observed in many laboratory and field data sets. The steepness is defined as

$$\bar{S}_o = \frac{2\pi}{g} \bar{f}^2 H_{rmso} \tag{1.2}$$

where $\bar{f}$ is either the average or peak frequency of the measured spectrum, and H_{rmso} is the root mean square wave height in deepwater. In Figure 1.5, the low steepness waves shoal more noticeably, reach a higher incipient condition, but dissipate energy more rapidly than the high steepness waves. This shoaling and "incipient breaking" behavior is completely consonant with theoretical and observed shoaling and incipient breaking of regular waves. The increased rate of decay of the low steepness waves would be expected since they tend to plunge rather than spill. Mase and Iwagaki developed a model to describe the transformation of statistically representative waves, but are limited to planar beaches. This model is reviewed in Chapter 3.

The last behavioral characteristic of random breaking waves to be discussed is the dependence of $\lambda_{rms} = H_{rms}/h$ on beach slope in the inner surf zone. This has been observed by several researchers, e.g., Thornton, Wu, and Guza (1984) and Sallenger and Holman (1985).

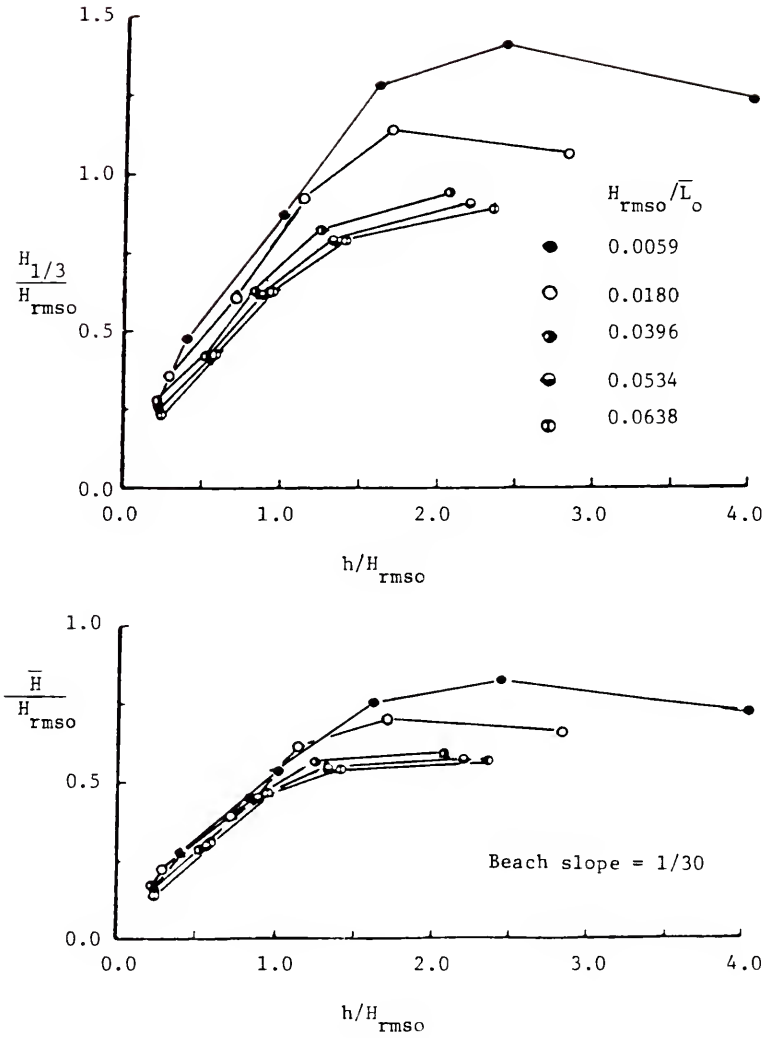

Figure 1.5 Transformation of mean wave height ($\bar{H}$) and significant wave height ($H_{1/3}$) across a plane beach for various average deepwater steepness ($H_{rmso}/\bar{L}_o$). Laboratory data and adapted figure from Mase and Iwagaki (1982).

Figure 1.6 is taken from Sallenger and Holman's paper and shows the behavior of λ_{rms} versus beach slope, m, for random wave data collected at several locations in the inner surf zone during several field experiments. The trend of increasing λ_{rms}/h with increasing slope is clearly discernible. This behavior is completely consonant with that observed for the regular wave experiments already discussed, and really should come as no surprise. The value of conducting regular wave studies in the laboratory before addressing the more complicated random wave problem is highlighted accordingly, and justifiably stressed. In fact, the model proposed by the author for regular wave breaking includes and predicts this behavior explicitly. So, as will be shown, when the model is adapted to random waves, the dependence of λ_{rms} on beach slope is contained inherently.

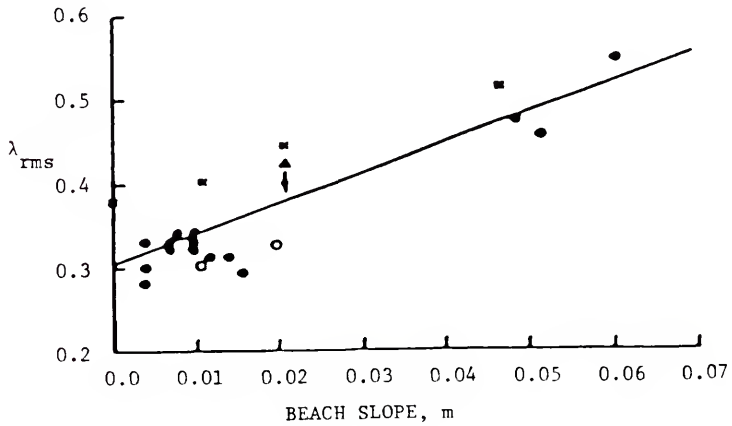

Figure 1.6 Observed dependence of the ratio $\lambda_{rms} = H_{rms}/h$ on beach slope. Figure adapted from Sallenger and Holman (1985).

CHAPTER 2

REGULAR BREAKING WAVES

2.1 Introduction and Brief Literature Review

The similarity model already mentioned, i.e. that breaking wave height is directly proportional to local water depth, is marginally accurate only for unrealistically steep, monotonic (and most often planar) beach profiles, as concluded by Horikawa and Kuo (1966). For the case of a non-monotonic profile, where perhaps a bar/trough formation is present, this model is especially inappropriate. Previous investigations over the past two decades devoted to improving this model have been based on the steady-state, depth-integrated equation governing the energy balance for waves propagating directly towards shore. The equation is simply

$$\frac{\partial ECg}{\partial x} = - \delta(x) \tag{2.1}$$

where E is wave energy per unit plan area, Cg is the group velocity, and δ is the rate of energy dissipation per unit plan area due to any dissipation mechanism--in this case breaking. Difficulties arise in finding representations for E and Cg that are accurate in the surf zone, although linear wave theory is most often applied. However, the most significant problem, to which most studies have been devoted, is the development of a rational and universally valid formulation for δ.

The most physically appealing approach, first suggested by LeMéhauté (1962), is the assumption that the rate of energy dissipation in a breaking wave is the same as a propagating bore. By strict definition, the dissipation in this model is proportional to the wave height cubed, although by order of magnitude arguments Battjes and Janssen (1978) developed a bore model for random waves in which δ was proportional to wave height squared. Horikawa and Kuo (1966) represent δ in terms of turbulent velocity fluctuations which are assumed to decay exponentially from the point of incipient breaking. The analytical solution for internal energy dissipation in waves due to viscosity (Lamb, 1945) is applied by Mizuguchi (1981), in which molecular viscosity is replaced by turbulent eddy viscosity. Also in these last two models, energy dissipation is proportional to wave height squared.

Observations and intuition supported by the laboratory experiments of Horikawa and Kuo (1966) indicate that a wave that was once a fully developed breaker which propagates over a horizontal bottom will gradually stop breaking, reform and continue on as a non-breaking "stable" wave of reduced height. An expression for δ originally proposed by the author in a master's thesis (Dally, 1980) includes this stabilization, and the model was later refined and subject to extensive calibration and verification in Dally, Dean and Dalrymple (1984, 1985). No other model developed to date includes the stabilization phenomenon in its dissipation function, although Mizuguchi (1981) did dictate stabilization in an ad hoc manner if the bottom became horizontal. Otherwise this model reverted to the similarity type.

The investigations to date of regular breaking waves and their concomitant dissipation models are listed in Table 2.1. Because the

major thrust of this dissertation is the application and extension of the author's original dissipation function to random breaking waves, waves on currents and wave interaction with surf beat, the other models for δ will not be reviewed in great length here. The reader is referred to Dally et al. (1985) or to the original papers for more information. Because the author's original investigation of regular breaking waves is the foundation for the models to be developed, it is reviewed in greater detail in the next section.

Table 2.1 -- Investigations of Regular Breaking Waves

Author(s)	Dissipation Model Used
LeMéhauté (1962)	propagating bore
Horikawa and Kuo (1966)	turbulent vel. fluc.
Divoky, LeMéhauté and Lin (1970)	propagating bore
Hwang and Divoky (1970)	propagating bore
Svendsen, Madsen and Buhr Hansen (1978)	propagating bore
Peregrine and Svendsen (1978)	propagating bore
Dally (1980)	wave stabilization
Mizuguchi (1981)	internal energy
Svendsen (1984)	propagating bore
Dally, Dean and Dalrymple (1984, 1985)	wave stabilization
Sakai, Hiyamizu and Saeki (1986)	propagating bore
Lin and Hwang (1986)	propagating bore

2.2 Review of Breaker Model for Regular Waves

2.2.1 Formulation and Governing Equations

Starting with regular waves propagating over an idealized bottom profile that rises in a gently sloping manner until becoming horizontal at some still water depth h' (see Figure 2.1), Dally (1980) proposed the following rationale. If deepwater wave conditions and the local water

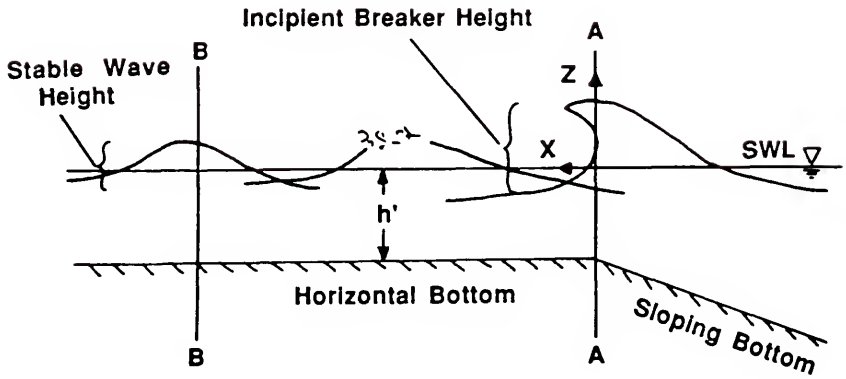

Figure 2.1 Wave decay on a shelf beach and model concepts for regular waves.

depth are such that the wave shoals and begins fully developed breaking near the beginning of the horizontal bottom (section A-A in Figure 2.1), breaking will not instantaneously stop as dictated by the similarity model, but will continue for some distance at an ever-decreasing rate until the wave reforms and a stable height is attained (section B-B). It is then hypothesized that the dissipation function $\delta(x)$ in (2.1) is proportional to the difference between the actual local depth-averaged energy flux per unit volume and that associated with the stable wave; i.e.

$$\delta(x) = \frac{K}{h} [ECg - ECg_s] \tag{2.2}$$

or

$$\frac{\partial ECg}{\partial x} = \frac{-K}{h} [ECg - ECg_s] \tag{2.3}$$

where the subscript s refers to the stable wave and K is a decay coefficient which must be calibrated. Shallow water linear wave theory is adopted and the stable wave height is assumed directly proportional to the local water depth as indicated by the measurements of Horikawa and Kuo (1966); see Figure 1.2. This results in

$$\frac{\partial\left(H^2\sqrt{h'}\right)}{\partial x} = \frac{-K}{h} \left[H^2\sqrt{h'} - \Gamma^2(h')^{5/2}\right] \tag{2.4}$$

where H is breaking wave height and Γ is the stable wave coefficient ($H_s = \Gamma h'$) and also must be calibrated.

As demonstrated by Longuet-Higgins and Stewart (1963) there exists a set-up in mean water level in the surf zone induced by the gradient in depth-integrated onshore momentum flux, S_{xx} (termed radiation stress), for which the governing equation is

$$\frac{\partial \bar{\eta}}{\partial x} = \frac{-1}{\rho g(h' + \bar{\eta})} \frac{\partial S_{xx}}{\partial x} \tag{2.5}$$

where $\bar{\eta}$ is the deviation of the mean water level (m.w.l.) from the still water level (s.w.l.), ρ is the mass density of water and g the acceleration due to gravity. If shallow water linear wave theory is again adopted, the radiation stress is given by

$$S_{xx} = \frac{3}{16} \rho g H^2 \tag{2.6}$$

and (2.5) becomes

$$\frac{\partial \bar{\eta}}{\partial x} = \frac{-3}{16} \frac{1}{(h' + \bar{\eta})} \frac{\partial H^2}{\partial x} \tag{2.7}$$

If (2.4) and (2.7) are coupled, the mean water depth, $h = h' + \bar{\eta}$, replaces h' in (2.4).

2.2.2 Analytical Solutions

If set-up is neglected, closed form solutions to (2.4) exist for several idealized bottom topographies. These solutions are derived in Dally et al. (1985) and just the final results are stated here. For the shelf beach previously described, the solution is

$$\frac{H}{h'} = \left\{\left[(\gamma^2 - \Gamma^2) \exp\left(- K \frac{x}{h'}\right)\right] + \Gamma^2\right\}^{1/2} \tag{2.8}$$

where γ denotes the ratio of wave height to water depth at incipient breaking (i.e. $\gamma = H_b/h'_b$) as defined in Chapter 1.

For a planar beach given by

$$h' = h'_b - mx \tag{2.9}$$

where m is the bottom slope and the origin of x is at the breaker line, the solution is

$$\frac{H}{H_b} = \frac{1}{\gamma} \cdot \left[\left(\frac{h'}{h'_b}\right)^{(K/m - 1/2)} (\gamma^2 + \alpha) - \alpha \left(\frac{h'}{h'_b}\right)^2\right]^{1/2} \tag{2.10a}$$

where

$$\alpha = \frac{(K/m)\ \Gamma^2}{(5/2 - K/m)} \tag{2.10b}$$

If K/m = 5/2, which turns out to occur only for unnaturally steep beaches, the solution is

$$\frac{H}{H_b} = \frac{h'}{h'_b}\left[1 - 5/2(\Gamma/\gamma)^2 \ln\left(\frac{h'}{h'_b}\right)\right]^{1/2} \tag{2.11}$$

Solutions (2.10) and (2.11) are displayed in Figure 2.2 for various values of K/m and γ.

As shown by Dean (1977), a profile shape which better represents those found in nature is of the form

$$h' = A(x_b - x)^{2/3} \tag{2.12}$$

where x_b is the distance from the breaker line to the still water line, and A is a shape factor dependent on sediment characteristics, the most notable being sand particle fall velocity. The solution to (2.4) for this bottom configuration is given by

$$\frac{H}{H_b} = \left\{\chi - \left[(\Gamma/\gamma)^2 120 \sum_{n=0}^{5} \left(\chi - \left(\frac{h'}{h'_b}\right)^{(4-n)/2}\right) \cdot \frac{\phi^n}{(5-n!)}\right]\right\}^{1/2} \tag{2.13a}$$

where

$$\chi = \left(\frac{h'}{h'_b}\right)^{-1/2} \exp\left\{\frac{1}{\phi}\left[\left(\frac{h'}{h'_b}\right)^{1/2} - 1\right]\right\} \tag{2.13b}$$

and ϕ is a similarity parameter

$$\phi = A/(3K\, x_b^{1/3}) \tag{2.13c}$$

Figure 2.3 displays (2.13) and the dependence of breaker decay on ϕ and γ.

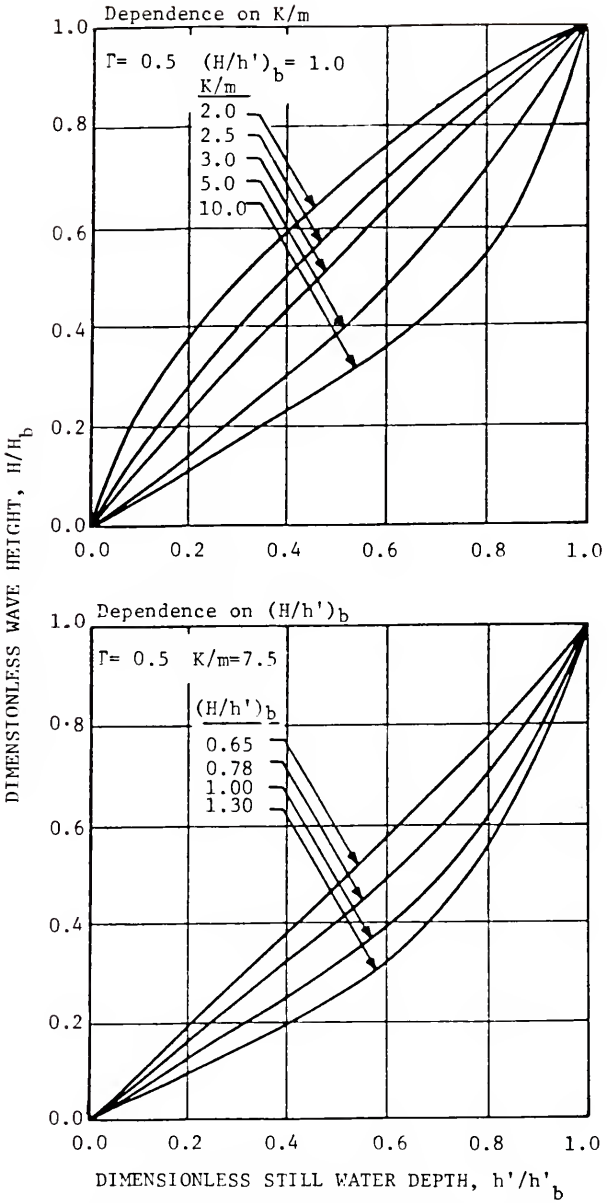

Figure 2.2 Analytical solution (2.10) of Dally et al. (1985) for wave decay on plane slopes, showing dependence on beach slope (m) and incipient condition $(H/h)_b = \gamma$.

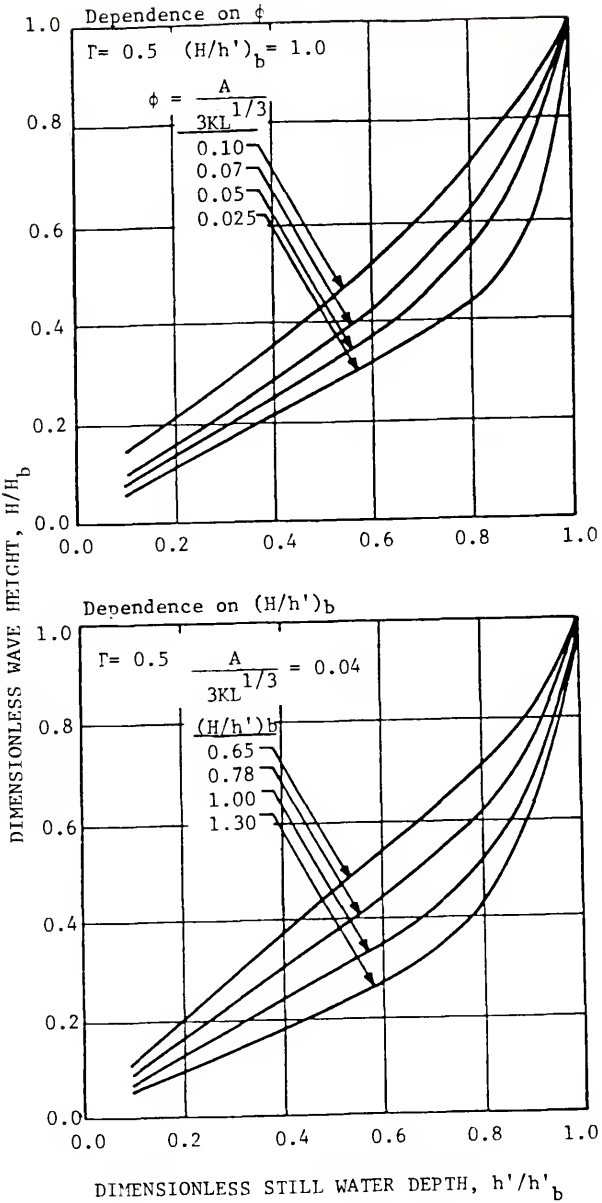

Figure 2.3 Analytical solution (2.13) of Dally et al. (1985) for wave decay on equilibrium beach profiles, showing dependence on similarity parameter (ϕ) and incipient condition (γ).

2.2.3 Numerical Solution

If set-up or bottom profiles of more arbitrary shape are included, solutions to (2.4) and (2.7) must be obtained numerically. Such a scheme was developed in Dally et al. (1984), and proved capable of describing the one-dimensional transformation of wave height over realistic bottom topography due to shoaling, breaking, reformation and bottom friction, although bottom friction was found to be negligible in the surf zone. In brief summary, (2.4) and (2.7) are finite-differenced, using central averages where appropriate; then because set-up is required but not known a priori, the program iterates at each spatial step until convergence is attained. The bottom profile, the initial wave height and incipient condition are the only information required to run the model. Because shallow water linear wave theory is used to shoal the waves up to incipient breaking, wave period is not required.

Extensive calibration and verification to the small scale laboratory data of Nakamura, Shiraishi and Sasaki (1966) and Horikawa and Kuo (1966) by Moore (1982) and Dally et al. (1984) yield best-fit values for the decay coefficient K and stable wave factor Γ. For the analytic solutions (without set-up) $K = 0.17$ and $\Gamma = 0.5$, while if set-up is included, $K = 0.15$ and $\Gamma = 0.4$. Although there is some dependence of K and Γ on beach slope, and slight dependence on wave period, these average values provide good agreement over a wide range of conditions which encompasses those found on natural beaches.

2.3 Verification of Breaker Model for Regular Waves to Prototype-Scale Data

To ensure that scale effects are not encountered when applying the small-scale calibration values of K and Γ to prototype conditions, the numerical model is now verified to three large-scale experiments. One experiment was conducted on a natural beach and the other two in large wave tanks with movable sand beds.

Suhayda and Pettigrew (1977) filmed a series of graduated wave staffs that were deployed in a transect across the surf zone, often referred to as the "photopole technique." Although the actual waves were of course random, they were rendered "regular" by choosing 10 waves of nearly identical breaking characteristics from the record and averaging their height at each location in the surf zone. These results are shown in Figure 2.4, as well as the wave transformation as predicted

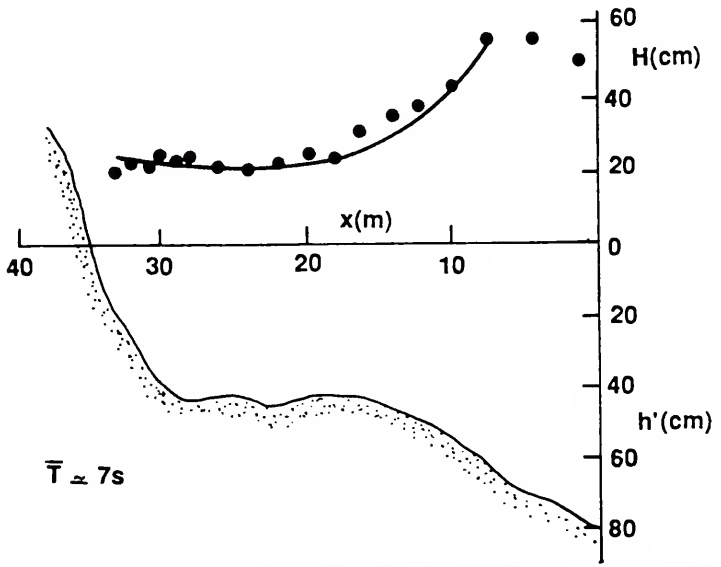

Figure 2.4 Verification of laboratory calibration of model of Dally et al. (1985) to full-scale field data of Suhayda and Pettigrew (1977).

by the numerical model using K = 0.15 and Γ = 0.4 and starting from incipient breaking. The measurements and predictions are in very good agreement.

Results of regular wave transformation measured visually in a large wave flume and reported by Stive (1985) are displayed in Figure 2.5. The major purpose of the original test was to study beach profile evolution, and it is noted that the wave data were not taken concurrently with the profile measurements. However, the model was run (again with K = 0.15 and Γ = 0.4) on each profile starting from incipient breaking. The average decay for the two runs is also shown in Figure 2.5 and compares well to the measurements.

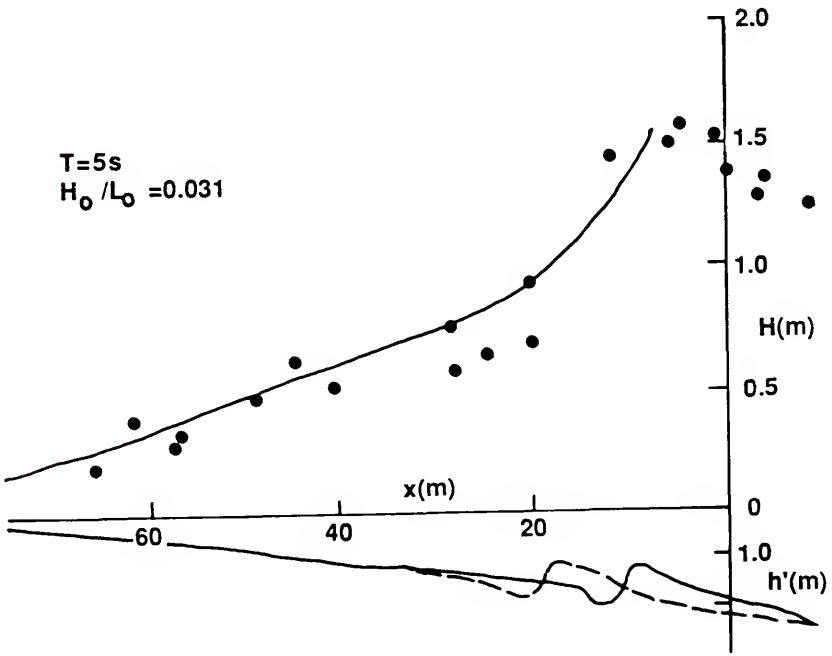

Figure 2.5 Verification of laboratory calibration of model of Dally et al. (1985) to full-scale large wave tank data of Stive (1985).

An experimental study of breaker decay conducted in a large wave tank utilizing the photopole technique by Maruyama, Sakakiyama, Kajima, Saito and Shimizu (1983) appears to be the most extensive prototype-scale data available in the literature for regular waves. Comparisons of the model ($K = 0.15$, $\Gamma = 0.4$) to these data are shown in Figure 2.6 and are in generally good agreement.

In conclusion it appears that the original calibration of K and Γ to small-scale laboratory measurements was not subject to scale effects in either energy dissipation or stable wave condition. The above comparisons verify the model over a wide range of deepwater heights, wave periods and bottom slopes and configurations. Unless otherwise noted, the decay factor K and stable wave coefficient Γ are hereafter fixed at the values of 0.15 and 0.4 respectively if set-up is included, and 0.17 and 0.5 if set-up is neglected.

2.4 Improvements to Breaker Model for Regular Waves

Before the regular wave model of Dally et al. (1985) is applied to the problem of random breaking waves, it is generalized in two respects. First, the shallow water assumption is removed during shoaling by incorporating the approximate solution to the dispersion relation given by Hunt (1979)

$$(kh)^2 = (k_o h)^2 + \frac{k_o h}{1 + \sum_{n=1}^{6} d_n (k_o h)^n} \tag{2.14}$$

where k is local wave number, k_o is deepwater wave number ($k_o = \omega^2/g = (2\pi)^2/gT^2$) and $d_1 = 0.66\overline{6}$, $d_2 = 0.35\overline{5}$, $d_3 = 0.1608465608$, $d_4 = 0.0632098765$, $d_5 = 0.0217540484$, $d_6 = 0.0065407983$. The accuracy was

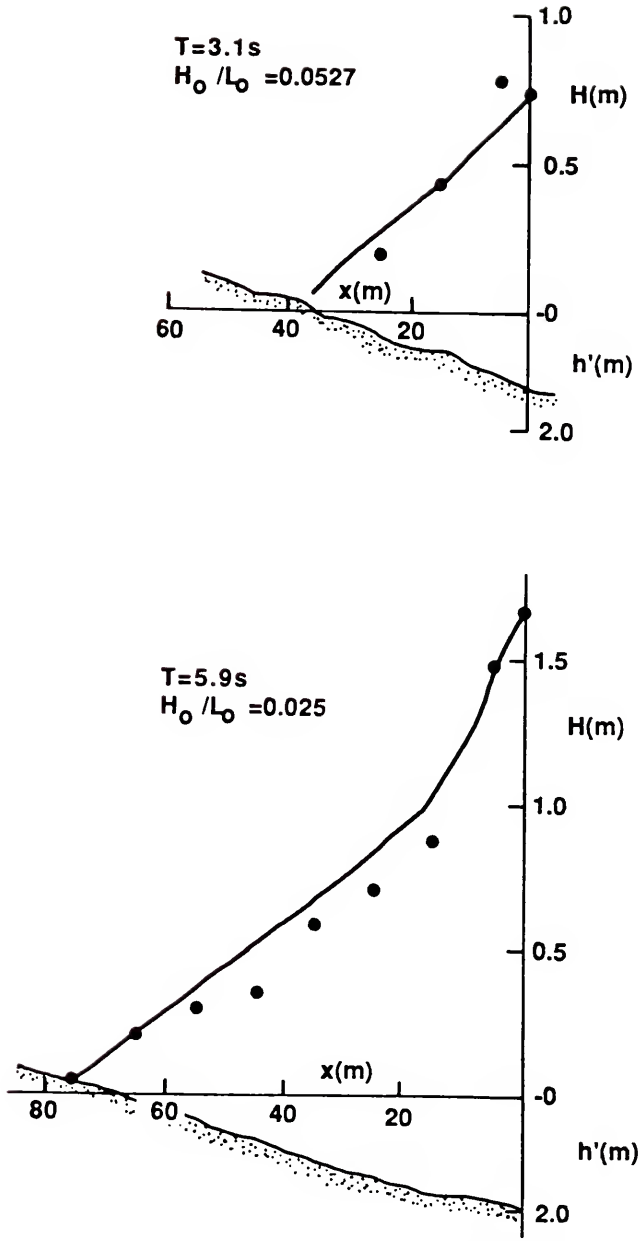

Figure 2.6 Verification of laboratory calibration of model of Dally et al. (1985) to full-scale large wave tank data of Maruyama et al. (1983).

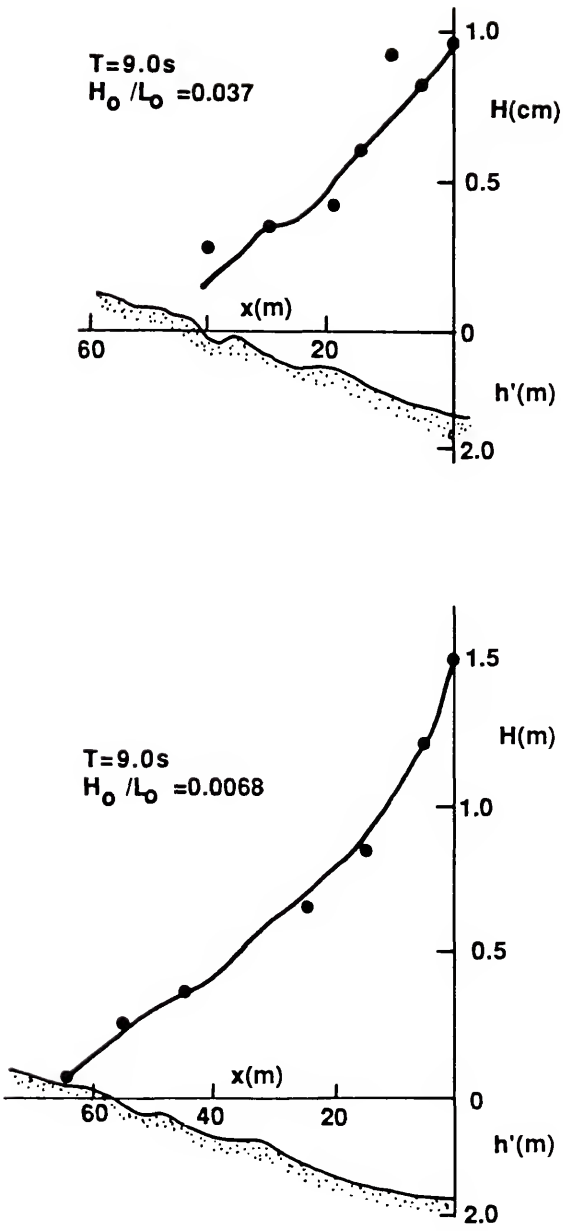

Figure 2.6 -- continued

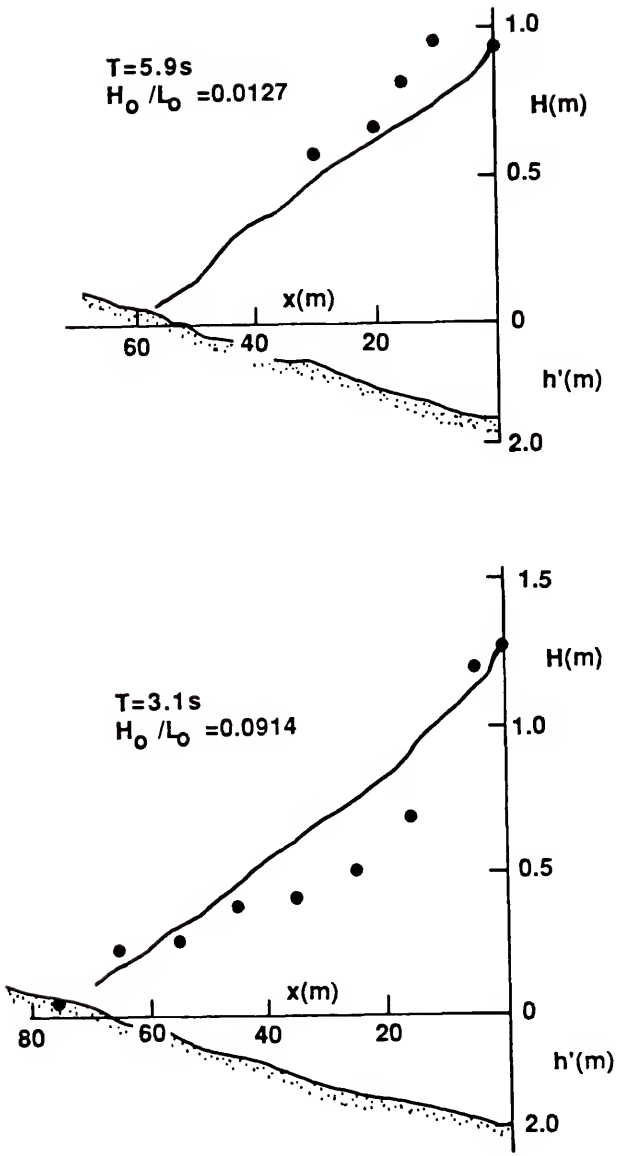

Figure 2.6 -- continued

stated by Hunt to be better than 0.01% over the range $0 < k_o h < \infty$. With the local relative depth thereby determined for a given wave period, the group velocity is calculated from linear wave theory and the shoaling wave height found by applying conservation of energy flux, i.e.

$$Cg = \frac{g(\tanh kh + kh\,\mathrm{sech}^2 kh)}{2(gk\tanh kh)^{1/2}} \tag{2.15}$$

and

$$H = H_o \left(\frac{Cg_o}{Cg}\right)^{1/2} \tag{2.16}$$

where Cg_o is group velocity in deep water ($Cg_o = gT/4\pi$) and H_o is deepwater wave height.

The regular wave shoals according to (2.16) and (2.15) until an incipient condition is attained, which in this improved version is given by a hybrid of the empirical expressions of Weggel (1972) and Komar and Gaughan (1972), and was first utilized by Moore (1982). This expression is

$$\gamma = b(m) - a(m)\left[\frac{0.36}{(2\pi)^{4/5}}\left(\frac{H_o}{L_o}\right)^{4/5}\right] \tag{2.17a}$$

where

$$a(m) = 43.8(1.0 - e^{-19m}) \tag{2.17b}$$

$$b(m) = 1.56/(1.0 + e^{-19.5m}) \tag{2.17c}$$

On realistically shaped bottom profiles, the question arises as to definition of the effective beach slope to be used in (2.17), especially when bar/trough systems are present. Based on laboratory tests conducted at the University of Florida, it was observed that the bottom slope just seaward of the break point more directly affected the breaking characteristics in the trough than the local bottom configuration. Consequently, the beach slope used in determining incipient breaking is calculated by averaging the slope over the profile just seaward of the point of interest, for a distance of one wave length. The negative slopes occurring on the landward side of a bar are treated as zeros in the averaging process.

Having shoaled according to (2.16) and attained incipient breaking as dictated by (2.17), the wave decays according to the numerical solution of (2.4) with h replacing h'. Set-down/up is determined iteratively as described. A flow chart of the improved model for regular waves is displayed in Figure 2.7.

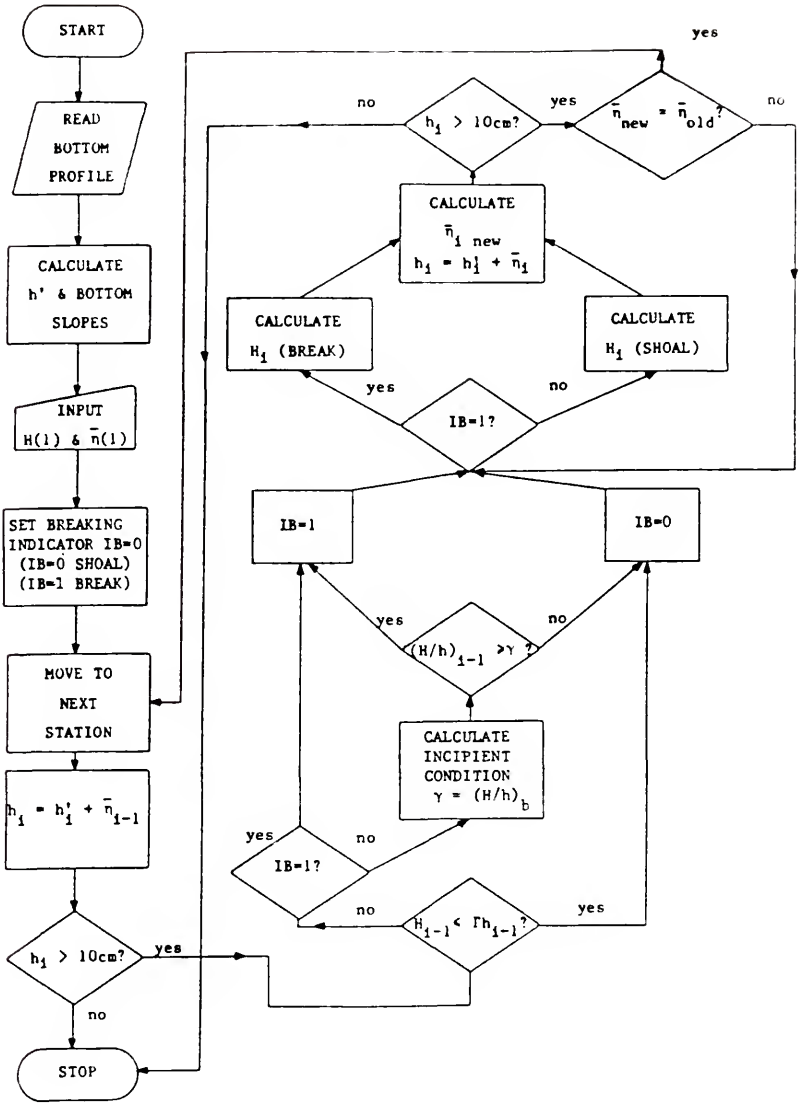

Figure 2.7 Flow chart of transformation model for regular waves.

CHAPTER 3

INTRODUCTION AND LITERATURE REVIEW OF RANDOM BREAKING WAVES

Extension of breaking models for regular waves to random waves not only involves the obvious problem of dealing with many waves of different heights and periods, but also the less apparent, but possibly important effects of breaking induced by wave-wave interaction. This interaction can be either between individual wind-waves, or with long waves driven by any groupiness displayed by the short waves. These are hereafter referred to as wave-short-wave and wave-long-wave interactions, respectively. While breaking of regular waves is depth-limited, i.e., occurs only in shallower water, breaking due to wave-short-wave interaction is steepness-limited and can occur in any water depth, while it can be both depth and steepness-limited for wave-long-wave interaction.

All previous studies of random breaking waves in the surf zone (which will be reviewed shortly), as well as this dissertation, neglect wave-short-wave interactions in their formulations. Only two of these studies have attempted to include the effects of wave-long-wave interactions, but addressed only the varying water level which the short wave sees and not the "current" associated with the long wave water particle velocities. In this chapter, discussion is restricted to the case with no wave-wave interaction. Individual waves documented at some offshore location are treated individually; i.e., it is assumed each wave shoals, reaches incipient breaking, breaks, reforms, etc. independently.

The essence of the random breaking wave problem is, starting with a known probability density function (pdf) for wave height (and perhaps period) at some offshore location, to describe the transformation of the pdf(H) due to shoaling and breaking across the nearshore region and surf zone. Attempts to model this transformation are complicated by the existence of both breaking and non-breaking waves at any location in the surf zone, and that waves of the same height can be found in each category. Collins (1970) appears to be the first to address the random breaking wave problem. He utilized linear wave theory to shoal the waves, an empirical relation to determine incipient breaking, and the similarity model ($H = \gamma h$) to limit wave heights due to breaking.

Collins applied conceptually the standard transformation of random variables

$$\text{pdf}(X_1, X_2, \ldots) = \text{pdf}(Y_1, Y_2, \ldots) \cdot |J| \tag{3.1a}$$

where $|J|$ is the Jacobian matrix

$$|J| = \begin{vmatrix} \partial Y_1/\partial X_1 & \partial Y_1/\partial X_2 \cdots \\ \partial Y_2/\partial Y_1 & \partial Y_2/\partial X_2 \\ \cdot & \\ \cdot & \\ \cdot & \end{vmatrix} \tag{3.1b}$$

and X_1, Y_1, etc., are random variables (wave height, period, etc.). But, due to the transcendental nature of the dispersion relation, closed form solutions could not be attained and so several of the required gradients and the Jacobian were evaluated numerically. Starting with a

Rayleigh pdf in deep water, the numerically transformed pdf retains this shape over most of the range of wave height in which waves are shoaling, but has a spike at the limiting breaker height as dictated by the local water depth (see Figure 3.1). This is the wave height where all the breaking waves "gather"; however, this behavior is not supported by either laboratory or field measurements.

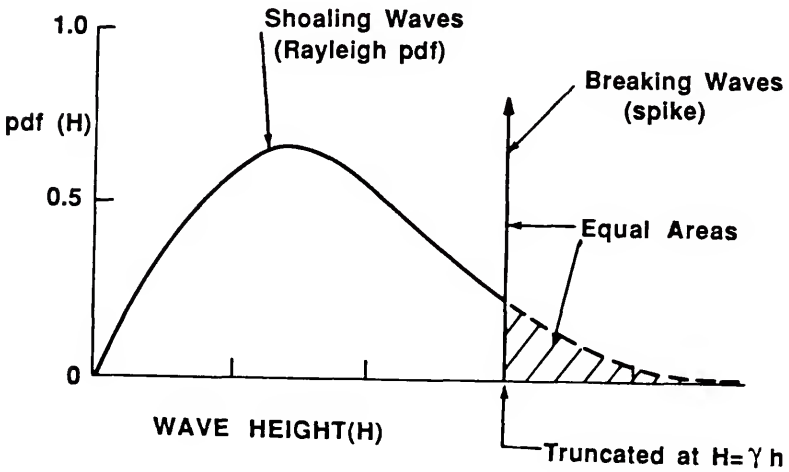

Figure 3.1 Conceptual model of Collins (1970) for the probability density function (pdf) of wave height in the surf zone.

Kuo and Kuo (1975) also assume the Rayleigh shape, but remove the spike at the limiting wave height and redistribute the associated area by normalizing the truncated pdf by the area lost above the truncation point (see Figure 3.2). As a result, the distinction between breaking and non-breaking waves is lost. This is a seemingly contrived treatment

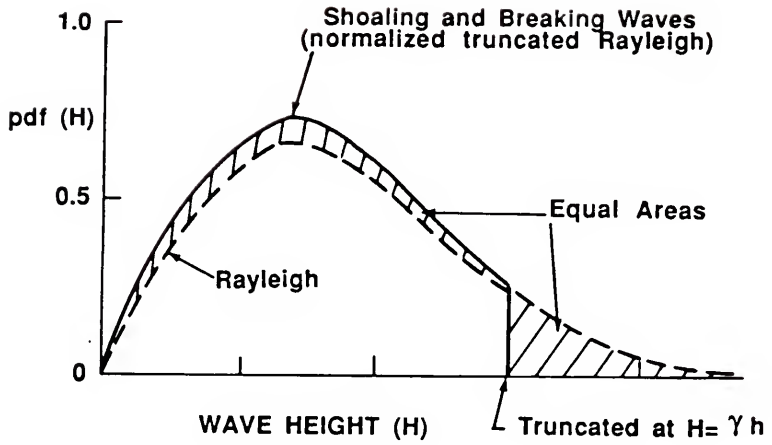

Figure 3.2 Conceptual model of Kuo and Kuo (1975) for the probability density function (pdf) of wave height in the surf zone.

which has little physical basis, and the resulting shape (a truncated Rayleigh distribution) does not compare well to measured histograms of waves in the surf zone.

Goda (1975) removes the delta function by reducing the Rayleigh pdf in an ad hoc manner over a range of heights that included the limiting value as shown in Figure 3.3. The pdf is then re-normalized in the same manner as Kuo and Kuo (1975). Although the behavior of the pdf induced by wave breaking is still contrived, this treatment leads to better comparison to histograms of wave height (combined shoaling and breaking) from laboratory experiments on a 1/10 slope after fitting to the data.

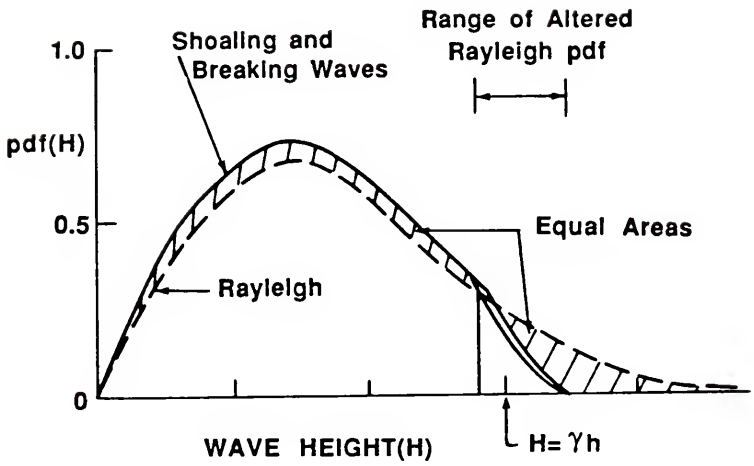

Figure 3.3 Conceptual model of Goda (1975) for the probability density function (pdf) of wave height in the surf zone.

However, this model is not verified to any additional histograms to ensure a universally applicable calibration. Wave set-up is calculated using (2.7) and interpreting H as H_{rms}. Mean water level variations due to surf beat are included stochastically by assuming the mean water level is normally distributed about the mean mean-water level, with variance given by an empirical expression based on field observations of surf beat. Runs for each stage of surf beat elevation and their accompanying probabilities are used to determine an average breaking wave behavior.

Battjes and Janssen (1978) regress to the pdf shape of Collins (1970) which contains a spike at the local limiting wave height, but apply (2.1) in a gross sense to dictate the decay in H_{rms}. By utilizing an approximate form for the rate of energy dissipation per unit plan

area for a hydraulic jump, defining a local limiting wave height, and deriving an expression for the probability of breaking waves (i.e., the area under the spike), an expression for $\delta(x)$ in (2.1) is developed. Energy density is assumed proportional to H_{rms}^2 and the group velocity, C_g, is calculated using linear wave theory and the average wave frequency, $\bar{f}$. Set-up is calculated from (2.7) also using H_{rms} and $\bar{f}$, and iteration to achieve convergence. Battjes and Janssen chose reasonable values for the two coefficients in their model and displayed favorable comparison to four laboratory tests. Battjes and Stive (1985) calibrated this model to each of sixteen laboratory and four field experiments and found a range of almost 32% in the coefficient that controls the fraction of breaking waves. This coefficient is somewhat analogous to γ for regular breaking waves. There is a distinct trend towards increasing the fraction of breaking waves (decreasing the coefficient) with decreasing average deepwater wave steepness, which Battjes and Stive parameterize in an empirical fashion. No justification is given by the authors for the behavior of this coefficient, which is in fact opposite to the trend observed for γ, i.e., <u>increasing</u> γ with decreasing wave steepness. However, Appendix G contains an explanation for this observed behavior dealing with the questionable assumption of Battjes and Janssen (1978) and Battjes and Stive (1985) that H_{rms}^2 is directly proportional to the energy in a wave record measured in the surf zone.

Mase and Iwagaki (1982) provide the most logically appealing approach to date for (numerical) transformation of the pdf of wave height across the surf zone. They first develop a breaker model for regular waves on planar beaches, with dissipation proportional to that

given by the bore representation. (Unfortunately, the proportionality factor varies in an ad hoc fashion with beach slope and distance from the break point.) Then, starting from a known joint histogram of wave height and period, each representative wave is shoaled according to linear theory until an empirical breaker index is satisfied, after which the regular wave model is employed to dictate wave decay. With the accompanying probability for each representative wave, histograms of wave height at any location can be constructed and statistically representative waves (i.e., H_{rms}, $H_{1/3}$, etc.) calculated. Surf beat is included in a manner similar to Goda (1975) and only treats m.w.l. fluctuations. Mase and Iwagaki display comparisons to laboratory measurements taken on planar beaches of slopes 1/10 and 1/30 for both histograms and mean wave height ($\bar{H}$) and significant wave height ($H_{1/3}$). Generally there is good agreement, especially for high steepness waves on the 1/30 slope. Filtering of the raw data significantly affected the shape of the measured histograms for low deepwater steepness waves in shallow water. The model is limited in application however, due to the assumption of a planar beach.

Based on field observations of the Nearshore Sediment Transport Study (NSTS), Thornton and Guza (1983) argue for adopting the complete, unmodified Rayleigh pdf for the entire nearshore region, including the surf zone. They define a subpopulation of waves that are breaking as did Battjes and Janssen (1978), but devise a "pdf" for the waves to spread out the area under the spike by making the physically unfounded assumption that waves break in proportion to the distribution for all waves. This pdf is shown conceptually in Figure 3.4. They fit this pdf for the subpopulation empirically and display calibrated comparisons to

one field data set. As is discussed in Appendix F, it is believed that much of the behavior of the data used to develop and calibrate this model was artificially induced by filtering during the initial treatment of the raw data.

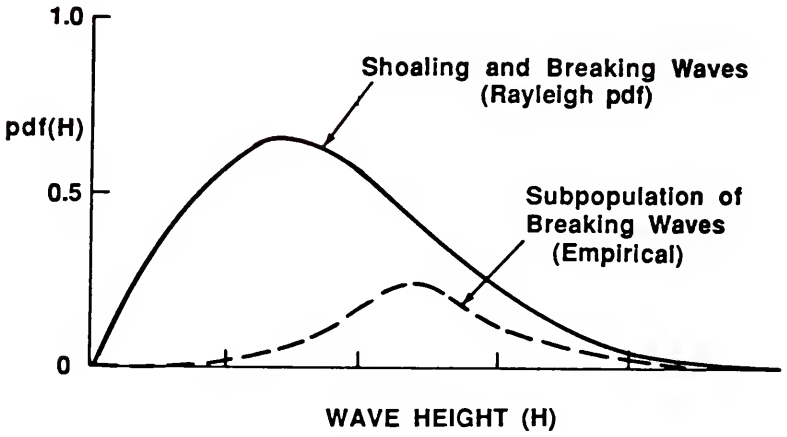

Figure 3.4 Conceptual model of Thornton and Guza (1983) for the probability density function (pdf) of wave height in the surf zone.

As is apparent from this literature review, with the exception of Mase and Iwagaki (1982), previous studies which deal with the probability density function of wave height in the surf zone have adopted the Rayleigh pdf and subjected it to somewhat contrived modifications to include the effects of wave breaking. However, both laboratory and field data indicate that inside the surf zone the Rayleigh form is not a valid assumption (for the most part due to wave breaking) while seaward of the surf zone and out into deep water, the Rayleigh pdf is well

substantiated for wave height. It is also well established that, due to nonlinearity in wave form, the free surface displacement (η) is a non-Gaussian random process in shallow water, and has been the subject of several investigations for non-breaking waves (see e.g. Ochi and Wang, 1984). Although the classical derivation of the Rayleigh pdf for wave height in deep water starts from the assumption that the free surface is a Gaussian random process, this places no restriction on the assumption that wave height is Rayleigh distributed for non-breaking waves in shallow water. In fact, the assumption that non-breaking wave height is Rayleigh in deep water is better substantiated by data than the assumption that the free surface is Gaussian, particularly during storm conditions; see Goodknight and Russell (1963). For these reasons, throughout the remainder of this study it is assumed that the pdf of wave height starts as a Rayleigh distribution well seaward of the surf zone, but the pdf will be transformed in an uncontrived manner due to shoaling and breaking. By invoking this assumption, it is not required to even consider the pdf of free surface displacement.

CHAPTER 4

CLOSED FORM SOLUTIONS FOR PLANAR BEACHES

4.1 Introduction

To date, no closed form solutions for the probability density function of random breaking waves in the surf zone have appeared in the literature. However, by applying a standard transformation of random variables and utilizing the analytical solution to the regular wave model of Dally et al. (1985), two closed form solutions for the probability density function of shoaling and breaking wave heights for a planar beach profile can be derived. In the first formulation, it is assumed that waves shoal according to shallow water linear wave theory, and that they all begin breaking at the same incipient height to depth ratio γ. Although displaying two features not supported by field data, this pdf is nevertheless more realistic than the other (ad hoc) forms that have been adopted to date, and is quite useful in an instructional sense. In the second formulation, the shallow water assumption is removed, and the incipient height to depth ratio varies and is systematically defined for each wave using any of several empirical expressions for γ available in the literature. This significantly improves at least qualitative comparison to observed histograms of wave height in the surf zone.

4.2 Closed Form Solution #1

As an initial condition, we adopt the Rayleigh pdf for wave height, truncate it at some realistically large wave height, and assume no waves

are breaking, i.e.,

$$\text{pdf}(H_i) = \frac{2H_i}{H^2_{rmsi}} \exp -\left[\frac{H_i^2}{H^2_{rmsi}}\right] \qquad H_i \leq \gamma h_i$$

$$= 0 \qquad H_i > \gamma h_i \qquad (4.1)$$

where H is the wave height, h the water depth (since set-up is not included, h = h'), γ the incipient breaker index (assumed constant), and the subscript "i" denotes initial conditions.

The area lost above the truncation point, Ω_t, is equal to

$$\Omega_t = \int_{\gamma h_i}^{\infty} \text{pdf}(H_i)\, dH_i = \exp -(\gamma h_i / H_{rmsi})^2 \qquad (4.2)$$

which shows that starting in water much deeper than the root mean square wave height will make Ω_t negligible. Otherwise, the pdf should be normalized by dividing by the quantity $(1 - \Omega_t)$. The random variable H_i is now transformed to local wave height H due to either shoaling or breaking, as a function of the local water depth, h.

4.2.1 Shoaling waves

It is now assumed that linear shallow water wave theory is valid, so that from Green's Law

$$H_i = H\,(h/h_i)^{1/4} \qquad (4.3)$$

and performing a standard transformation of random variable, i.e.,

$$\text{pdf}(H)_{sh} = \text{pdf}(H_i) \cdot \left|\partial H_i / \partial H\right| \qquad (4.4)$$

where subscript "sh" denotes the pdf for shoaling waves, and

$$|\partial H_i/\partial H| = (h/h_i)^{1/4} \tag{4.5}$$

yields

$$pdf(H)_{sh} = \frac{2H}{H_{rmsi}^2} (h/h_i)^{1/2} \exp[\frac{-H^2}{H_{rmsi}^2} (h/h_i)^{1/2}] \tag{4.6}$$

This distribution must be truncated at the largest wave height that can occur at the local water depth, i.e., $H \leq \gamma h$. If the random variable is non-dimensionalized by H_{rmsi}, we obtain

$$pdf(A)_{sh} = 2A\, \hat{h}^{1/2} \exp(-A^2\, \hat{h}^{1/2}) \qquad A \leq A_{max} \tag{4.7}$$

where $A = H/H_{rmsi}$, $A_{max} = \gamma h/H_{rmsi}$, and $\hat{h} = h/h_i$.

4.2.2 Breaking waves

The probability density function of wave height for broken waves is derived in a similar manner, but in two steps. The random variable H_i is first transformed to h_b, the water depth at which incipient breaking is attained, by applying Green's Law

$$H_i = \gamma\, h_b^{5/4}\, h_i^{-1/4} \tag{4.8}$$

Again the transformation is accomplished by

$$pdf(h_b) = pdf(H_i) \cdot |\partial H_i/\partial h_b| \tag{4.9}$$

where $$|\partial H_i/\partial h_b| = 5/4\ \gamma\, h_b^{1/4}\, h_i^{-1/4} \tag{4.10}$$

which yields

$$pdf(h_b) = \frac{5}{2} \frac{\gamma^2}{H_{rmsi}^{2\ 1/2}\ h_i} h_b^{3/2} \exp -\left(\frac{\gamma^2 h_b^{5/2}}{H_{rmsi}^{2\ 1/2}\ h_i}\right) \quad h_b \leq h_i \qquad (4.11)$$

To transform from h_b to H, we utilize the analytical solution to the model of Dally et al. (1985) for regular waves breaking on a planar beach (neglecting set-up). By inverting (2.10) we obtain

$$h_b = \left[\frac{H^2 + \alpha h^2}{(\gamma^2 + \alpha)\ h^{(K/m-1/2)}}\right]^{1/(5/2-K/m)} \qquad (4.12)$$

recalling that

$$\alpha = \frac{(K/m)\Gamma^2}{(5/2 - K/m)} \qquad (2.10b)$$

m is beach slope, K is the decay coefficient (~ 0.17), and Γ the stable wave factor (~ 0.50). Performing

$$pdf(H)_{br} = pdf(h_b) \cdot |\partial h_b/\partial H| \qquad (4.13)$$

where

$$|\partial h_b/\partial H| = \frac{1}{|5/2 - K/m|} \left[\frac{H^2 + \alpha h^2}{(\gamma^2 + \alpha)\ h^{(K/m-1/2)}}\right]^{\frac{(K/m-3/2)}{(5/2-K/m)}}$$

$$\cdot \left|\frac{2H}{(\gamma^2 + \alpha)\ h^{(K/m-1/2)}}\right| \qquad (4.14)$$

and again nondimensionalizing by H_{rmsi}, the portion of the pdf due to broken waves is

$$pdf(A)_{br} = \frac{5\, A\, \hat{h}^{(1/2-K-m)}\, B^{K/m}}{|(5/2 - K/m)|(\gamma^2 + \alpha)} \exp\left[-\left(\frac{\gamma h_i}{H_{rmsi}}\right)^2 B^{5/2}\right] \; ; \; A_{min} \leq A \leq A_{max} \tag{4.15a}$$

where

$$B = \left[\frac{\left(\frac{H_{rmsi}}{h_i}\right)^2 A^2 + \alpha \hat{h}^2}{(\gamma^2 + \alpha)\, \hat{h}^{(K/m-1/2)}}\right]^{1/(5/2-K/m)} \tag{4.15b}$$

This distribution must be truncated not only at the upper limit $A_{max} = \gamma h/H_{rmsi}$, but also at the lower bound given by the breaking wave height that corresponds to the largest wave of the original $pdf(H_i)$. By applying (2.10), we find

$$A_{min} = \left[\hat{h}^{(K/m-1/2)}\, (\gamma^2 + \alpha) - \alpha \hat{h}^2\right]^{1/2} (h_i/H_{rmsi}) \tag{4.15c}$$

If γ and m are such that the decay profiles are convex, A_{max} and A_{min} switch.

The expressions (4.7) and (4.15) are plotted in Figure 4.1 for a beach slope m = 1/80 and γ = 0.78, Figure 4.2 for m = 1/50 and γ = 1.0, and Figure 4.3 for m = 1/20 and γ = 1.2. Note that for the mild beach slope, as one moves into the surf zone, area is taken from the shoaling pdf and "piled up" at the lower breaking wave heights of the breaking pdf and not the upper limiting wave height, as is the case for the steep beach and was assumed by Collins (1970) and Battjes and Janssen (1978). This is in qualitative agreement with lab and field data, but the discontinuities at the upper and lower limits of the breaking pdf, the discontinuity at the upper limit of the shoaling pdf, and the anomaly in the breaking pdf are not realistic. These characteristics result from neglecting the mechanisms present in nature which smooth the pdf, such

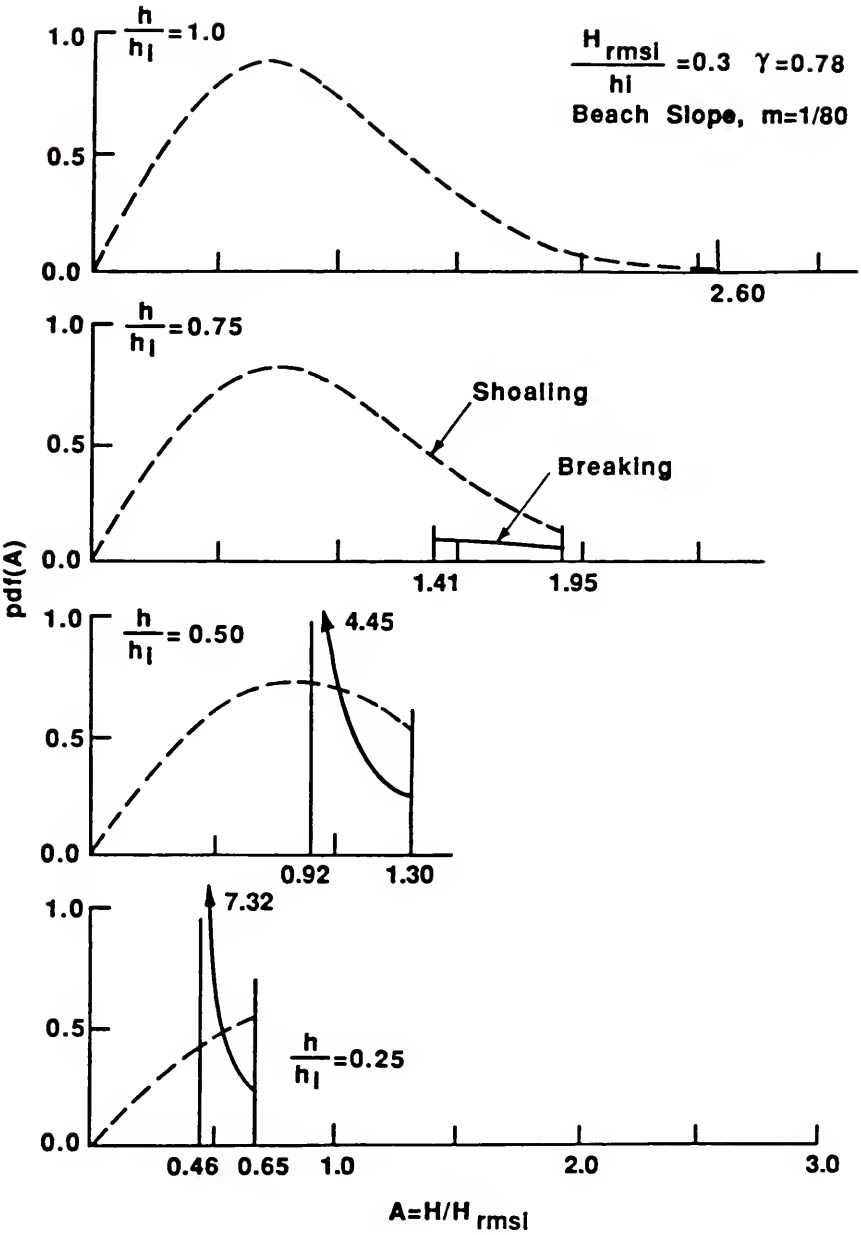

Figure 4.1 Transformation of the pdf of wave height across the surf zone according to closed-form solution #1 (4.7) and (4.15). Beach slope, m = 1/80.

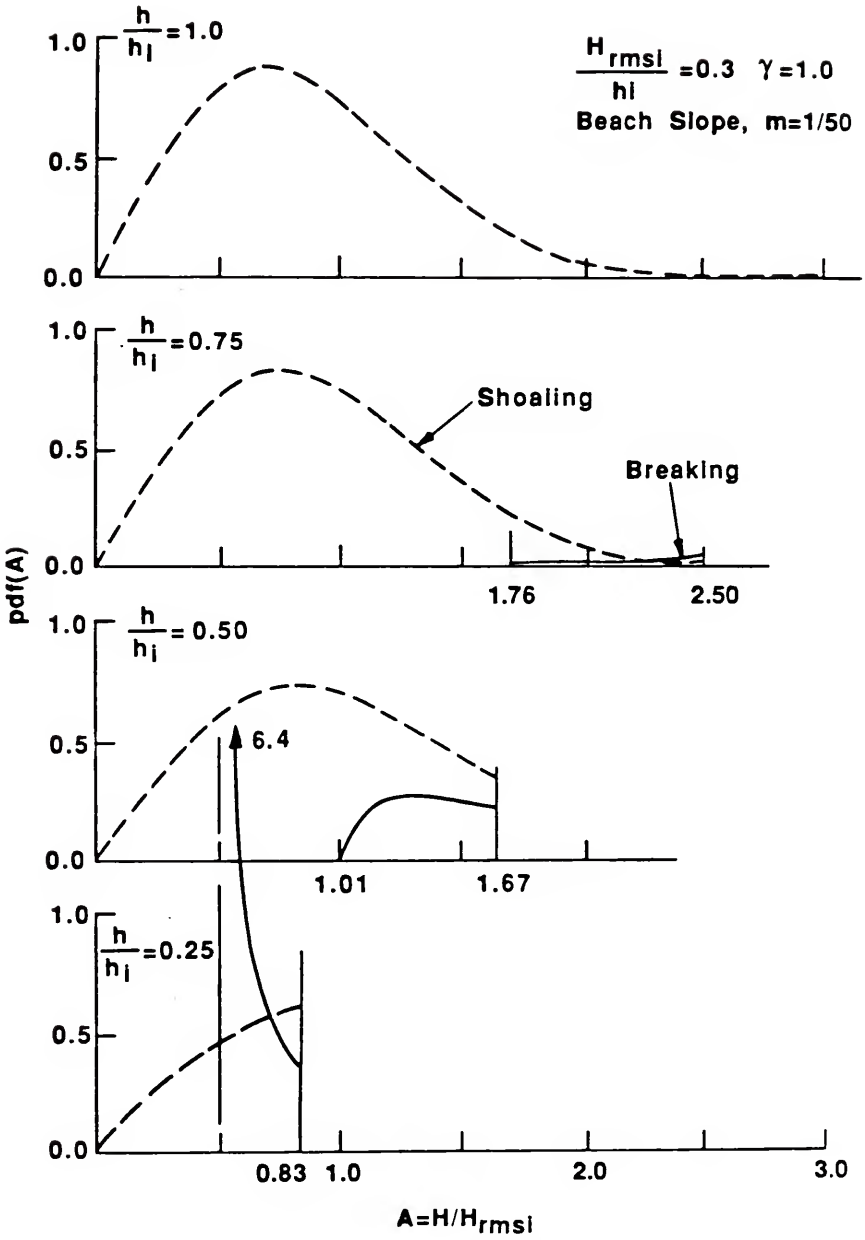

Figure 4.2 Transformation of the pdf of wave height across the surf zone according to closed-form solution #1 (4.7) and (4.15). Beach slope, m = 1/50.

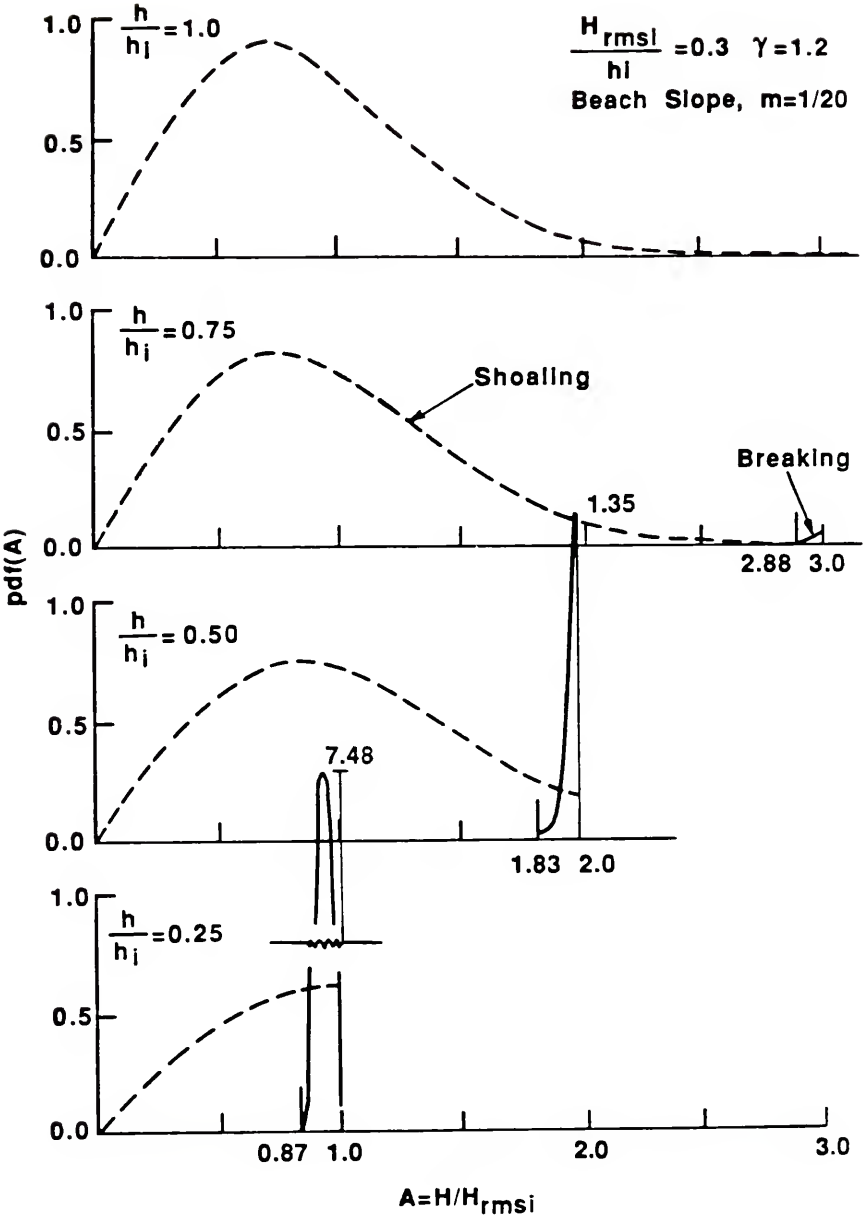

Figure 4.3 Transformation of the pdf of wave height across the surf zone according to closed-form solution #1 (4.7) and (4.15). Beach slope, m = 1/20.

as surf beat and a varying height to depth ratio at incipient breaking. The pdf is also in qualitative agreement to measured histograms in that, in the inner surf zone, the portion below the mean value rises gradually while the portion for A greater than the mean value drops sharply.

Because (2.10) includes beach slope explicitly, the effect of beach slope on the transformation of statistically representative waves commonly observed in the laboratory and nature and noted in Chapter 1 can be examined. By multiplying (4.7) and (4.15) by A^2 and integrating over proper limits, H_{rms} can be determined. The shoaling portion of the pdf is integrated from zero to A_{max} in closed form, while the breaking portion must be integrated from A_{min} to A_{max} numerically. Unfortunately, the anomaly at the lower bound of the breaking pdf precludes accurate numerical integration for mild beach slopes. Figure 4.4 displays the behavior of $\lambda_{rms} = H_{rms}/h$ with beach slope and deepwater steepness at a location in the inner surf zone ($H_{rmsi}/h = 2.0$) as predicted by the model. The trend of increasing H_{rms} with increasing slope noted in Chapter 1 is clearly evident, while the effect of wave steepness is minimal, as was noted by Sallenger and Holman (1985). The data of Sallenger and Holman from Figure 1.6 are also displayed. Because the field data were collected on bottom profiles that departed significantly from a planar slope, plus the sampling rate of the instruments was only 2.0 Hz and may not be sufficient to accurately resolve the wave height, only a qualitative comparison can be made.

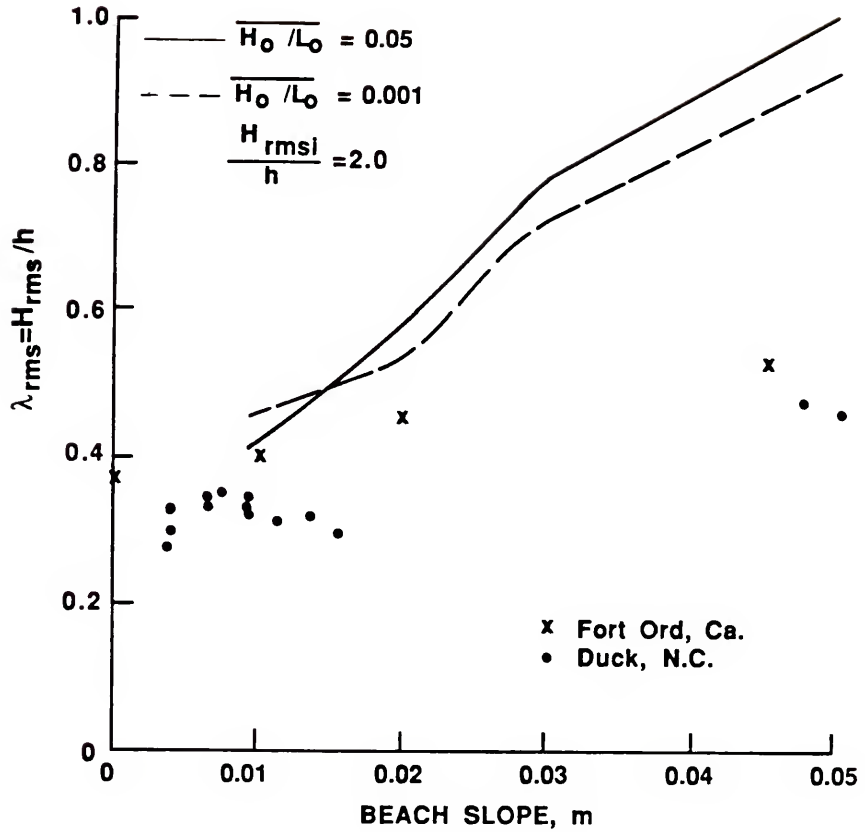

Figure 4.4 Predicted behavior of λ_{rms} in the inner surf zone from closed form solution #1, with dependence on beach slope (m) and deepwater steepness ($\overline{H_o/L_o}$). Field data is from Sallenger and Holman (1985), for qualitative comparison only.

4.3 Closed Form Solution #2

To improve upon the first closed form solution, in the following the shallow water assumption is removed and the incipient condition varies according to a general form for the empirical expressions available in the literature, e.g., the expression of Weggel (1972) previously noted in (2.17). These improvements require knowledge of the distribution of wave period, and so we will conduct a series of transformations of a joint pdf in two random variables. In the final step the second random variable is integrated out to obtain the marginal pdf of shoaling and breaking wave heights.

The initial condition is taken to be the joint probability density function for wave height and period in deep water as derived by Longuet-Higgins (1983), which is

$$\text{pdf}(R_o,\tau) = C_1 \frac{R_o^2}{\tau^2} \exp\{-R_o^2[1 + \frac{1}{\nu^2}(1 - \frac{1}{\tau})^2]\} \tag{4.16a}$$

where $$R_o = H_o/H_{rmso} = H_o/\sqrt{8a_0} \tag{4.16b}$$

and $$\tau = T/\bar{T} = T\frac{a_1}{2\pi\, a_0} \tag{4.16c}$$

The subscript "o" denotes deepwater conditions, T and $\bar{T}$ are wave period and average wave period, and a_0 is the area under the measured spectral density function in deep water and a_1 is the first moment of this area. The coefficient C_1 is given by

$$C_1 = \frac{4}{\sqrt{\pi}\,\nu}\left[1 + (1 + \nu^2)^{-1/2}\right]^{-1} \tag{4.16d}$$

and ν is the band-width parameter determined by the first three moments of the spectrum

$$\nu = \left[\frac{a_0\, a_2}{(a_1)^2} - 1\right]^{1/2} \tag{4.16e}$$

4.3.1 Shoaling waves

Although the transformation could be performed in one step, for better tractibility, the pdf for shoaling waves will be developed in two steps. The first is to transform τ to deepwater relative depth, D_o

$$D_o = k_o h = \frac{(2\pi)^2}{gT^2} h \tag{4.16}$$

and so

$$\tau = \frac{2\pi}{\overline{T}} \left(\frac{h}{gD_o}\right)^{1/2} \tag{4.18}$$

Because only one random variable changes, the Jacobian becomes simply

$$\left|\partial\tau/\partial D_o\right| = \left|-\frac{1}{2}\frac{2\pi}{\overline{T}} \left(\frac{h}{g}\right)^{1/2} D_o^{-3/2}\right| \tag{4.19}$$

and the joint pdf is transformed to

$$\text{pdf}(R_o, D_o) = \frac{C_1}{2} R_o^2 \frac{\overline{T}}{2\pi} \left(\frac{g}{hD_o}\right)^{1/2} \exp\left(-R_o^2\left[1 + \frac{1}{\nu^2}\left[1 - \frac{\overline{T}}{2\pi}\left(\frac{gD_o}{h}\right)^{1/2}\right]^2\right]\right) \tag{4.20}$$

The second step is to transform the deepwater wave height to the local shoaling wave height. By applying conservation of energy flux

$$E_o C g_o = E_{sh} C g_{sh} \tag{4.21}$$

and invoking linear wave theory yields

$$R_o^2 \frac{gT}{4\pi} = R^2\left[\frac{g \tanh kh + gkh(1 - \tanh^2 kh)}{2(gk \tanh kh)^{1/2}}\right] \tag{4.22}$$

From the dispersion relation

$$k_o h = kh \tanh kh \tag{4.23}$$

and adopting the notation D = kh, (4.22) reduces to

$$R_o^2 = R^2\left[\frac{D_o + D^2 - D_o^2}{D}\right] \tag{4.24}$$

As previously discussed, the approximate solution to (4.23) given by Hunt (1979) is

$$D^2 = D_o^2 + \frac{D_o}{1 + \sum_{n=1}^{6} d_n D_o^n} \tag{2.14}$$

in the present notation, and (4.24) can now be expressed explicitly in terms of D_o

$$R_o = R\left\{\frac{1 + 1/(1 + \Sigma)}{[1 + 1/D_o(1 + \Sigma)]^{1/2}}\right\}^{1/2} \tag{4.25}$$

where Σ denotes the summation in (2.14). Again because only one random variable is being transformed, the Jacobian reduces to

$$\left|\partial R_o/\partial R\right| = \left|\left\{\frac{1 + 1/(1 + \Sigma)}{[1 + 1/D_o(1 + \Sigma)]^{1/2}}\right\}^{1/2}\right| \tag{4.26}$$

Finally, the joint probability density function of shoaling wave height and deepwater relative depth is produced

$$pdf(R,D_o)_{sh} = \frac{C_1}{2} \overline{D}_o^{-1/2} D_o^{1/2} \{\}^{3/2} R^2 \exp\left(-R^2 \{\} \{1 + \frac{1}{\nu^2} [1 - (\frac{D_o}{\overline{D}_o})^{1/2}]^2\}\right) \quad (4.27)$$

in which $\{\}$ denotes the expression within the braces of (4.25) and

$$\overline{D}_o = \overline{k}_o h = \frac{2\pi}{\overline{L}_o} h = 2\pi \frac{H_{rmso}}{\overline{L}_o} \frac{h}{H_{rmso}} = 2\pi \overline{S}_o \hat{h} \quad (4.28)$$

$\overline{S}_o$ is mean deepwater wave steepness and $\hat{h}$ is dimensionless water depth.

The marginal pdf for dimensionless shoaling wave height is found by integrating between proper limits (numerically) with respect to deepwater relative depth D_o. These limits are defined by the incipient condition, which is a function of deepwater steepness and bottom slope. This function can be expressed in a general form which encompasses most of the empirical relationships for γ available in the literature:

$$S_o = H_o/L_o = \frac{D_o R_o}{2\pi \hat{h}} = [F(m, \gamma)]^p \quad (4.29)$$

As an example, for γ given by (2.17)

$$F = \left[\frac{b(m) - \gamma}{a(m)} \frac{(2\pi)^{4/5}}{0.36}\right] \quad (4.30a)$$

and

$$p = 5/4 \quad (4.30b)$$

The essence of the problem at hand is, given the local water depth and choosing a wave height of interest, what is the deepwater relative

depth of the single wave that is at incipient breaking, if such a wave exists. If it does exist, all waves of that height but with smaller relative depth are still shoaling, while all waves of that height but greater relative depth are already breaking. Thus to determine the marginal pdf of shoaling wave height, the joint pdf $(R,D_o)_{sh}$ is integrated according to

$$\text{mpdf}(R)_{sh} = \int_{o}^{D_{oI}} \text{pdf}(R,D_o)_{sh}\, dD_o \tag{4.31}$$

where D_{oI} is the relative depth of the wave with height R at incipient breaking. Returning to (4.29), substituting (4.25) and collecting D_o to one side yields

$$D_o\{\ \}^{1/2} = \frac{2\pi\hat{h}}{R}\,[F(m,\gamma)]^p \tag{4.32}$$

For a chosen wave height R and given water depth h, the wave at incipient breaking of course has a γ value

$$\gamma_I = R/\hat{h} \tag{4.33}$$

so that

$$D_o\{\ \}^{1/2} = C_2 \tag{4.34a}$$

where

$$C_2 = \frac{2\pi}{\gamma_I}\,[F(m,\ \gamma_I)]^p \tag{4.34b}$$

Straightforward manipulation of (4.32) leads to

$$(C_2)^4[D_o(1 + 2\Sigma + \Sigma^2) + 1 + \Sigma] - D_o^5[4 + 4\,\Sigma + \Sigma^2] = 0 \tag{4.35}$$

which is a polynomial in D_o of degree seventeen (C_2 is known). By applying Müller's Method and Hotteling's Deflation, the seventeen complex roots can be found numerically. There exists one acceptable root which is purely real and positive, and this root is the upper limit on the integration, D_{oI} in (4.31). The acceptable root to (4.35) for conditions $m = 0.05$, $\hat{h} = 1.67$, and the incipient condition given by (2.17), is displayed in Figure 4.5. Note that (2.17) does prescribe an upper limit on γ for a given beach slope.

The original joint pdf (R_o,τ) is limited by the Miche type wave steepness criterion

$$\frac{H_o}{L_o} \leq 1/7 \tag{4.36a}$$

or

$$\frac{D_o R_o}{2\pi \hat{h}} \leq 1/7 \tag{4.36b}$$

which, after utilizing (4.24), has exactly the same form as (4.35)

$$(C_3)^4[D_o(1 + 2\Sigma + \Sigma^2) + 1 + \Sigma] - D_o{}^5[4 + 4\Sigma + \Sigma^2] = 0 \tag{4.37a}$$

$$\text{where} \quad C_3 = \frac{1}{7}\frac{2\pi\hat{h}}{R} \tag{4.37b}$$

and whose acceptable root is found in the same manner as described above. The two criterion match when $H_o/L_o = 1/7$ is inserted in the breaker criterion expression, which for (2.17) yields

$$\gamma_{match} = b(m) - (0.017166)\, a(m) \tag{4.38}$$

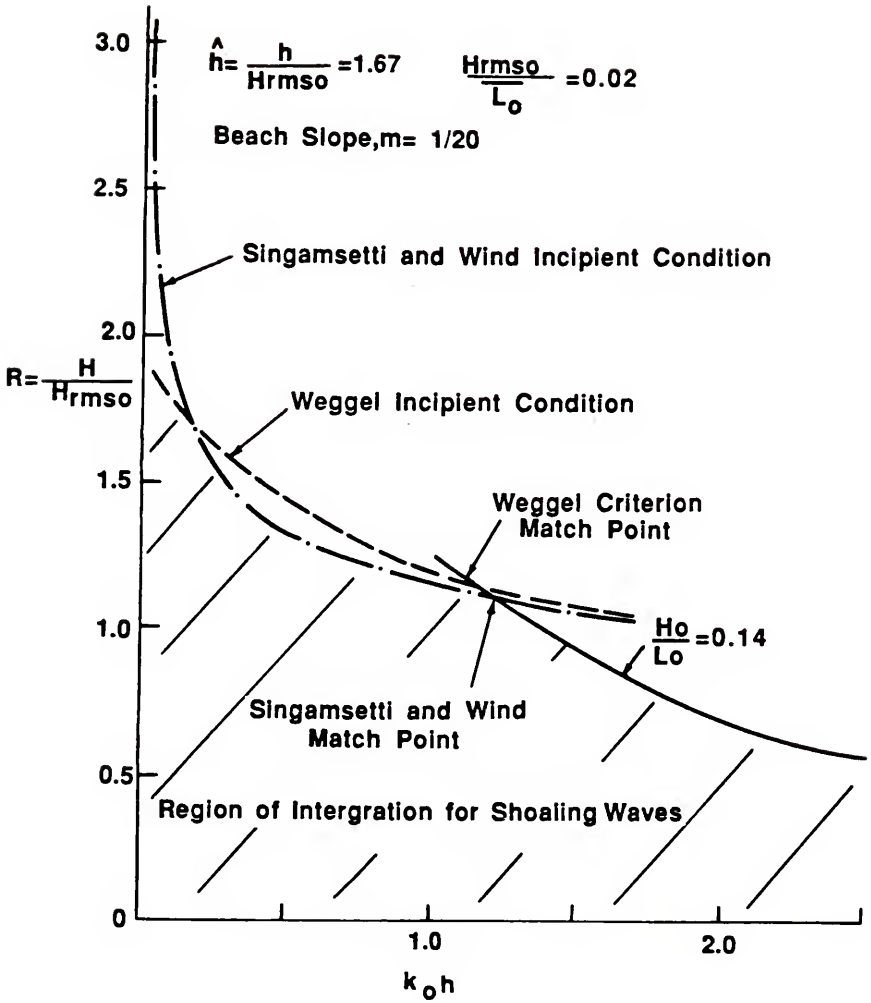

Figure 4.5 Example of region of integration for pdf of shoaling waves for closed-form solution #2 determined by solving (4.24) and (4.26) numerically.

The solution to (4.37) is also drawn in Figure 4.5 and completes the boundary of the region to be integrated in determining $mpdf(R)_{sh}$. We now turn our attention to the pdf for breaking waves.

4.3.2 Breaking Waves

Four steps will be required to derive the pdf of wave height due to breaking, represented conceptually by

$$pdf(H_o,T) \Rightarrow pdf\ (H_o, \frac{H_o}{L_o}) \Rightarrow pdf(H_o,\gamma) \Rightarrow pdf(h_b,\gamma)$$

$$\Rightarrow pdf(H,\gamma)_{br}\ ;\ mpdf(H)_{br} = \int_{\gamma_1}^{\gamma_2} pdf(H,\gamma)_{br}\, d\gamma \qquad (4.39)$$

Again starting with (4.16) and applying

$$\tau = \left(\frac{R_o}{S_o}\frac{H_{rmso}}{\bar{L}_o}\right)^{1/2} = \left(\frac{R_o}{S_o}\bar{S}_o\right)^{1/2} \qquad (4.40)$$

$$\left|\partial\tau/\partial S_o\right| = \left| -\frac{1}{2}\left(R_o \bar{S}_o\right)^{1/2} S_o^{-3/2}\right| \qquad (4.41)$$

we obtain

$$pdf(R_o,S_o) = \frac{C_1}{2}\frac{R_o^{3/2}}{S_o^{1/2}}(\bar{S}_o)^{-1/2}\exp\left(-R_o^2\left\{1+\frac{1}{\nu^2}\left[1-\left(\frac{R_o}{S_o}\bar{S}_o\right)^{-1/2}\right]^2\right\}\right) \qquad (4.42)$$

In the second step, (4.29) is employed

$$S_o = [F(m,\gamma)]^p \qquad (4.29)$$

$$\left|\partial S_o/\partial\gamma\right| = p[F(m,\gamma)]^{p-1}\cdot\left|\partial F/\partial\gamma\right| \qquad (4.43)$$

so that

$$pdf(R_o,\gamma) = \frac{C_1}{2}(\bar{S}_o)^{-1/2} R_o^{3/2}\ p\ F^{(P/2-1)} |\partial F/\partial\gamma| \cdot$$

$$\exp\left(-R_o^2\left\{1 + \frac{1}{\nu^2}\left[1 - \left(\frac{R_o}{F^p}\bar{S}_o\right)^{-1/2}\right]^2\right\}\right) \qquad (4.44)$$

We now apply conservation of energy flux between the deepwater wave and the same wave at incipient breaking (which is in shallow water)

$$E_o Cg_o = E_b\ Cg_b \qquad (4.45)$$

or

$$\frac{R_o^2\ L_o^{1/2}\sqrt{g}}{2\sqrt{2\pi}} = R_b^2\sqrt{gh_b} = \frac{\gamma^2\ h_b^2}{H_{rmso}^2}\sqrt{gh_b} \qquad (4.46)$$

Rearranging and applying (4.29) yields

$$R_o = \hat{h}_b(8\pi)^{1/5}\ \gamma^{4/5}[F(m,\gamma)]^{p/5} \qquad (4.47)$$

where $\hat{h}_b = h_b/H_{rmso}$, from which

$$|\partial R_o/\partial\hat{h}_b| = (8\pi)^{1/5}\gamma^{4/5}[F(m,\gamma)]^{p/5} \qquad (4.48)$$

and the joint pdf of $\hat{h}_b$ and γ is determined

$$pdf(\hat{h}_b,\gamma) = \frac{C_1}{2}(\bar{S}_o)^{-1/2}(8\pi)^{1/2}\ \gamma^2\ p\ F^{(p-1)}\ |\partial F/\partial\gamma|\ \hat{h}_b^{3/2} \cdot$$

$$\exp\left(-\hat{h}_b^2(8\pi)^{2/5}\ \gamma^{8/5}F^{2p/5}\left\{1 + \frac{1}{\nu^2}\left[1 - \left(\frac{\hat{h}_b(8\pi)^{1/5}\ \gamma^{4/5}\ \bar{S}_o}{F^{4p/5}}\right)^{-1/2}\right]^2\right\}\right) \qquad (4.49)$$

The final transformation again utilizes the inverted analytic solution for wave decay on planar beaches (4.12) which in the present dimensionless notation is

$$\hat{h}_b = \left[\frac{R^2 + \alpha \hat{h}^2}{\hat{h}^{(K/m-1/2)}(\gamma^2 + \alpha)}\right]^{\frac{1}{5/2-K/m}} \tag{4.50}$$

and so

$$|\partial \hat{h}_b/\partial R| = \frac{1}{|5/2 - K/m|} \frac{2R}{\hat{h}^{(K/m-1/2)}(\gamma^2 + \alpha)} [\ ]^{\left(\frac{K/m-3/2}{5/2-K/m}\right)} \tag{4.51}$$

where [ ] denotes the quantity in the brackets of (4.50). Finally, the joint pdf of R and γ for breaking waves is

$$\text{pdf}(R,\gamma)_{br} = \frac{C_1}{2}(\bar{S}_o)^{-1/2} (8\pi)^{1/2} \gamma^{2p} F^{(p-1)} |\partial F/\partial \gamma| [\ ]^{\left(\frac{K/m}{5/2-K/m}\right)}$$

$$\cdot \frac{1}{|5/2 - K/m|} \frac{2R}{\hat{h}^{(K/m-1/2)}(\gamma^2 + \alpha)}$$

$$\cdot \exp\{-[\ ]^{\left(\frac{2}{5/2-K/m}\right)} (8\pi)^{2/5} \gamma^{8/5} F^{2p/5}$$

$$\{1 + \frac{1}{\nu^2}[1 - (\frac{[\ ]^{\frac{1}{5/2-K/m}} (8\pi)^{1/5} \gamma^{4/5} \bar{S}_o}{F^{4p/5}})^{-1/2}]^2\}) \tag{4.52}$$

In examining (4.52) and in particular (4.50) it is noted that for real solutions the quantity [ ] must be positive. Thus in order for the value of the pdf to be real, $(\gamma^2 + \alpha)$ and $(R^2 + \alpha\hat{h}^2)$ must have the same sign. This defines two regions in the R-γ plane where the integration will take place; see Figure 4.6. Note that the function is well-behaved

(in fact, equal to zero) along the lines $(\gamma^2 + \alpha) = 0$ and $(R^2 + \alpha\hat{h}^2) = 0$ except at the point of intersection where there is a simple pole. The range of γ is limited by (4.38) on the lower end, and the largest value for a given beach slope dictated by (2.17). Waves that are at incipient breaking are found along the line $H/h = \gamma$ or in terms of the present variables

$$R = \hat{h}\,\gamma \tag{4.53}$$

Combinations of R and γ that fall above this line, meaning that the height to depth ratio of the already broken wave is greater than its height to depth ratio was at incipient breaking, corresponds to wave decay profiles that are convex. The region below this line corresponds to concave profiles, while the singular point is where decay profiles that are linear "collect." The similarity model is valid at this point as is seen when the special case $\alpha = -\gamma^2$ is inserted in (2.10). The existence of the singularity might well have been expected because given only γ, the local height of an already broken wave and that its decay profile is linear, there is no way to determine where it started breaking. This is the point where the transformed pdf loses its one-to-one correspondence with the original pdf.

The integration of the $\text{pdf}(R,\gamma)_{br}$ is accomplished numerically using Simpson's rule to obtain the marginal pdf of dimensionless wave height due to breaking. Due to the singularity that exists in (4.50) whenever α is negative, the final transformation does not preserve the volume under the joint pdf and therefore does not preserve the area under the marginal pdf of breaking wave height. However, the area under the mpdf

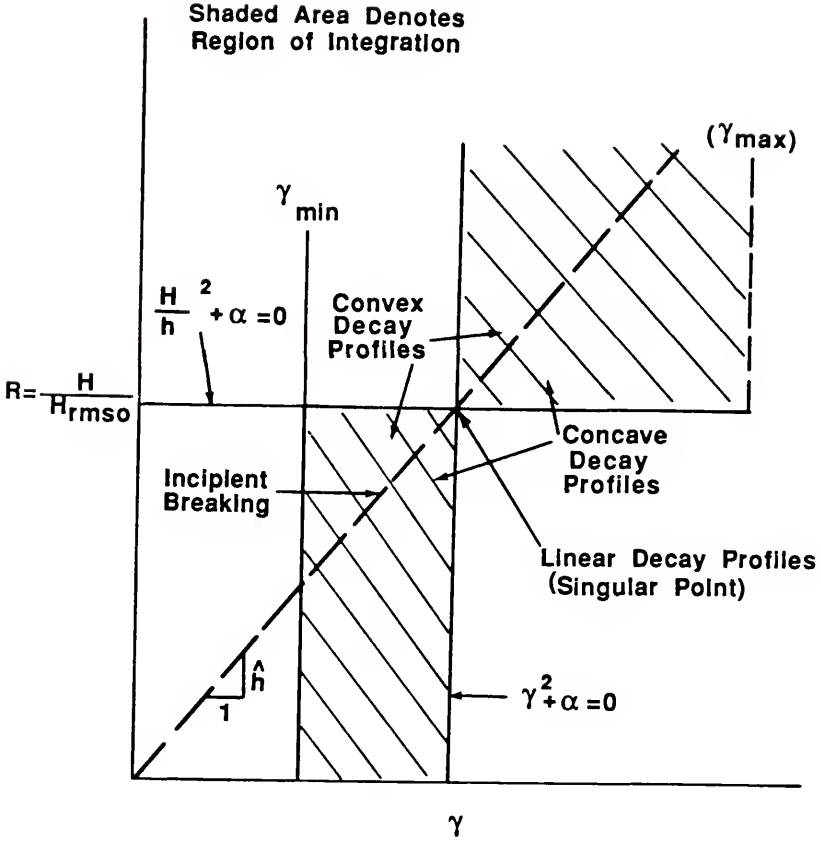

Figure 4.6 Region of integration for pdf of breaking waves for closed-form solution #2.

of shoaling waves is preserved, and the total area under the two mpdf's must equal one. Therefore, we normalize the breaking mpdf by

$$\text{mpdf}(R)_{\text{br(normalized)}} = \frac{1 - \Omega_{sh}}{\Omega_{br}} \text{mpdf}(R)_{br} \tag{4.54}$$

where Ω_{sh} is the area under the shoaling mpdf and Ω_{br} is the area under the breaking mpdf before normalization. Example results are displayed in Figures 4.7 and 4.8. Note that the anomaly present in the first closed form solution for breaking on the 1/20 slope has been smoothed and that the discontinuity at the upper bound of the shoaling pdf's has been eliminated and significantly reduced for breaking. For mild beach slopes, the anomaly in the lower range of values for breaking waves displayed by the first model (Figure 4.1) still exists as shown in Figure 4.8 for a beach slope of 1/80.

To test the sensitivity of the model to the expression chosen to dictate incipient breaking, that given by Singamsetti and Wind (1980),

$$\gamma = 0.568\ m^{0.107}\left(\frac{H_o}{L_o}\right)^{-0.237} \tag{4.55}$$

is also applied and results for the same conditions as Figure 4.7 are displayed in Figure 4.9. This breaker criterion allows more range in values of γ than (2.17), perhaps more than is actually found in nature and in fact has no upper limit. This is responsible for the broad and flat shape of the pdf for broken waves, and the upper tail of the pdf for shoaling waves as compared to Figure 4.7. The incipient condition (4.55) is also shown in Figure 4.5 for comparison to Weggel's criterion.

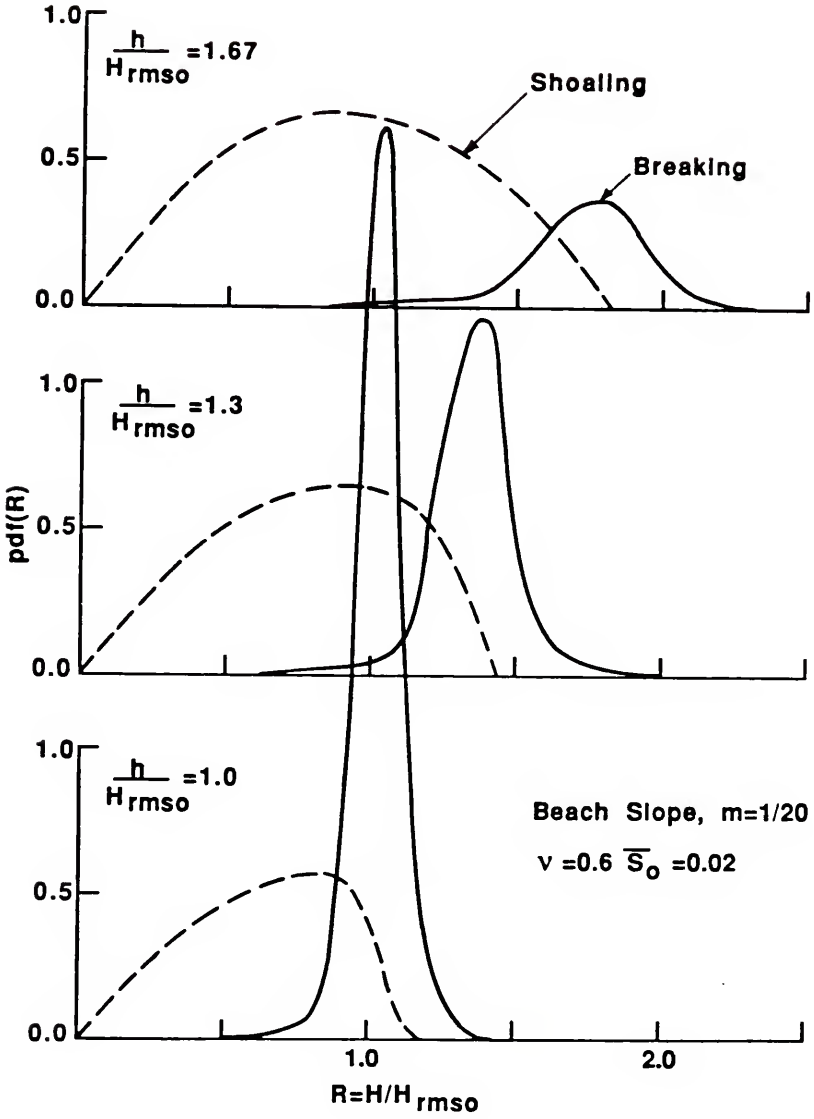

Figure 4.7 Transformation of the marginal pdf of wave height across the surf zone according to closed-form solution #2 (4.27) and (4.52). Beach slope, m = 1/20.

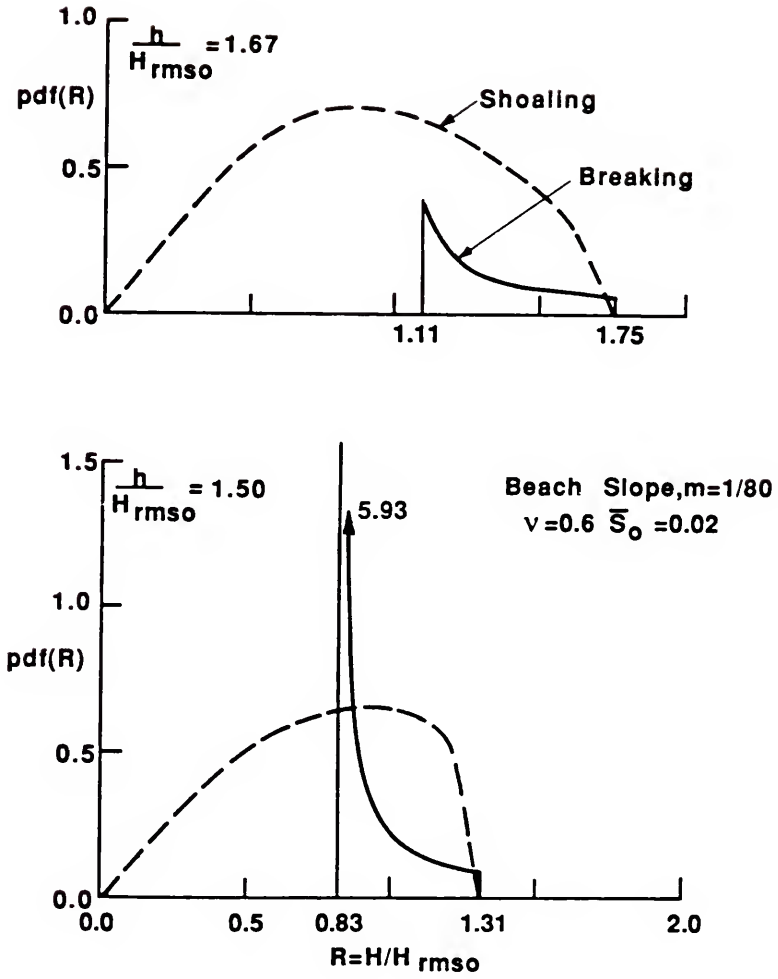

Figure 4.8 Transformation of the marginal pdf of wave height across the surf zone according to closed-form solution #2 (4.27) and (4.52). Beach slope, m = 1/80.

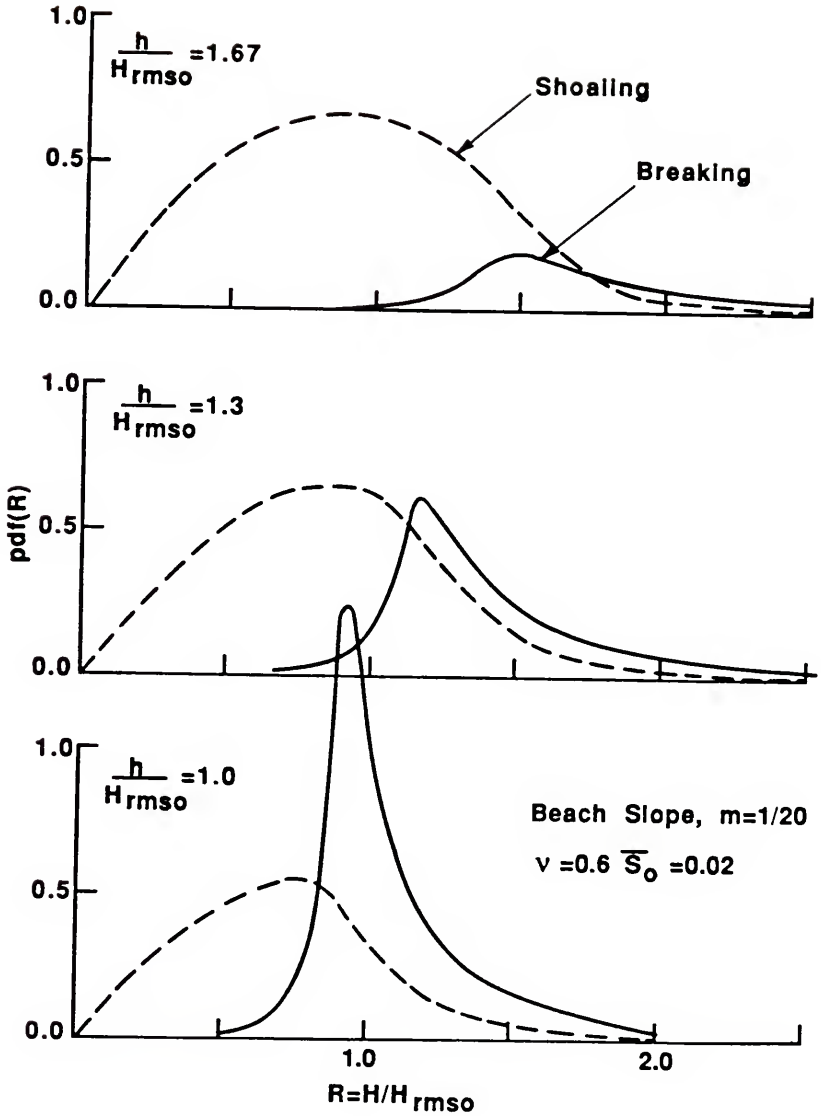

Figure 4.9 Transformation of the marginal pdf of wave height across the surf zone according to closed-form solution #2 (4.27) and (4.52). Beach slope, m = 1/20. Incipient criterion of Singamsetti and Wind (1980) used.

CHAPTER 5

NUMERICAL SOLUTION FOR RANDOM WAVES

5.1 Introduction

Beach profiles found in nature often depart significantly from the planar form assumed in Chapter 4. The monotonic but concave-up shape of (2.12) is generally accepted as more representative of nature, but unfortunately the analytical solution (2.13) cannot be explicitly inverted for h_b and therefore a closed form solution for random waves analogous to those of Chapter 4 is unobtainable. Profiles are often non-monotonic and contain bar/trough systems where many waves will break and reform. Attaining the ability to address profiles of arbitrary shape will permit comparison of the model to available field data, which if successful will verify the conceptual basis (r.e. section 2.2.1) of all the models presented herein.

Set-up/down in the mean water level induced by the onshore gradient in radiation stress accompanying shoaling and breaking waves was also neglected in Chapter 4. In regular wave studies however, it has often been noted that set-up can significantly affect breaker decay in the inner surf zone, particularly at the still water line where there exists a surviving wave height (see Figure 1.1). It is therefore desirable to include the effects of set-up in some fashion in the random wave model. To accomplish this and to treat profiles of arbitrary shape, a numerical solution involving conceptually the coupling of (2.4) and (2.7) is sought.

5.2 Formulation

We again start with the joint probability density function of wave height and period in deep water given by (4.16) and discretize it into a joint histogram of N × N bins where N is an arbitrary integer. The wave height and period corresponding to the center of each bin, along with the volume of the bin, identify a representative wave and its associated probability. Invoking the assumption that each representative wave transforms independently and wave-wave interactions can be neglected, the finite difference solution to the regular wave model, described in 2.2.3, is used to shoal, dictate incipient breaking, break, reform, etc. each representative wave across the nearshore region and surf zone. With the heights of the N × N waves in any depth determined and the probability weights retained, histograms of wave height are easily constructed. By ordering the transformed waves at a location from largest to smallest, and averaging over a desired range, statistically representative waves such as $H_{1/3}$ and $H_{1/10}$ can be computed and their transformation across the surf zone monitored. In the algorithm the ordering is accomplished by using a fast "heap" sorting routine given by Williams (1964).

Because the incident waves are random, the mean water level that an individual wave encounters is not simply given by the regular wave model run for that particular wave. The mean water level for random waves is in fact dynamic due to the presence of surf beat generated by groupy waves, and complete treatment of this aspect of the problem is outside the scope of interest at this stage of development and is deferred until Chapter 7. Instead the set-up in the mean mean-water level, i.e., the time average of the free surface over the period of the surf beat, is

approximated by the set-up calculated using the regular wave numerical model with H_{rmso} and $\overline{T}$ as input conditions. It would perhaps be more appealing to calculate the mean mean-water level using the calculated value of local H_{rms} in the set-up equation (2.7) and iterating with wave decay to converge on a value for the water level. This is much like the procedure used in the regular wave model, and has been utilized in other investigations of random waves (Battjes and Janssen, 1978; or Mase and Iwagaki, 1982). However, this greatly increases run time of the model and does not significantly change the results for wave decay from those found using the first method.

The information required to run the model consists of 1) root mean square wave height and band width parameter as the deepwater initial condition, or a joint histogram of wave height and period at a known water depth, and 2) the bottom profile. If the spectrum is not available for calculating the moments required to determine the band width parameter (4.16e), a value of $\nu = 0.3$ is used for gentle swell conditions and $\nu = 0.6$ for "confused" or storm conditions. A flow chart of the random wave model is shown in Figure 5.1.

5.3 Verification

The random wave numerical model was tested against the field data sets of Hotta and Mizuguchi (1980, 1986). Hotta and Mizuguchi (1980) utilized the photopole technique with a series of sixty wave staffs established at 2 to 3 m intervals across the nearshore region to a point well outside the surf zone. The measured bottom profile contained a large bar/trough formation, but unfortunately the cameras documenting the trough area failed during the experiment. Nevertheless, it is still

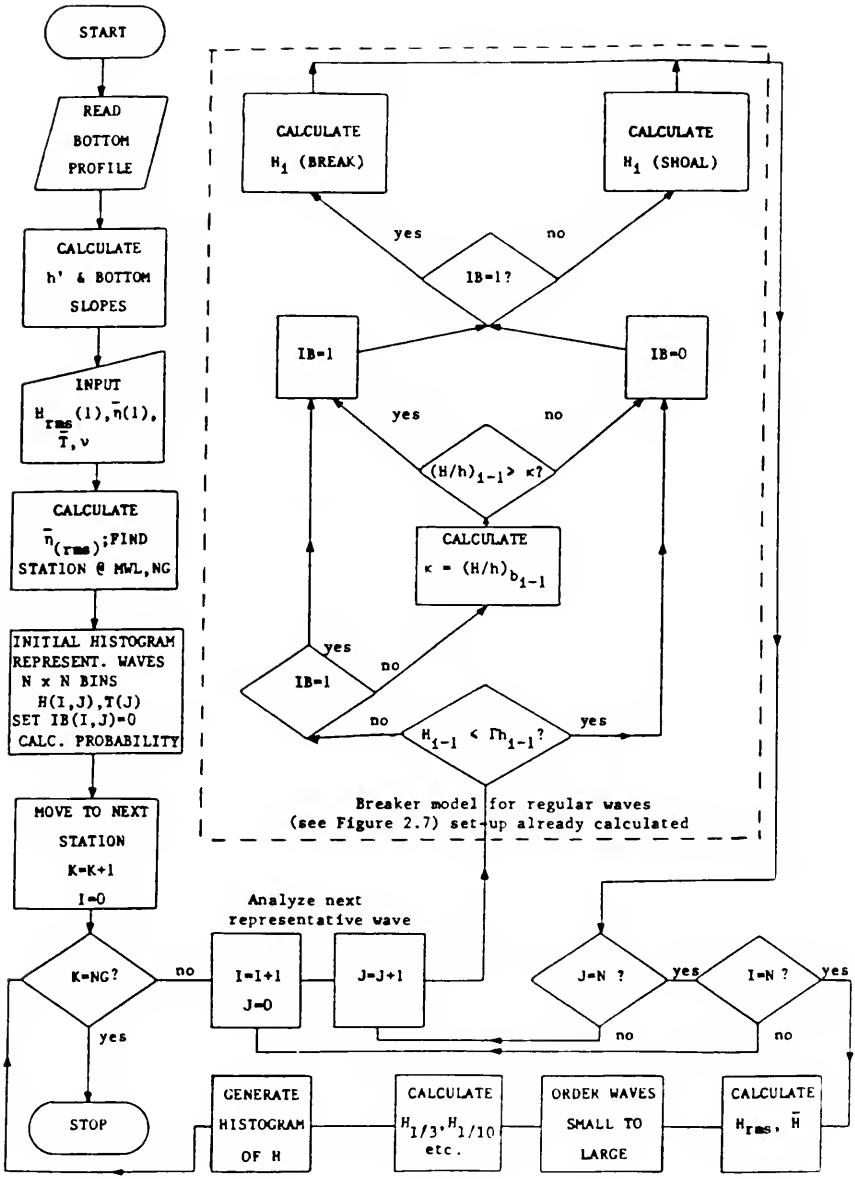

Figure 5.1 Flow chart of random wave numerical model.

an excellent data set. They retrieved the free surface time series at each pole by projecting the film and recording the instantaneous water elevation for each frame. The frames were exposed at a frequency of 5 Hz so an accurate digital representation of the waves was obtained. The raw data were then analyzed using both the zero-up-crossing and zero-down-crossing techniques to obtain wave heights and periods, from which statistically representative waves were calculated and histograms of wave height generated (shoaling and breaking combined).

The bottom profile and transformation of several statistically representative waves (H_{rms}, $H_{1/3}$, $H_{1/10}$) are displayed in Figure 5.2. The model-predicted results generated using the values for the empirical coefficients as found in the laboratory calibration of the regular wave model ($K = 0.15$, $\Gamma = 0.40$) are also shown. The agreement is quite satisfactory, except for $H_{1/10}$ and perhaps $H_{1/3}$ in the region just seaward of the surf zone. This discrepancy is because linear theory underpredicts the rate of shoaling in shallow water, especially for waves of low deepwater steepness.

Figure 5.3 displays comparison of the transformation of the histogram of wave height (up and down-crossing results have been averaged) with results of the model. Wave height has been nondimensionalized by the local average wave height, $\overline{H}$. Note that the Rayleigh distribution represents the actual initial histogram fairly well (station 57) but would not compare well at stations in the inner surf zone. The basic shape of the predicted pdf appears correct, especially for $(H/\overline{H}) > 1.0$. However, in the inner surf zone the model overpredicts the number of waves near $H/\overline{H} = 1.0$ and underpredicts for $H/\overline{H} < 1.0$.

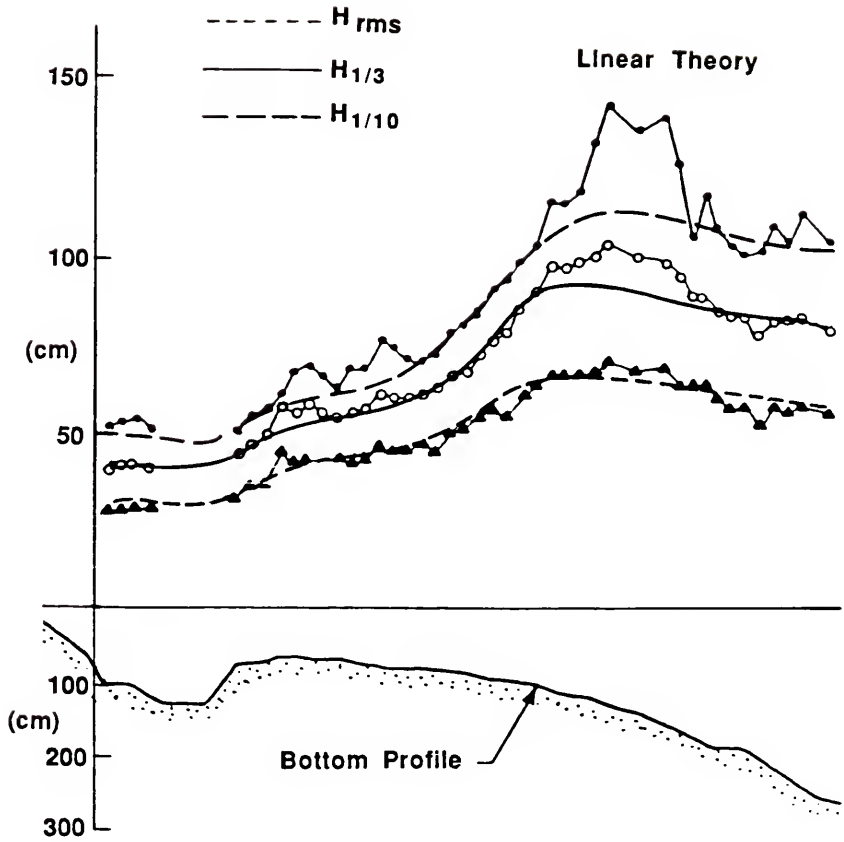

Figure 5.2 Comparison of model, using linear wave theory, to field data of Hotta and Mizuguchi (1980) for transformation of statistically representative waves.

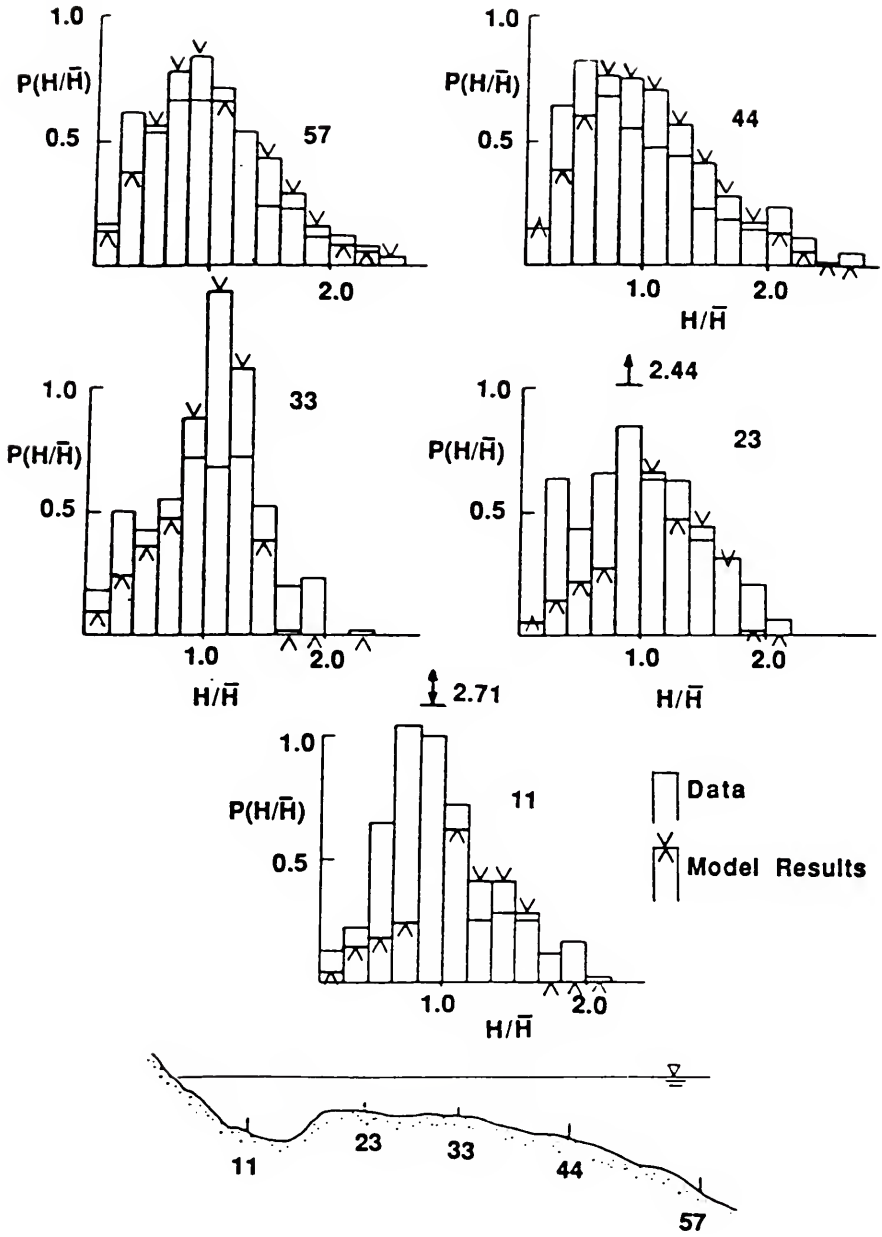

Figure 5.3 Comparison of model, using linear wave theory, to field data of Hotta and Mizuguchi (1980) for transformation of histogram of wave height.

Even though a gap in the data in the trough region prevents verification of the wave reformation aspects of the model, the favorable comparison landward of this section lends support to the stable wave assumption in the original formulation (2.4). It is noted that the random wave model predicted that the majority of the waves reformed in the trough, consistent with visual observations made during the experiment.

To investigate the effects of nonlinear shoaling on the transformation of statistically representative waves, Cnoidal wave theory is applied using the results and recommendations of Svendsen and Buhr Hansen (1977). Because Cnoidal theory is valid only in shallower water, linear theory is applied to shoal each wave until the relative depth, h/L_o equals 0.1. Shoaling then continues by using a table generated by Svendsen and Hansen which provides values of H/H_o given h/L_o and H_o/L_o, and a simple linear interpolation scheme to determine intermediate values. Incipient breaking and wave decay calculations proceed as before.

Results of the "Cnoidal model" in comparison to the data of Hotta and Mizuguchi (1980) for statistically representative waves H_{rms}, $H_{1/3}$, and $H_{1/10}$ are displayed in Figure 5.4. They show significantly improved agreement in the shoaling region while retaining the already favorable comparison over most of the breaking region. However, just before the trough region the model predictions begin to show more decay than was observed. This is because when using Cnoidal theory to shoal the waves they reach incipient breaking sooner than with linear theory, and as a result have undergone more breaking before reaching the bar crest. This is especially true for waves in the original histogram that are of low

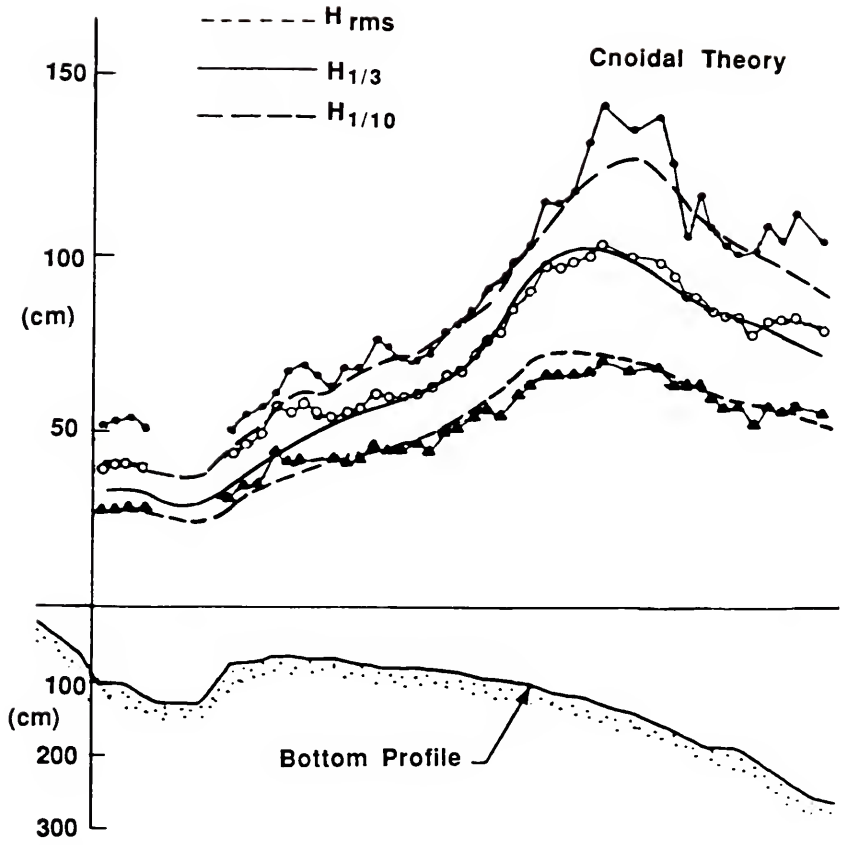

Figure 5.4 Comparison of model, using Cnoidal wave theory for shoaling, to field data of Hotta and Mizuguchi (1980) for transformation of statistically representative waves.

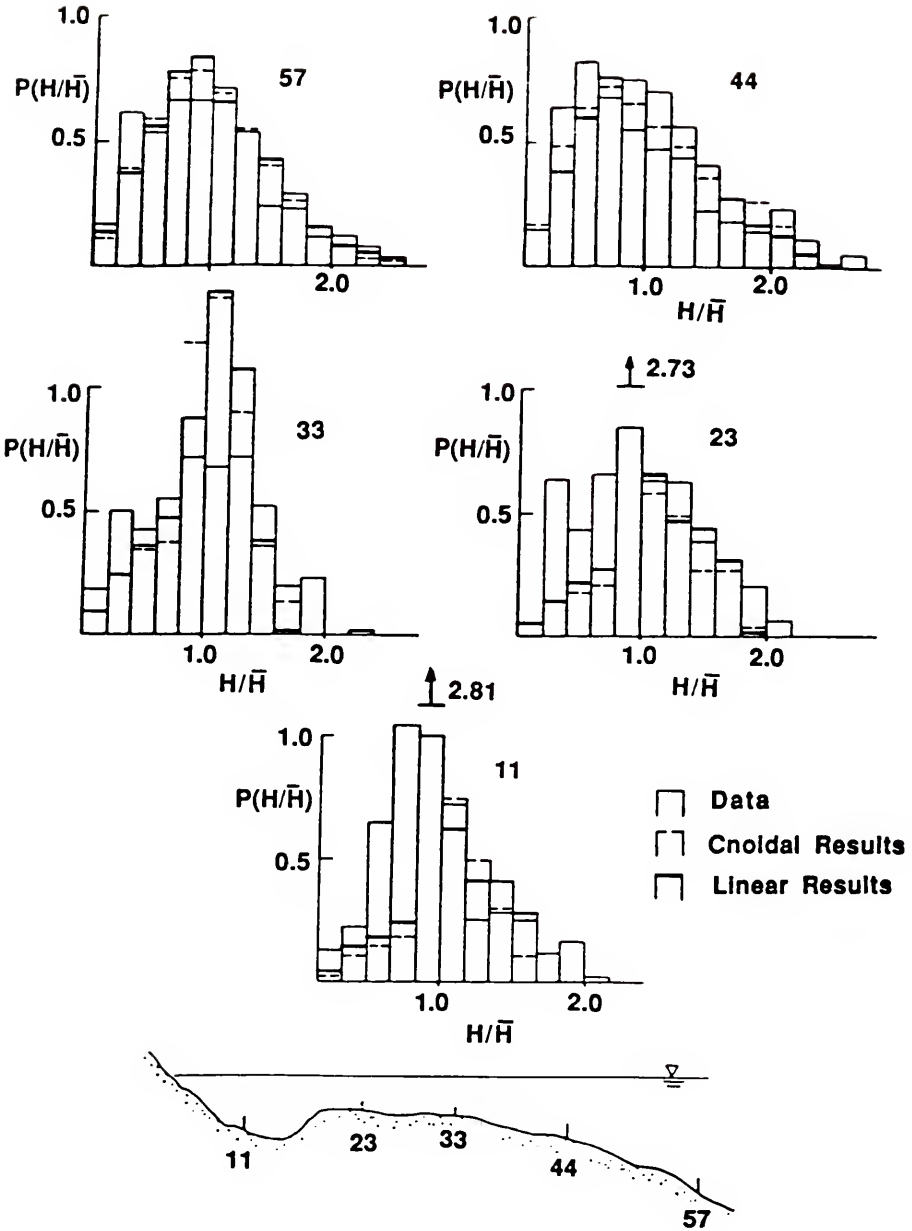

Figure 5.5 Comparison of model-predicted histogram transformation, using linear and Cnoidal theory for shoaling, to field data of Hotta and Mizuguchi (1980).

deepwater steepness. Histograms of wave height are shown in Figure 5.5 and show little change from the linear results.

Comparisons of the linear and Cnoidal models to four more photopole data sets reported in Hotta and Mizuguchi (1986) are shown in Figures 5.6, 5.7, 5.8 and 5.9. The measured bottom profile contains two bar/trough formations and poses a rigorous test for the models. The tests were conducted over a period of two days so some variability in the bottom profile might be expected. Different tide stages during each test were responsible for the 40 cm range in still water level. Although only significant wave period $T_{1/3}$ was provided by Hotta and Mizuguchi (1986), Hotta and Mizuguchi (1980) found an almost constant ratio of $T_{1/3}/\overline{T} = 1.3$ and this relationship was used to calculate average wave period for each test. The average period and significant height at the outermost station was 6.9 s and 65 cm, 6.4 s and 77 cm, 5.8 s and 80 cm, and 5.4 s and 83 cm for each experiment respectively. Because H_{rms} is required to start the models but was not provided, values were chosen that produced an $H_{1/3}$ that roughly matched the data at the outermost station. With these initial conditions the models were run with $K = 0.15$ and $\Gamma = 0.4$.

In general, the models faithfully represent the observations, and in several regions display good quantitative agreement. The model with shoaling by linear theory follows the trend of the data in all cases, but as expected underpredicts the amount of shoaling on the outer bar. In fact in Figure 5.6, almost no waves broke on the outer bar using the linear model. As with Hotta and Mizuguchi (1980), Cnoidal theory improves the agreement to a remarkable degree in the outer shoaling and breaking regions. The only significant problem with both models is that

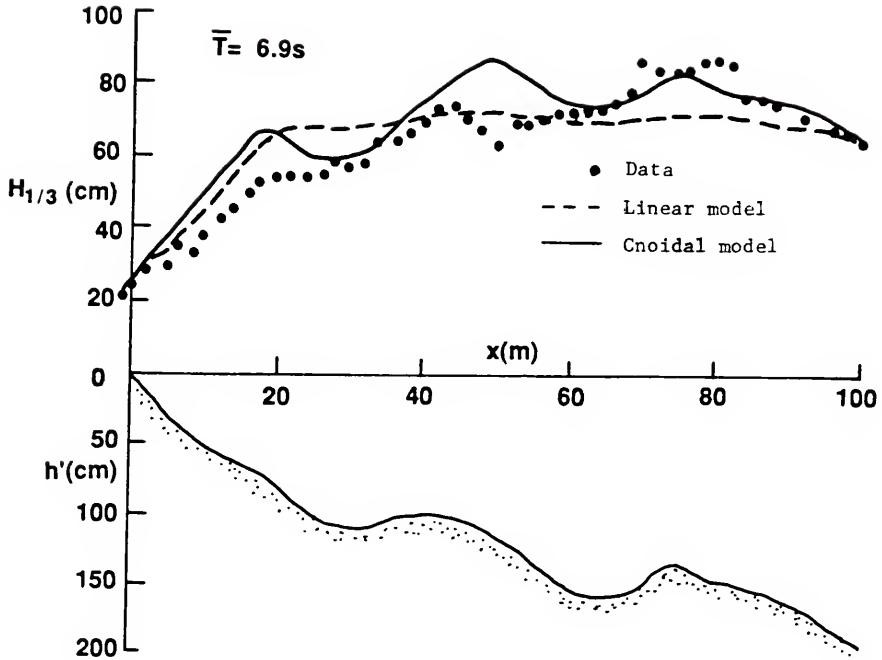

Figure 5.6 Comparison of linear and Cnoidal models to field data of Hotta and Mizuguchi (1986) for transformation of significant wave height. High tide conditions, $\bar{T}$ = 6.9 s.

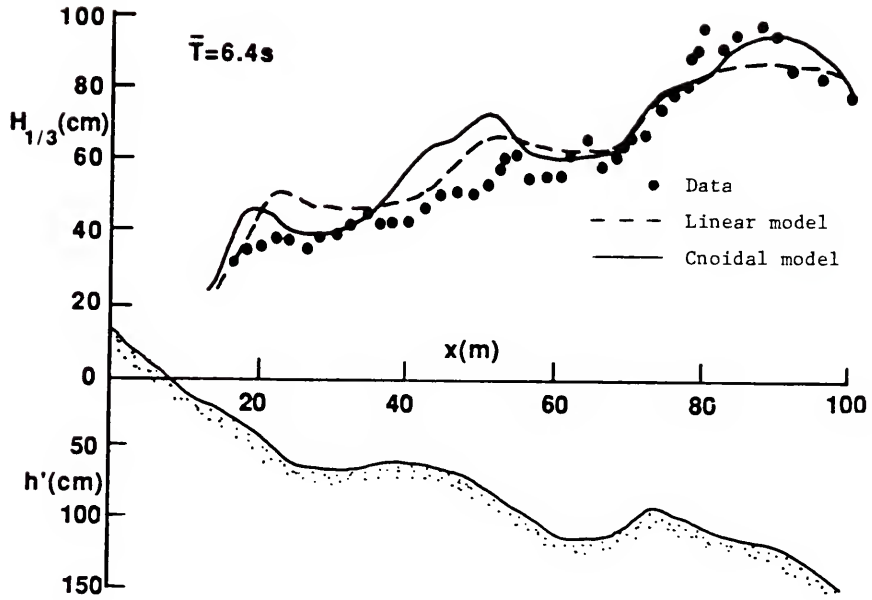

Figure 5.7 Comparison of linear and Cnoidal models to field data of Hotta and Mizuguchi (1986) for transformation of significant wave height. Low tide conditions, $\bar{T}$ = 6.4 s.

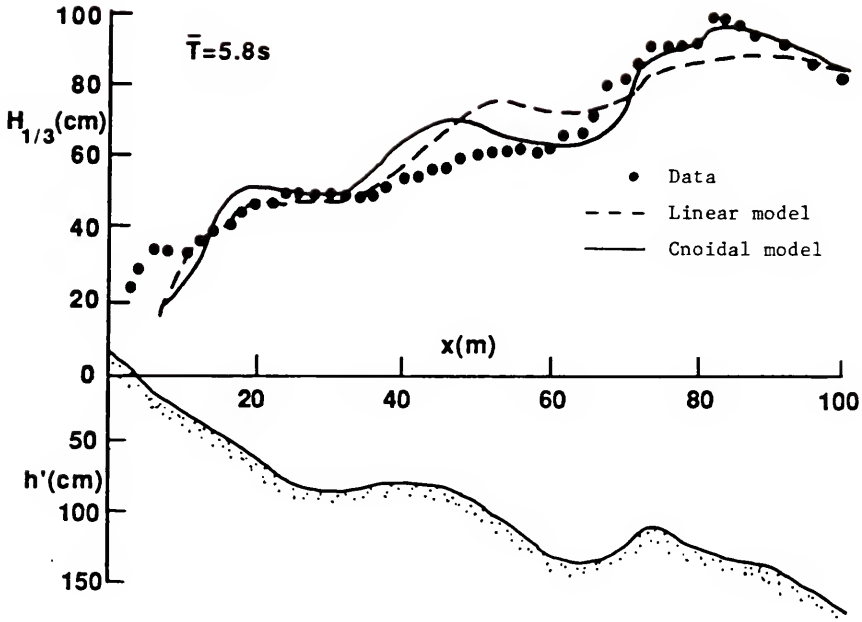

Figure 5.8 Comparison of linear and Cnoidal models to field data of Hotta and Mizuguchi (1986) for transformation of significant wave height. Mid-tide conditions, $\bar{T}$ = 5.8 s.

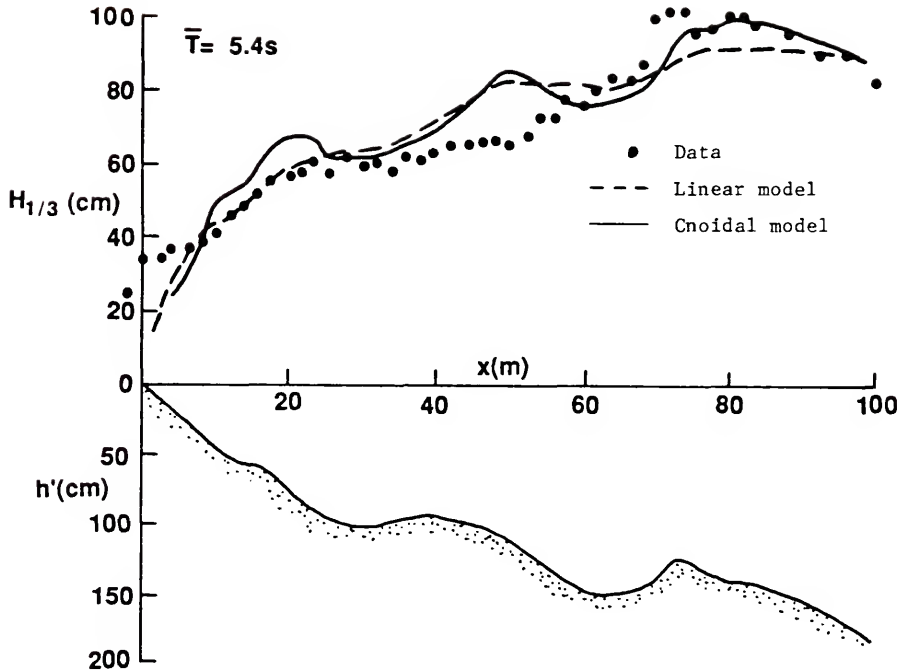

Figure 5.9 Comparison of linear and Cnoidal models to field data of Hotta and Mizuguchi (1986) for transformation of significant wave height. High tide conditions, $\bar{T}$ = 5.4 s.

they appear to allow too many waves to reform, especially in the outer trough. This results in strong shoaling on the inner bar and again in the inner surf zone. Only in Figure 5.6 and 5.7 was there observed evidence of wave reformation and a subsequent increase in $H_{1/3}$ due to shoaling.

CHAPTER 6

REGULAR WAVES BREAKING ON STEADY CURRENTS

6.1 Introduction and Literature Review

One of the major goals of this study is to investigate the effects of long waves such as surf beat on wind-wave transformation in the surf zone. Because the surf beat period is an order of magnitude longer, and the height and order of magnitude smaller than the short waves that drive it (Lo, 1981; Guza and Thornton, 1985), it is hypothesized that its effect on short waves can be closely represented as that of a slowly ocsillating current and mean water level. The effect of a slowly changing water level (depth) on shoaling and breaking is of course the essence of the investigation up to this point, as well as all previous studies. However, the effect of currents on the transformation of breaking waves has received very little attention in the literature. To simplify the problem, the effect of a steady, collinear current on the breaking of regular waves is first examined in this chapter, with these results applied to surf beat in the next chapter.

The earliest study of breaking waves on steady currents appears to have been by Yu (1952) who performed a theoretical and laboratory investigation of the surviving wave height after a wave encounters and breaks on an opposing current. Conditions were limited to deep water where it was found that complete breaking, i.e., reducing the wave height to zero, took place when the opposing current was 1/4 the wave celerity in still water. Partial breaking took place when the current

was between 1/7 and 1/4 the still water celerity. Unfortunately only the reformed wave height was measured, and the process of wave decay up to that point was not addressed.

Dalrymple and Dean (1975) using Stream Function Theory also studied the limiting height of (nonlinear) waves on steady, uniform currents, and found that in deep water the arresting current could be as strong as 0.3 times the still-water celerity. Limiting heights for milder currents were related to those of the stream function tables without currents (see Dean, 1974). It was found that in shallow water the current had little effect on the maximum height a given water depth can sustain, that is $H/h \sim 0.78$ regardless of current strength. Again the process of wave breaking on a (non-uniform) steady current which, as the forthcoming laboratory observations will show is clearly dependent on current strength, was not addressed.

The only study appearing in the literature to date which relates directly to the present investigation is that of Sakai and Saeki (1984). They collected laboratory measurements of wave transformation due to shoaling and breaking on planar slopes with steady opposing currents, and found that the shoaling behavior was governed by the deepwater steepness H_o/L_o (in still water) and the per-unit-width discharge q rendered non-dimensional by the ratio of wave period to the square of the deepwater wave length, T/L_o^2; see Figure 1.3. A fourth order Stokes' solution for waves on currents was presented but only one direct comparison to data was displayed. Although it appeared to represent the shoaling portion of the transformation faithfully in this single case, plots of the "limits of applicability" showed generally only a narrow range of (h/L) where the theory predicted within ±5%, with this range

becoming increasingly narrow with increasing current strength. Increasing discharge moves the incipient break point offshore and decreases steepness at incipient breaking, $(H/L)_b$. This followed the Miche criterion for small currents in shallow water, but drops below it significantly for values of $(h/L)_b > 0.08$ and high discharge rates. The present author compared the deepwater results of Yu (1952) to the Miche criterion and also found the measured limiting heights well below it.

For breaking, Sakai and Saeki (1984) conclude that the shape of the decay profile depends mostly on the slope of the sea bed and to a small extent on the incipient condition, which agrees with regular wave studies without currents. However, the authors did not attempt to model the decay process after breaking is initiated.

6.2 Governing Equations

6.2.1 Kinematical Conservation

The expression which governs the response of the wave number vector $\vec{k}$ of small amplitude waves to a current is the Kinematical Conservation equation which is

$$\frac{\partial \vec{k}}{\partial t} + \vec{\nabla}(\sigma + \vec{k} \cdot \vec{U}) = 0 \qquad (6.1)$$

in which $\vec{U}$ is the current vector which is arbitrary in direction and can be non-steady and non-uniform (see Phillips, 1977). The intrinsic frequency σ is the wave frequency an observer sees when moving with the current and is assumed to be given by the dispersion relation for linear wave theory

$$\sigma = (gk \tanh kh)^{1/2} \tag{6.2}$$

where k is the magnitude of $\vec{k}$. $\vec{\nabla}$ is the horizontal spatial gradient vector operator. Restricting our attention to collinear currents and waves, and inserting (6.2) into (6.1) yields

$$\frac{\partial k}{\partial t} + \frac{\partial}{\partial x}\left[(gk \tanh kh)^{1/2} + kU\right] = 0 \tag{6.3}$$

which is a first order, quasi-linear, hyperbolic partial differential equation. If the waves are regular and the current is steady (6.3) reduces to

$$(gk \tanh kh)^{1/2} + kU = \omega \tag{6.4}$$

where ω is the absolute frequency and is constant, i.e., it is the wave frequency in the absence of a current. This dispersion relation is of course transcendental, and "exact" solutions must be found iteratively. However, following the procedure used by Nielsen (1984) for dispersion without currents, an approximate series solution can be derived. As shown in Appendix A, this solution is

$$kh \simeq \frac{\sqrt{k_o h}}{\hat{U}}\left\{1 + \frac{1}{6\hat{U}^3}(k_o h) + \left[\frac{1/9 - 1/15\,\hat{U} + 1/72(\hat{U} - 2)}{\hat{U}^6}\right](k_o h)^2\right\} \tag{6.5}$$

where $\hat{U}$ is the dimensionless relative current

$$\hat{U} = \left(1 + \frac{U}{\sqrt{gh}}\right) \tag{6.6}$$

This expression is exact in shallow water and according to Nielsen is better than 0.5% accurate out to $(k_o h)/\hat{U}^3 \approx 2.51$. With the effect of a steady, non-uniform collinear current on wave length so determined, the effect on wave height is now explored.

6.2.2 Conservation of Wave Action

As derived by Bretherton and Garrett (1969) and discussed also in Phillips (1977), the equation governing the change in planform energy density E for waves on a current with no energy dissipation is given by

$$\frac{\partial(E/\sigma)}{\partial t} + \vec{\nabla} \cdot \left[(\vec{U} + \vec{C}g)\,\frac{E}{\sigma}\right] = 0 \qquad (6.7)$$

and is called Conservation of Wave Action, wave action being E/σ and Cg the group celerity. This equation is a first order, hyperbolic partial differential equation and is linear if the group velocity is not dependent on energy density (i.e., no amplitude dispersion). By examining the Lagrange Systems for (6.1) and (6.7), it can be shown that the phase plane trajectories of k and E/σ coincide at all relative depths. The coupled system of (6.1) and (6.7) is parabolic so there is only one characteristic. If the complete temporal and spatial description of the current and bottom topography is available, the change in wave number and energy density could be tracked through time and space using numerical techniques.

Rendering (6.7) steady and collinear yields

$$\frac{\partial}{\partial x}\left[(U + Cg)\,\frac{E}{\sigma}\right] = 0 \qquad (6.8)$$

and with a known dispersion relation for the intrinsic frequency, e.g. (6.2), the energy density for a given local current magnitude and given reference conditions can be determined. Until now, no energy dissipation has been included. Because (6.4) indicates that k or σ is not dependent on energy density, the dissipation of wave action is directly proportional to the dissipation of energy density. For steady non-uniform currents and regular waves this means

$$\frac{\partial}{\partial x}\left[(U + Cg)\frac{E}{\sigma}\right] = \frac{-\delta(x)}{\sigma} \tag{6.9}$$

where $\delta(x)$ is again the rate of energy dissipation per unit planform area, for which an expression is formulated in the next section.

6.2.3 Proposed Governing Equation for Regular Waves Breaking on Steady Currents

Returning to the idealized shelf beach bottom profile described in chapter 2, a constant discharge of water is introduced which could be either opposing or assisting waves incident from deep water. The current associated with this discharge is assumed to be uniform with depth, and due to the bottom configuration, is assumed spatially uniform in the horizontal section and dies off as 1/h in the sloping portion as shown in Figure 6.1. For the moment, an opposing current is adopted and incident conditions are such that the wave shoals on the current and sloping bottom and again attains incipient breaking where the beach becomes horizontal. The wave then breaks for some distance and eventually reforms. Applying (6.9) to the horizontal section and adopting a reference frame that moves with the speed of energy propagation, i.e., the actual group velocity (U + Cg),

$$x = (U + Cg)t \tag{6.10}$$

$$\frac{\partial}{\partial x} = \frac{\partial t}{\partial x}\frac{\partial}{\partial t} = \frac{1}{U + Cg}\frac{\partial}{\partial t} \tag{6.11}$$

and (6.9) becomes

$$\frac{\partial(E/\sigma)}{\partial t} + \frac{E}{\sigma}\frac{1}{U + Cg}\frac{\partial(U + Cg)}{\partial t} = \frac{-\delta(t)}{\sigma} \tag{6.12}$$

and in the horizontal section reduces to

$$\frac{\partial E}{\partial t} = -\delta(t) \tag{6.13}$$

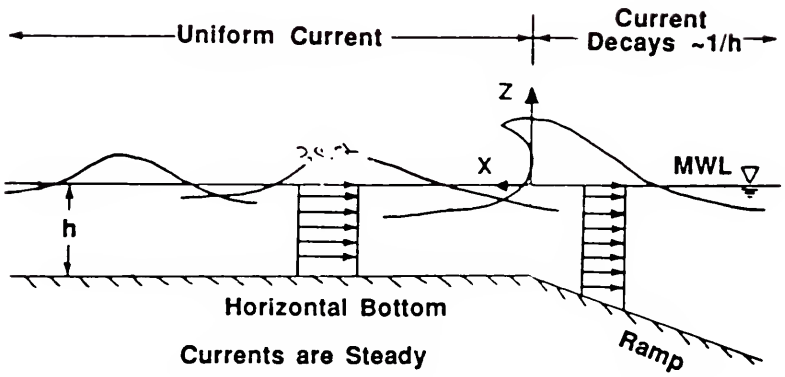

Figure 6.1 Concepts of model of regular waves breaking on a shelf beach with collinear currents.

It is now hypothesized that the rate of energy dissipation $\delta(t)$ observed when moving at the actual group velocity is independent of the strength or direction of the collinear current. To reiterate, as long as one moves with the speed of energy propagation of the breaking waves, the same rate of decay in wave height is observed. For no current $\delta(t)$ is already "known" and given by (2.2) after making the transformation from x to t. Since $\delta(t)$ is the same regardless of current strength it is finally concluded that (2.2) can be utilized directly in (6.9) and the governing equation for regular waves breaking on a collinear, steady, non-uniform current is therefore

$$\frac{\partial}{\partial x}\left[(U + Cg)\,\frac{E}{\sigma}\right] = \frac{-K}{\sigma h}\left[ECg - ECg_s\right] \tag{6.14}$$

Linear wave theory is adopted and if the stable wave height is depth-limited as before, (6.14) becomes

$$\frac{\partial}{\partial x}\left[\frac{(U + Cg)}{\sigma}\,H^2\right] = \frac{-K}{h}\,\frac{Cg}{\sigma}\,\left[H^2 - \Gamma^2\,h^2\right] \tag{6.15}$$

where it is hoped the previous calibration of the decay coefficient K and the stable wave factor Γ still applies, at least in shallow water. As noted, Dalrymple and Dean (1975) found theoretically that the maximum wave height in shallow water was depth-limited and independent of current strength; and, as indicated by the results of the laboratory experiment described in section 6.5, the previous stable wave assumption appears valid for cases where breaking was fully developed. The decay coefficient also seems to remain unchanged.

6.3 Analytical Solution for Uniform Depth

For the bottom configuration of Figure 6.1, a closed form expression can be derived for waves that attain incipient breaking in or very close to the section of uniform depth. Rewriting (6.15) yields

$$\frac{\partial}{\partial x}\left[\frac{(U + Cg)}{\sigma} H^2\right] + \frac{K\ Cg}{h(U + Cg)}\left[\frac{(U + Cg)}{\sigma} H^2\right] = \frac{K\ \Gamma^2\ h^2\ Cg}{h\ \sigma} \tag{6.16}$$

The general solution to the first order ordinary differential equation

$$G'(x) + P(x)\ G(x) = Q(x) \tag{6.17}$$

is

$$G = \exp(-\int P dx)\ \left[\int Q\ \exp(\int P dx)\ dx + F\right] \tag{6.18}$$

where F is a constant and it is observed that for (6.16)

$$G = \frac{(U + Cg)}{\sigma} H^2 \tag{6.19a}$$

$$P = \frac{K}{h}\ \frac{Cg}{(U + Cg)} \tag{6.19b}$$

$$Q = \frac{K\ \Gamma^2\ h^2\ Cg}{h\ \sigma} \tag{6.19c}$$

A bottom of uniform depth is now adopted so that U, Cg, and h are not functions of x. Inserting (6.19) into (6.18) and performing the integrations produces

$$\frac{(U + Cg)}{\sigma} H^2 = \exp -\left[\frac{K}{h}\ \frac{Cg}{(U + Cg)}\ x\right]$$

$$\left\{\Gamma^2\ h^2\ \frac{(U + Cg)}{\sigma}\ \exp\left[\frac{K}{h}\ \frac{Cg}{(U + Cg)}\ x\right] + F\right\} \tag{6.20}$$

Applying the boundary condition

$$H = H_b = \gamma h \qquad @\ x = 0 \tag{6.21}$$

the integration constant is determined

$$F = \frac{(U + Cg)}{\sigma} [H_b^2 - \Gamma^2 h^2] \tag{6.22}$$

and (6.20) becomes

$$\frac{H}{h} = \left\{[\gamma^2 - \Gamma^2] \exp -[\frac{K}{h} \frac{Cg}{(U + Cg)} x] + \Gamma^2\right\}^{1/2} \tag{6.23}$$

If U = 0, this expression reduces to the original analytical solution for uniform depth (2.8) as should be expected. Invoking the transformation from x to t via (6.10), (6.23) becomes

$$\frac{H}{h} = \left[(\gamma^2 - \Gamma^2) \exp(-K \hat{t}) + \Gamma^2\right]^{1/2} \tag{6.24a}$$

where $\hat{t}$ is dimensionless time

$$\hat{t} = \frac{Cg}{h} t \tag{6.24b}$$

With K and Γ known and fixed, it is noted that the decay in height observed when moving with the actual group velocity (U + Cg) is only a function of $\hat{t}$ and incipient condition γ.

If it is assumed that discharge is uniform across a beach profile so that the current magnitude is determined simply by dividing by the local water depth (as was assumed by Sakai and Saeki, 1984), or other

such contrived current distributions adopted, additional closed form solutions for other idealized bottom topographies (e.g., planar and $Ax^{2/3}$ shapes) are possible but difficult because U, Cg, and h are now functions of x and the integrations in (6.18) might not be realizable. A more useful approach for natural beaches is to solve (6.15) numerically.

6.4 Numerical Solution for Arbitrary Currents and Bottom Profiles

With an arbitrary but known collinear current distribution and bottom profile, (6.15) can be solved numerically with relative ease. For convenience the governing equation is restated

$$\frac{\partial}{\partial x}\left[\frac{(U + Cg)}{\sigma} H^2\right] = \frac{-K}{h} \frac{Cg}{\sigma}[H^2 - \Gamma^2 h^2] \tag{6.15}$$

Using a central finite difference on the left hand side and central averages for those quantities on the right (6.15) becomes

$$\frac{\left(\frac{(U + Cg)}{\sigma}\right)_{I+1} H^2_{I+1} - \left(\frac{(U + Cg)}{\sigma}\right)_{I} H^2_I}{\Delta x} =$$

$$- K \frac{\left(\frac{Cg}{h\sigma}\right)_{I+1} + \left(\frac{Cg}{h\sigma}\right)_{I}}{2} \left[\frac{H^2_{I+1} + H^2_I}{2} - \Gamma^2 \frac{h^2_{I+1} + h^2_I}{2}\right] \tag{6.25}$$

Collecting the unknown H_{I+1} to one side yields

$$H^2_{I+1} = \frac{H^2_I\left\{\left(\frac{U + Cg}{\sigma}\right)_I - \frac{K\Delta x}{4}\left[\left(\frac{Cg}{h\sigma}\right)_{I+1} + \left(\frac{Cg}{h\sigma}\right)_I\right]\right\} + \frac{K\Delta x}{4}\Gamma^2 (h^2_{I+1} + h^2_I)}{\left\{\left(\frac{U + Cg}{\sigma}\right)_{I+1} + \frac{K\Delta x}{4}\left[\left(\frac{Cg}{h\sigma}\right)_{I+1} + \left(\frac{Cg}{h\sigma}\right)_I\right]\right\}} \tag{6.26}$$

In many cases to be examined the intrinsic group velocity can be assumed to be given by shallow water approximations. However, in the event an opposing current is strong enough to shorten the wave length and place the wave in transitional water, the complete expression for Cg, i.e., (2.15) is used. In Appendix B, this numerical solution was applied to produce results for comparisons to data from the laboratory test reviewed in the next section.

6.5 Verification to Laboratory Data

6.5.1 Overview of Experiment

A series of tests was conducted in the "tilting flume" of the University of Florida Coastal and Oceanographic Engineering Laboratory. This flume is 15.5 m long, 0.6 m wide, and 0.9 m high with one wall constructed of glass panels. It is equipped with a piston type mechanical wave maker used to generate regular waves in the frequency range 0.3 to 1.0 Hz. A shelf beach as shown in Figure 6.1 and a special apparatus for generating opposing currents was designed and constructed by the author, and is fully described in Appendix B. Waves generated in still water would propagate down the tank, encounter the sloping bottom and opposing currents, shoal, break and finally reform somewhere in the horizontal section. Because the apparatus was designed so that the waves could be generated in still water, the effect of varying current strength could be observed directly. Nineteen tests were conducted with various combinations of incident wave conditions, water levels, and current magnitudes. Test conditions are summarized in Table 6.1. Current magnitude is calculated by dividing the measured discharge of

the pump by the nominal cross-sectional area of the flow. Group velocity is calculated using linear wave theory and the expansion solution to the dispersion relation with currents (6.5) and the local measured mean water level. Procedure and measurement techniques are also described in Appendix B.

TABLE 6.1 -- Test Conditions for Laboratory Experiment of Regular Breaking Waves on Steady Opposing Currents

			Conditions in Uniform Depth Section			
Test #	Offshore Height, H(cm)	Period T(s)	Nominal Depth, h'(cm)	Current U(cm/s)	Grp Vel. Cg(cm/s)	$\sqrt{gh'}$ (cm/s)
824C	4.0	1.8	7.9	-17.7	83	88
824B	4.0	1.8	7.9	-25.5	80	88
824A	4.0	1.8	7.9	-31.4	74	88
84A	7.0	3.0	10.0	0.0	99	99
86A	7.0	3.0	10.0	-23.4	96.5	99
89A	12.8	1.8	10.0	0.0	96	99
810A	12.5	1.8	10.0	-22.6	92	99
811A	9.7	1.15	10.0	0.0	85.5	99
811B	9.5	1.15	10.0	-16.8	77	99
827A*	4.4	1.8	11.0	0.0	97	104
827B	4.7	1.8	11.3	-15.5	95	105
827C	4.8	1.8	11.3	-25.6	92.5	105
825A	5.0	1.8	12.5	-26.3	97	111
825B	5.1	1.8	12.5	-36.1	89	111
812D*	9.5	1.15	14.7	-7.9	92	120
812C	9.5	1.15	14.7	-11.9	90	120
812B	9.5	1.15	14.7	-19.8	80.5	120
811C	10.0	1.15	15.0	0.0	97	121
812A	10.5	1.15	15.0	-15.1	87	121

6.5.2 Comparison of Model to Data

Figure 6.2 displays sample results of the laboratory measurements and comparisons of the numerical solution (6.26). Wave conditions at the generator are the same for each test, but the opposing current strength increases from top to bottom. Note that by increasing the current the incipient break point is moved offshore slightly while the point where the wave reforms moves substantially, i.e., the surf zone is displaced seaward and compressed. The decay profile also becomes more concave. The model comparisons indicate that the stable wave criterion $(H/h)_s = 0.4$ is reasonable except for the uppermost case. In this

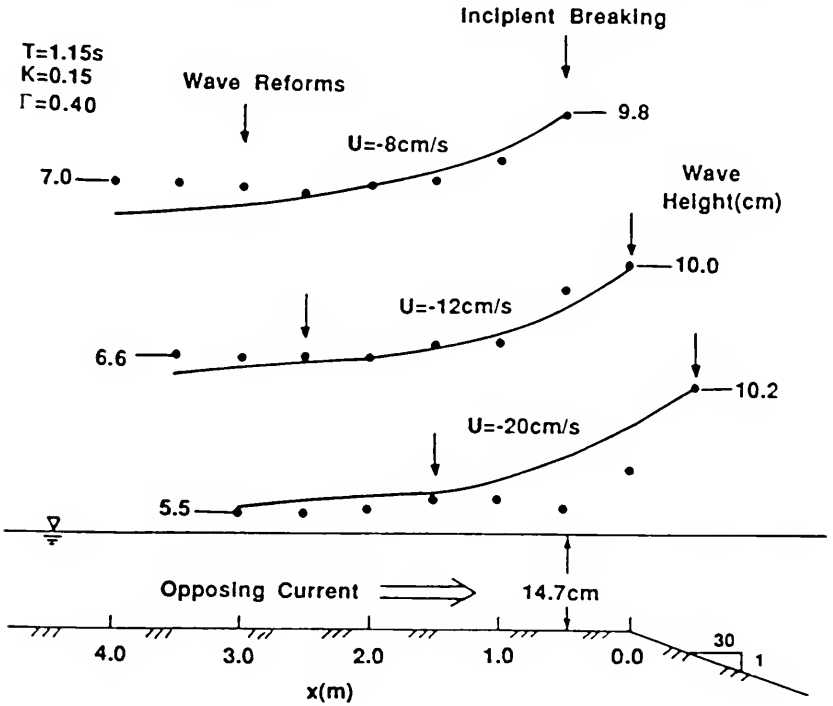

Figure 6.2 Sample of results of laboratory investigation of regular breaking waves encountering opposing currents.

instance the current was just strong enough to barely "trip" the wave, and breaking did not become fully developed. It is noted that without a current, no breaking took place at all. The decay coefficient $K = 0.15$ performs satisfactorily except in the strong current case.

Results of the six tests where incipient breaking occurred at or very close to the beginning of the horizontal section are displayed in Figure 6.3. Breaking wave height has been non-dimensionalized by the average mean water depth, and distance from the breakpoint has been converted to dimensionless elapsed time, $\hat{t}$ via (6.24b) and (6.10). Note that the dimensionless treatment has significantly collapsed the behavior of the data as desired and that the stable wave criterion $H_s = 0.4h$ appears quite valid except for the case where breaking was not fully developed, as previously discussed. Model predictions using the closed form solution (6.24) with the average γ value (0.672) and $K = 0.15$ and $\Gamma = 0.4$ are also displayed and show good agreement to the data. The results of all nineteen tests and numerical solutions of the model are displayed and discussed in Appendix B, and generally show good agreement. At this point it appears safe to conclude the model is valid, at least for shallow water conditions. The governing equation (6.15) is now applied to a stochastic model of random wave transformation on surf beat.

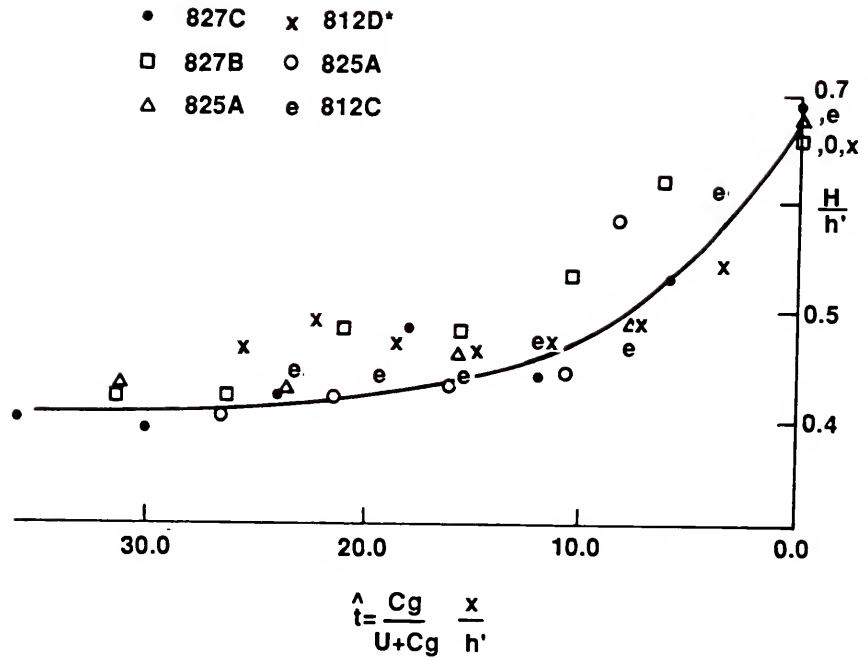

Figure 6.3 Comparison of analytical solution (6.24) to laboratory data for waves breaking on collinear currents in a uniform depth.

CHAPTER 7

SURF BEAT EFFECTS ON RANDOM WAVE TRANSFORMATION

7.1 Introduction and Literature Review

Surf beat is a long period wave, generally of small amplitude, which is driven due to groupiness displayed by the shorter wind waves. The group periods are an order of magnitude longer than that of the wind waves and in nature are in the range of 30 seconds to 3 minutes. To date, there have been two mechanisms identified for their generation, both associated with mean water level response to gradients in the radiation stress accompanying the short waves. Longuet-Higgins and Stewart (1962) describe a long wave which is "locked" and has its trough located under the high waves of the group and its crest under the small waves, and is in essence a dynamic set-down in the mean water level. They contend that this wave is released as a free wave as the short waves break upon entering the surf zone. Lo (1981) and Symonds, Huntley and Bowen (1982) describe a long wave driven by the time-varying break point associated with groupy waves and is essentially a dynamic set-up in the mean water level. Lo (1981) includes both mechanisms in a numerical model and concludes that the wave generated by the second mechanism dominates the long wave activity in the surf zone. In any event, for the purposes of this study a single component of the surf beat can be regarded as a one-dimensional, standing or partially standing long wave which obeys shallow water linear wave theory.

Although the effect of the short waves in generating the long waves has been the emphasis of these and other studies, the impact of surf beat on the shoaling and breaking of short waves has received very little attention in the literature. The two major reasons for including these effects in a stochastic transformation model are that 1) surf beat smooths the histogram of wave height and reduces the magnitude of the peak, especially in the inner surf zone, and 2) the beat has the potential to affect the behavior of statistically representative waves. Although an individual wave approaching the surf zone passes through all phases of the generally broad-banded surf beat, when the currents oppose or the water level is low, breaking can be initiated sooner and may be of greater intensity than would otherwise be expected. Extending this scenario to the behavior of many waves and all phases of the beat, this implies that on the average, energy dissipation should begin sooner than in the situation with the same wind-wave train in the absence of surf beat. That is, the "incipient break point" for statistical waves, particularly H_{rms}, should move offshore. If conditions are such that the surf beat is particularly narrow-banded, phasing of the beat with the approaching wave groups may also be important. If large waves enter the surf zone during the phase when the mean water level is depressed or the associated water particle velocities are opposing, H_{rms} can decrease more rapidly than expected. If the large waves of the group enter the surf zone during the opposite phase, H_{rms} might experience less rapid decay and $H_{1/3}$ or $H_{1/10}$ will be enhanced in the inner surf zone.

As noted, because the surf beat period is an order of magnitude longer and its height an order of magnitude smaller than the wind waves that drive it, its effects on transformation of short waves can be

represented as a slowly varying current and mean water level. However, previous investigations have addressed only the mean water level fluctuations and not the currents.

Goda (1975) assumed the mean water level followed the Gaussian distribution, with its standard deviation at a location in the nearshore, σ_h, given by the empirical expression

$$\sigma_h = \frac{0.01\ H_{so}}{\left[\frac{H_{so}}{L_{so}}\left(1 + \frac{h'}{H_{so}}\right)\right]^{1/2}} \tag{7.1}$$

where H_{so} is the deepwater significant wave height of the wind waves, h' is the local mean mean-water depth and L_{so} is the deepwater wave length corresponding to the significant period. The Gaussian distribution was then discretized into a histogram, and the transformation model run for each representative elevation of the mean water level. The behavior for each representative pdf was then averaged over the surf beat, and statistically representative waves (H_{rms}) calculated.

Mase and Iwagaki (1984) also assumed the surf beat elevation is normally distributed and its standard deviation given by (7.1) from Goda (1975). However, they established the elevation using a random number generator rather than choosing representative values. Neither Goda (1975) nor Mase and Iwagaki (1984) identify or discuss any mean effects the surf beat may have on wave transformation.

Finally, Abdelrahman and Thornton (1986) addressed some of the effects of long waves on short wave transformation in the nearshore with a two-dimensional model, and investigated the generation of edge waves and time-varying longshore currents. However, wave breaking was due to

depth limitation only ($H = \gamma h$) and the effects of the long wave currents were not included in the breaking process.

Deterministic treatment of surf beat effects on wind-wave transformation across the surf zone would require simultaneous solution of the Kinematical Conservation (6.1) and Conservation of Wave Action (6.7) equations, with the dissipation function due to breaking in shallow water with currents added to the R.H.S. of (6.7). Utilizing a numerical scheme to integrate the differential equations along a characteristic also requires complete temporal and spatial description across the nearshore of the mean water level and currents induced by the surf beat. Preliminary attempts at such a scheme found it computationally time-consuming for even the simple case of a single wind-wave riding a single standing long wave. Expanding such a scheme to random wind-waves on broad-banded surf beat would seem impracticable, and a stochastic treatment is therefore pursued.

7.2 Stochastic Representation of Surf Beat

The stochastic transformation models of Goda (1975) and Mase and Iwagaki (1984) both assume the fluctuation in mean water depth (h) due to surf beat follows the Gaussian probability density function with mean h' and standard deviation σ_h. In the present formulation, the current (U) which the wind waves encounter is also assumed to be normally distributed with zero mean and standard deviation σ_u, with the additional assumption that h and U are uncorrelated. These assumptions are supported by the following formulation.

A standing wave system is established due to a long incident wave reflecting from a beach and consists of one frequency component ω_{sb}. Adopting shallow water linear wave theory, the free surface displacement, η_{sb}, and horizontal water particle velocities, u_{sb}, are given by

$$\eta_{sb} = Af_1(x) \cos \omega_{sb} t \tag{7.2a}$$

$$u_{sb} = Af_2(x) \sin \omega_{sb} t \tag{7.2b}$$

where $f_1(x)$ and $f_2(x)$ depend on the bottom profile shape, and A is an amplitude specified at some location such as the shoreline or in deep water. Because η_{sb} and u_{sb} are 90^o out of phase in time, they are statistically uncorrelated. Expanding the model to include a distribution in specified amplitude that is Rayleigh in shape, it can be shown that η_{sb} and u_{sb} each become normally distributed and of course remain uncorrelated. Therefore, the joint probability density function of current and mean water depth which the short waves will encounter at any location in the nearshore is

$$\text{pdf}(U,h) = \frac{1}{2\pi \sigma_u \sigma_h} \exp\{ - \frac{1}{2}[(\frac{U}{\sigma_u})^2 + (\frac{h - h'}{\sigma_h})^2]\} \tag{7.3}$$

where σ_u and σ_h are the standard deviations of current and mean water level respectively, and h' is the mean mean-water level. It is assumed that σ_u, σ_h, and h' are known quantities.

7.3 Equivalent Water Depths

7.3.1 Introduction

To perhaps gain a better understanding of the effect of currents and water depth on the processes of shoaling and breaking, and to seek some indication as to the surf beat magnitude required to have a significant effect on wave transformation in the surf zone, two "equivalent depths" are defined and their behaviors in response to varying current and mean water level are investigated. The first is an equivalent depth which relates to the kinematical behavior of waves, and the second is associated with wave action.

7.3.2 Kinematical Equivalent Water Depth

The kinematical equivalent water depth, h_{ek}, is defined using the dispersion relation (6.4)

$$\omega^2 = \left[(gk \tanh kh)^{1/2} + kU\right]^2 = gk \tanh kh_{ek} \qquad (7.4)$$

In physical terms, for a wave with still water frequency ω encountering a collinear current U and with the resulting wave number k, the kinematical equivalent depth is that fictitious depth which the wave of frequency ω would have to encounter in the absence of a current in order to retain the same wave number k. Solving (7.4) for h_{ek} yields

$$h_{ek} = \frac{1}{2k} \ell n\left[\frac{1 + (k_o/k)}{1 - (k_o/k)}\right] \qquad \text{for} \qquad \frac{k_o}{k} < 1 \qquad (7.5)$$

Thus for a given actual water depth and absolute frequency, for opposing currents, $h_{ek} < h$, and for assisting currents, $h_{ek} > h$.

If surf beat can be stochastically represented by (7.3), the behavior of h_{ek} in response to surf beat can be investigated, and the standard deviations of the beat σ_u and σ_h required to have a significant kinematical effect can be identified. This is accomplished by a transformation of random variables from (U,h) to $(h_{ek},h : k_o)$ and integrating with respect to h to obtain the marginal pdf of h_{ek}. Appendix C contains the details of this transformation, whose final result is

$$\text{pdf}(\hat{h}_{ek},\hat{h} : k_o h') = \frac{k_o h' \hat{h}^{1/2} |F_1||F_2|}{2\pi \hat{\sigma}_u \hat{\sigma}_h} \cdot$$

$$\exp - \frac{1}{2}\{\frac{\hat{h}}{\hat{\sigma}_u^2}[\frac{D_o^{1/2} - (D \tanh D)^{1/2}}{D}]^2 + [\frac{(\hat{h} - 1)}{\hat{\sigma}_h}]^2\} \qquad (7.6a)$$

where

$$\hat{h}_{ek} = h_{ek}/h'$$

$$\hat{h} = h/h'$$

$$\hat{\sigma}_u = \sigma_u/\sqrt{gh'} \qquad (7.6b)$$

$$\hat{\sigma}_h = \sigma_h/h'$$

$$D_o = k_o h' \hat{h}$$

$$F_1 = \{-D[\frac{\tanh D + D \operatorname{sech}^2 D}{2(D \tanh D)^{1/2}}] + (D \tanh D)^{1/2} - D_o^{1/2}\} D^{-2} \qquad (7.6c)$$

$$D = D_o\{1 + [D_{oek}(1 + \sum_{n=1}^{6} d_n D_{oek}^n)]^{-1}\}^{1/2} \qquad (7.6d)$$

$$D_{oek} = k_o h_{ek} = k_o h' \hat{h}_{ek} \qquad (7.6e)$$

$$F_2 = \frac{D_o}{2}\{\}^{-1/2}[\{\} - 1]^2 [1 + \sum_{n=1}^{6} (n + 1) d_n D_{oek}^n] \qquad (7.6f)$$

and $\{\}$ denotes the quantity inside the braces of (7.6c), and coefficients d_n are those of Hunt's approximation (1979) given by (2.14). The marginal probability density function for $\hat{h}_{ek}$ is found by integrating (7.6) with respect to $\hat{h}$ between the physically realizable limits $0 \to \infty$. Because (7.6c) contains a simple pole at $D = 0$, the volume under the pdf is not preserved. Using Simpson's Rule, (7.6) is first integrated with respect to $\hat{h}$, then again with respect to $\hat{h}_{ek}$ to determine the volume under the pdf with which to normalize (7.6).

Figure 7.1 displays the marginal pdf($\hat{h}_{ek}$) for typical surf zone conditions T = 8.0 s and h' = 150 cm and for dimensionless standard deviations of current and water depth of 5%, 10%, and 20%. The spread of these curves indicates that a significant amount of surf beat ($\hat{\sigma} \sim 10\%$) would be required to affect the average kinematical behavior of waves for the given period and mean mean-water depth. Increasing the wave period to 18 s, i.e., $k_o h' = (0.0186)$ does not affect the variance of the pdf to a noticeable degree.

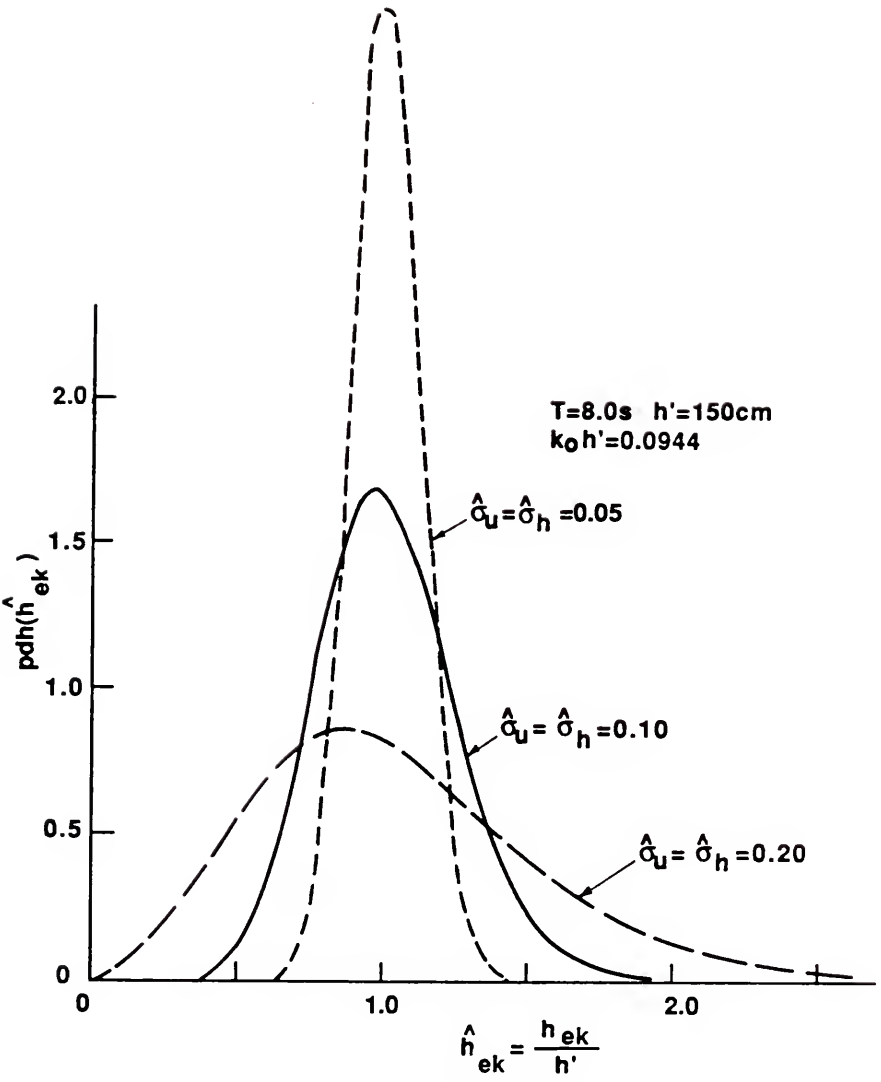

Figure 7.1 Dependence of pdf of kinematical equivalent water depth (7.6) on surf beat standard deviations.

Figure 7.2 shows the relative importance of the surf-beat-induced currents versus the mean water level fluctuations. Note that removing the currents from the problem ($\hat{\sigma}_u = 0$) narrows the pdf($\hat{h}_{ek}$) substantially and returns it to its Gaussian shape. However, retaining the currents and essentially removing the m.w.l. fluctuations ($\hat{\sigma}_h = 0.01$) does not significantly alter the pdf. In conclusion, when attempting to address surf beat effects in the kinematical behavior of waves in the surf zone, it is more important to include the associated currents than the mean water level fluctuations.

7.3.3 Wave Action Equivalent Water Depth

As indicated in chapter 6, changes in wave height are governed by gradients in the flux of wave action. The parameter ℓ_w given by

$$\ell_w = \frac{U + Cg}{\sigma} \tag{7.7}$$

is a characteristic length and is proportional to the distance an observer would move when traveling with the actual group velocity for an elapsed time of one intrinsic wave period. It is the change in this length scale over distance which governs the change in wave height due to shoaling and breaking according to (6.8) and (6.15). The equivalent water depth for wave action, h_{ew}, is defined as

$$\frac{\sqrt{gh_{ew}}}{\omega} = \frac{U + Cg}{\sigma} \tag{7.8}$$

and is the depth in which a long wave must travel for an elapsed time of one absolute period in order to move the same distance ℓ_w. The behavior

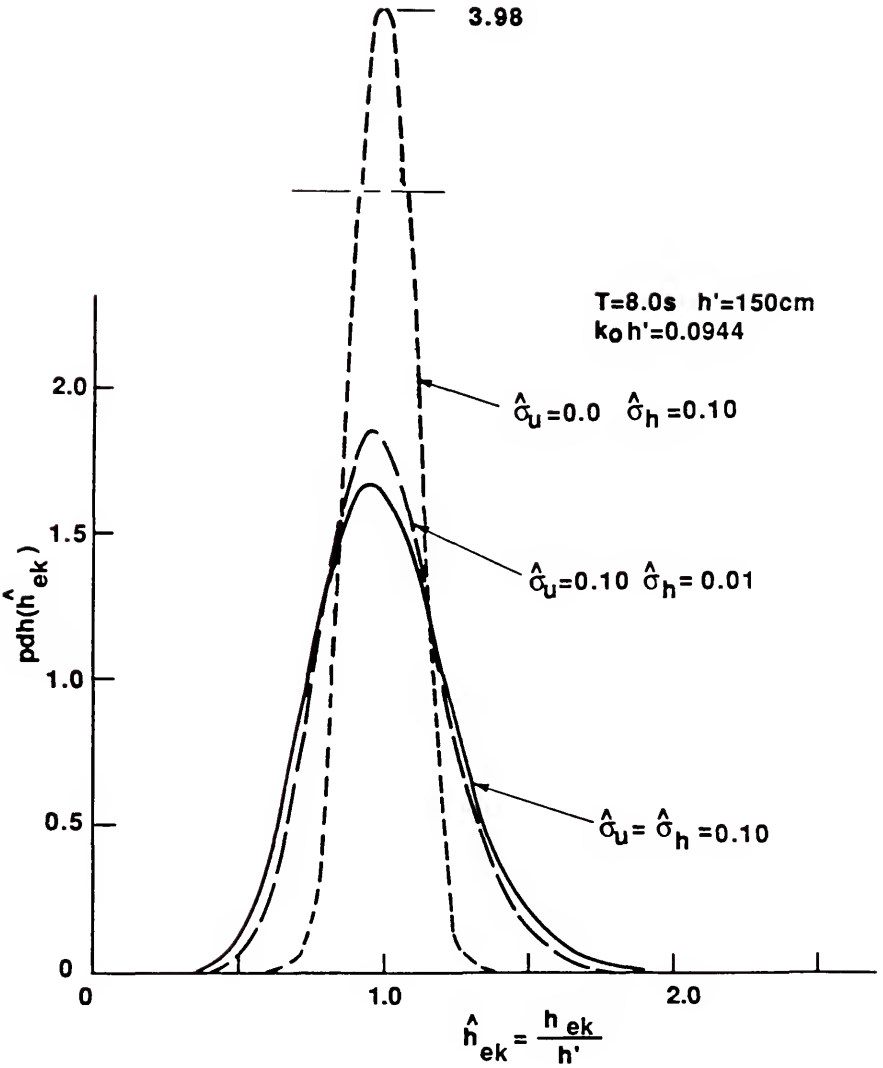

Figure 7.2 Relative importance of currents versus mean water level fluctuations in determining variance of pdf of kinematical equivalent water depth.

of this parameter in response to the stochastic surf beat model should yield some information as to the relative importance of the currents versus the mean water level fluctuations to wave height transformation due to the beat.

As in the previous section, the random variables (U,h) are transformed to (h_{ew}, h :k_o) which is fully described in Appendix D. The final result is

$$\text{pdf}(\hat{h}_{ew},\hat{h} :k_o) = \frac{|F_1||F_2|}{2\pi\ \hat{\sigma}_u\ \hat{\sigma}_h}\ \frac{\hat{h}^{3/2}}{\hat{h}_{ew}^{2}}\ \cdot$$

$$\exp -\frac{1}{2}\{\frac{\hat{h}}{\hat{\sigma}_u^2}[\frac{D_o^{1/2} - (D \tanh D)^{1/2}}{D}]^2 + [\frac{(\hat{h} - 1)}{\hat{\sigma}_h}]^2\} \qquad (7.9a)$$

where

$$\hat{h}_{ew} = h_{ew}/h' \qquad (7.9b)$$

$$D = D_o^{1/2}\ \tilde{h}_{ew}^{1/4}\{1 + [\frac{1}{12}\ \tilde{h}_{ew}^{1/2} - \frac{1}{6}\ \tilde{h}_{ew}^{3/4}]\ D_o + [\frac{1}{120}\ \tilde{h}_{ew} - \frac{7}{360}\ \tilde{h}_{ew}^{5/4} + \frac{1}{8}\ \hat{h}_{ew}^{3/2}]D_o^2\} \qquad (7.9c)$$

$$\tilde{h}_{ew} = h/h_{ew} = \hat{h}/\hat{h}_{ew} \qquad (7.9d)$$

$$F_3 = \frac{1}{4}\ \tilde{h}_{ew}^{-3/4}\ D_o^{1/2} + [\frac{1}{16}\ \tilde{h}_{ew}^{-1/4} - \frac{1}{6}]\ D_o^{3/2} + [\frac{1}{96}\ \tilde{h}_{ew}^{1/4} - \frac{7}{240}\ \tilde{h}_{ew}^{1/2} + \frac{7}{32}\ \tilde{h}_{ew}^{3/4}]\ D_o^{5/2} \qquad (7.9e)$$

and all other quantities are defined in (7.6). As in the kinematical case, the marginal pdf of $\hat{h}_{ew}$ is also found by integrating with respect to $\hat{h}$ numerically, and normalizing by the volume under the joint pdf.

Figure 7.3 contains examples of the marginal pdf of $\hat{h}_{ew}$ for the same values of $\hat{\sigma}_u$ and $\hat{\sigma}_h$ used in Figure 7.1. Note that surf beat has an even greater effect on the wave action equivalent depth, and that significant variance is generated even with only a 5% standard deviation in U and h.

The relative importance of currents and mean water level are again investigated by alternatively setting $\hat{\sigma}_h$ and $\hat{\sigma}_u$, respectively, at small values. Results are displayed in Figure 7.4 and it is observed that eliminating the currents while retaining m.w.l. fluctuations greatly reduces the variance of the marginal pdf($\hat{h}_{ew}$). In the reverse case, however, there is an almost indistinguishable change in the pdf; i.e., most of the variance in $\hat{h}_{ew}$ in response to surf beat is due to the currents and very little is accountable to m.w.l. fluctuations. It is noted that the mean value of $\hat{h}_{ew}$ is less than 1.0 because of the way h_{ew} is defined. Even without surf beat, h_{ew} is always less than the actual water depth.

From the analysis in the preceding two sections, it seems that if surf beat effects are to be correctly addressed in a wave transformation model, both the induced current and mean water level fluctuations should be included--most importantly the currents. As previously noted, no study to date has addressed the current aspects of the problem. In recalling the proposed governing equation for breaking waves on currents (6.15), it appears that currents will manifest themselves most in determining shoaling, incipient breaking, and the rate of decay, while the water level fluctuations will most directly affect the stable wave height (which also affects the rate of decay).

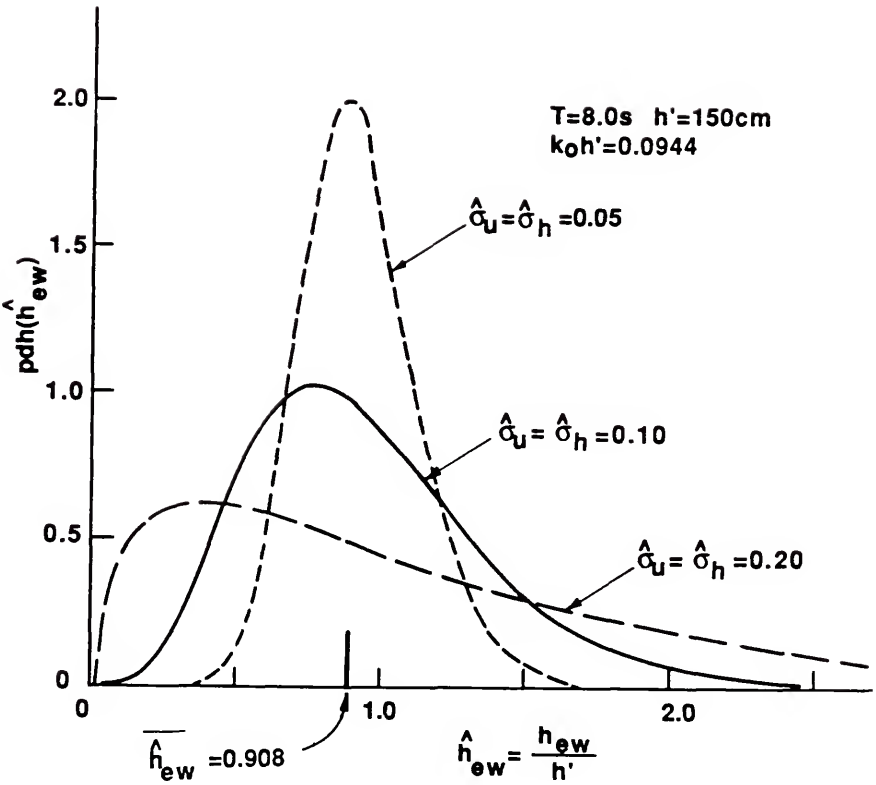

Figure 7.3 Dependence of pdf of wave action equivalent water depth (7.9) on surf beat standard deviations.

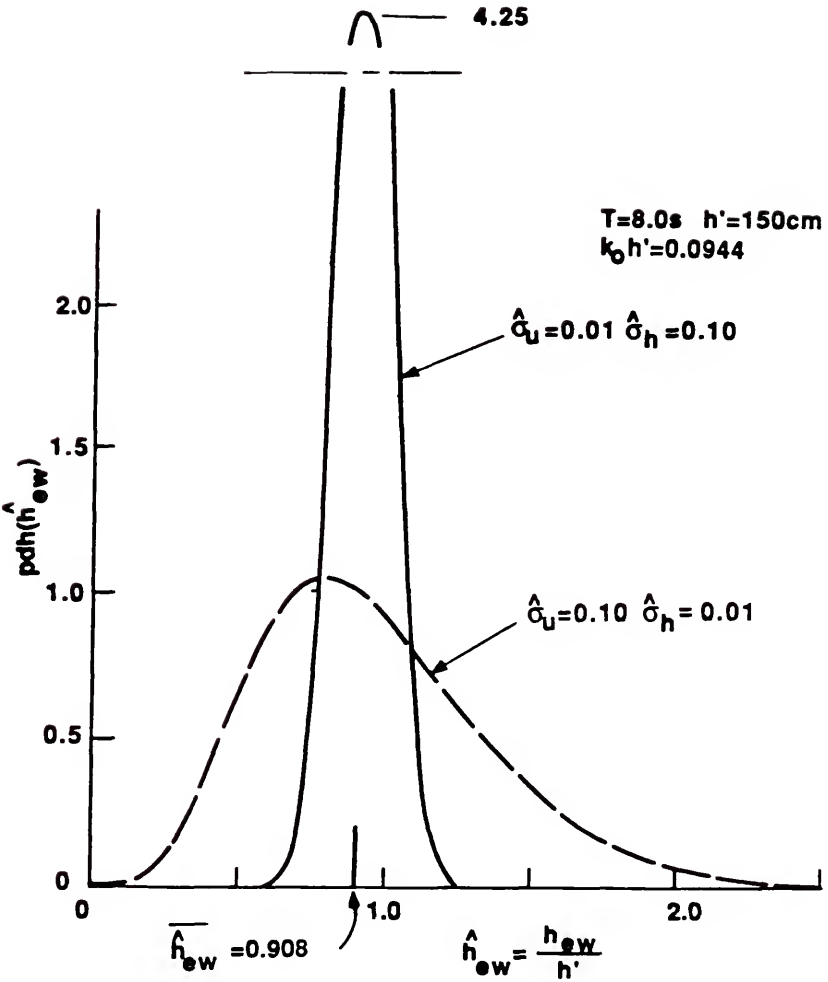

Figure 7.4 Relative importance of currents versus mean water level fluctuations in determining variance of pdf of wave action equivalent water depth.

7.4 Model for Wave Transformation Including Surf Beat

Surf beat is included in the numerical wave transformation model by returning to the original probability density function for induced currents and m.w.l. fluctuations (7.3) and discretizing it into a histogram of 9 x 9 = 81 bins of equal volume, each with an accompanying combination of current and mean water level. This is done at each location across the surf zone. The initial condition for the incident waves is again assumed to be given by (4.16), also discretized into a histogram. Each representative wave is then transformed 81 times across the surf zone, once for each of the 81 bins of surf beat. Statistics and histograms can then be calculated from the N x N x 81 transformed waves.

Transformation of each wave is carried out according to (6.26) with the decay factor K set equal to zero if the wave has not started breaking. Due to the currents and m.w.l. fluctuations, the incipient breaking criteria utilized previously are no longer applicable. Instead a Miche type expression is proposed

$$\frac{H_b}{L} = 0.124 \tanh kh_{ek} \tag{7.10}$$

which after applying (7.5) becomes simply

$$H_b = 0.124 \frac{L^2}{L_o} \tag{7.11}$$

where L is the local wave length including current effects and L_o is the deepwater wave length in the absence of currents. It is noted that in shallow water with no current this reduces to the familiar

$$H_b = 0.78\, h \tag{7.12}$$

Once this incipient condition (7.11) is satisfied, breaking and reformation take place according to (6.26) with $K = 0.15$ and $\Gamma = 0.40$.

7.5 Results and Comparison to Data

Although many laboratory and several field experiments of random breaking waves in the surf zone have been conducted and results reported in the literature, none of these studies reported measurements of surf beat taken synchronously with the wave transformation data. In fact, many writers have gone into great detail as to the problems encountered and techniques utilized when filtering the surf beat from the sensor records. In searching for a data set with which to compare the wave transformation/surf beat model, it was also realized that laboratory data are likely to display surf beat effects that are amplified as compared to nature because the long waves are trapped in the flume. Long waves with periods corresponding to the natural modes of the flume would be exceptionally energetic, especially for experiments run for a long period of time. Goda (1975) specifically pointed out that surf beat amplitude measured during his laboratory experiments were 1.7 and 2.1 times greater than the values predicted by his expression (7.1), for the 1/50 and 1/10 beach slopes respectively.

For these reasons, the search was limited to field experiments, which are necessarily elaborate and costly to conduct. One such experiment was the Nearshore Sediment Transport Study (NSTS) field experiment at Torrey Pines Beach, California which took place in late 1978. Thornton and Guza (1983) provide the measured transformation of H_{rms} from a depth of 10 m all the way to the inner surf zone, measured with a combination of current meters, pressure transducers and

resistance-wire wave staffs. These data, presented in Figure 7.5 along with comparison to the numerical model of chapter 5, displayed decay in H_{rms} that began much farther offshore and to a much greater degree as compared to the models or any other data set. This deviant behavior was the original impetus for including surf beat in the present wave transformation model, in hopes of achieving a better comparison to this data set. As will be shown however, surf beat did not improve the model comparison to the expected degree, and it was eventually realized that the unexpected behavior was an artifice of the manner in which the data were filtered during the original analysis (see Appendix F). Nevertheless, in a later paper, Guza and Thorton (1985) did report information from which the variances in mean water level and currents required to run the model could be extracted, and it was concluded that this was the best available data set.

To identify effects of the switch to (7.12) in prescribing incipient breaking from the original numerical solution in Figure 7.5, the surf beat model was run with σ_u and σ_h set equal to zero, which is equivalent to running the linear model of chapter 5 using the "0.78" criterion as the incipient condition. Results are displayed in Figure 7.6, and show a slight increase in the decay of H_{rms} as compared to the model using the incipient breaking criterion of Weggel (1972). This is because the waves during this experiment were of very low steepness and therefore the average incipient condition according to (2.17) was higher than 0.78.

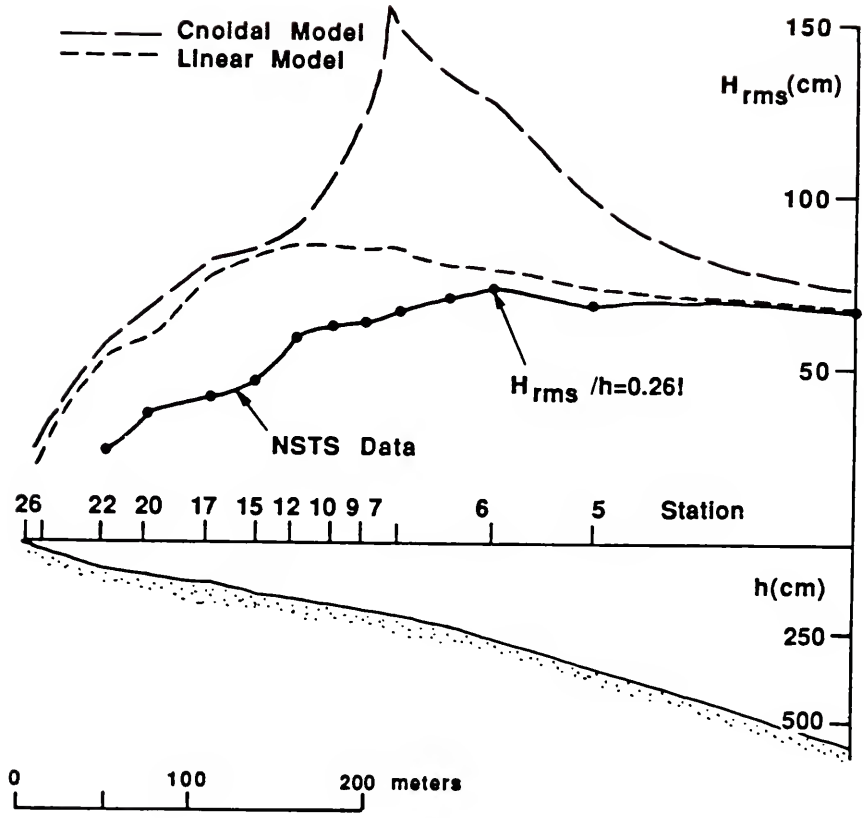

Figure 7.5 Comparison of numerical models of Chapter 5 with H_{rms} transformation of NSTS data from Thornton and Guza (1983).

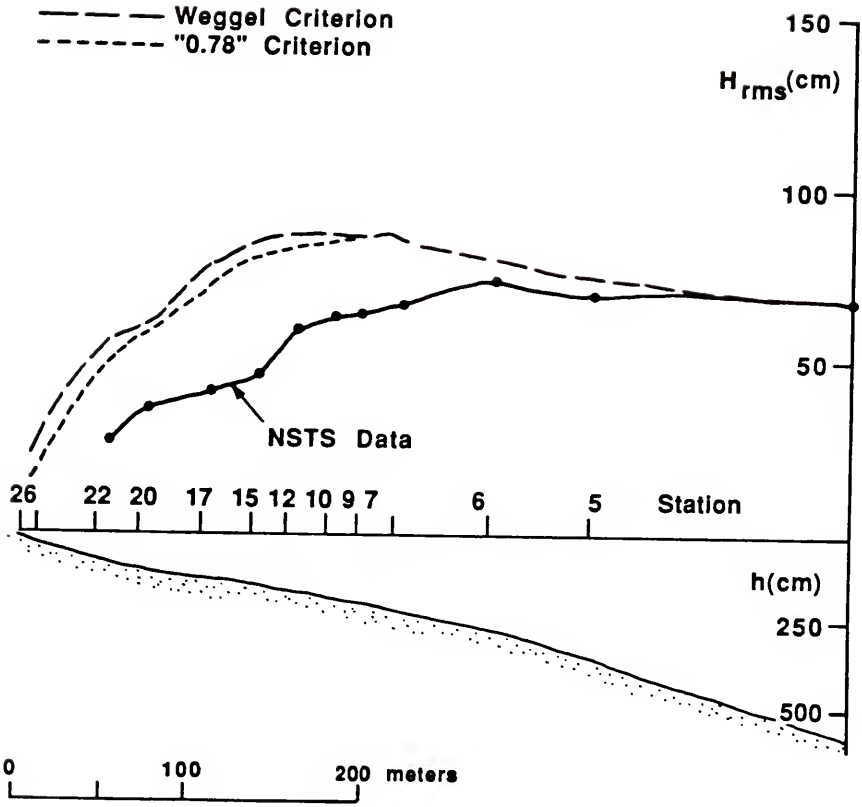

Figure 7.6 Transformation model with "0.78" incipient criterion (no surf beat) compared to criterion of Weggel (1972).

The surf beat model was then run in several different modes to explore the possible effects of surf beat. These modes are:

(a) Variances σ_u and σ_h set equal to the values reported by Guza and Thornton (1985),
(b) σ_u as in (a), but σ_h set equal to zero, and ...
(c) σ_h as in (a), but σ_u set equal to zero, to investigate the relative importance of currents and mean water level fluctuations in the predicted transformation.

Comparisons of model results will be made by calculating the percent change in H_{rms}, ε, at each station according to

$$\varepsilon = \frac{H_{rms}(\text{beat}) - H_{rms}(\text{w/o beat})}{H_{rms}(\text{w/o beat})} \tag{7.13}$$

As shown in Figure 7.7, with all waves encountering all phases of current strength and water level, there is only a very slight increase in the rate of decay in H_{rms} as compared to neglecting surf beat, with most of this increase accounted for by the currents, especially in the outer surf zone. This seems to indicate that if there is no correlation between a group of waves entering the surf zone and the phase of the surf beat it encounters, the <u>average</u> statistical behavior of the short waves is not significantly affected. Without a deterministic model, it is difficult to investigate the effects of the relative phase between the incoming wave groups and the surf beat. Conceptually, all incident waves pass through several outgoing long waves as they cross the near-shore region, but no significant net effect on wave height or other characteristics should be realized until breaking is initiated because up to this point the system is conservative. However, if the phase of the beat is such that the water level is low or the associated currents are opposing when the high waves of the group enter the surf zone, a substantial increase in mean dissipation could result.

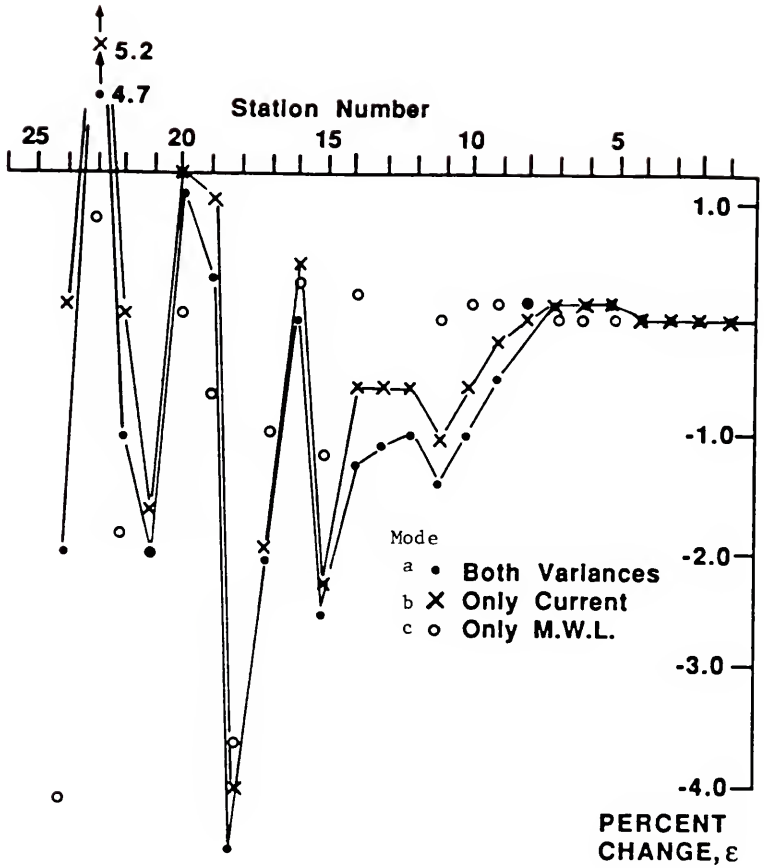

Figure 7.7 Percent change in H_{rms} from model without surf beat to model with only m.w.l. fluctuations (mode c), only current fluctuations (mode b), and complete surf beat (mode a). Phase of wave group and beat assumed independent.

Figure 7.8 shows percent change results of running the model in the following modes:

(d) σ_u and σ_h prescribed as in (a), but any wave whose initial height was greater than H_{rmso} encounters only the water levels at or below the mean mean-water level and currents of zero or negative value,

(e) same as in (d) with large waves encountering only lower water levels, but now allowed to encounter all currents,

(f) Same conditions as (d), but for waves of <u>less</u> initial height than H_{rmso}.

In examining Figure 7.8, the increase in dissipation for large waves encountering the "opposing beat" is quite apparent and on the order of 15% in the surf zone. The results of mode (e) lead us to conclude that at least half of this increase in dissipation is due to the opposing currents. In light of the results of mode (d), the result of mode (f), i.e., less rapid decay in H_{rms}, comes as no surprise.

The question now arises as to when such situations represented by the various modes, specifically (a), (d), and (f), might occur in nature. As described by Lo (1981) and Symonds et al. (1982), surf beat generated by the moving breaker line associated with wave groups can be represented conceptually as a wavemaker positioned at the mean break point which oscillates at the group frequency. The forward motion of the "paddle" corresponds to the phase when the high waves of the group enter the surf zone and the backward motion corresponds to the low waves. Therefore, as the high waves of the group approach the surf zone, they always encounter the long wave motion comprised of the opposing phase of the paddle (due to the low waves of the previous group) added to the long wave reflected from the shoreline. As noted by Symonds et al. (1982), depending on the relative phases of these two waves, their motions can potentially either enhance or cancel out. The

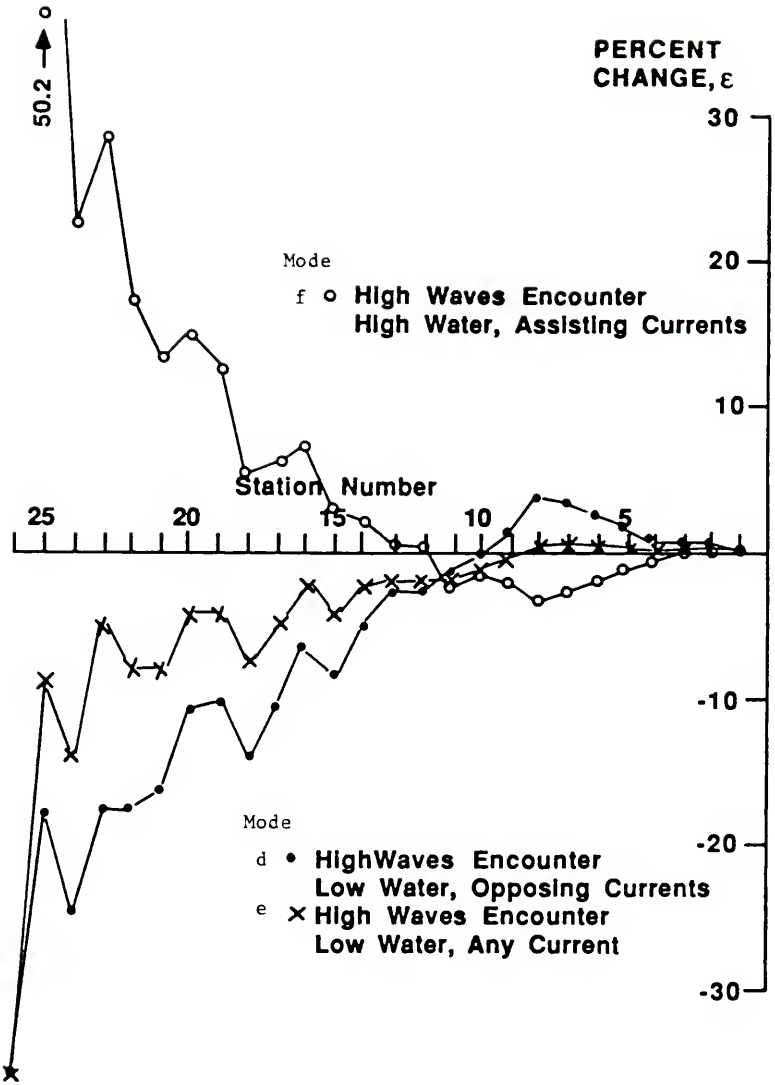

Figure 7.8 Percent change in H_{rms} from model without surf beat to model with high waves encountering lower water and opposing currents (mode d), lower water and all currents (mode e), and higher water and assisting currents (mode f).

relative phase depends on the geometry of the surf zone and the group period. If the wave maker (i.e., the mean break point) is positioned far enough offshore for several long waves to be in the surf zone at any one time, given the broad-banded nature of surf beat, the high waves are likely to encounter any phase of the previously generated beat and mode (a) would result. However, if the wave maker is within a distance of half a surf beat wave length of the shoreline, the motion of the paddle and the reflected wave are in phase. The high waves are likely to encounter opposing currents as they approach the breaking region, and reduced water levels in the interior of the surf zone, and mode (d) is realized. In view of the wave-maker analogy, mode (f) where the small waves of the group always encounter opposing beat, is not physically possible.

For the mean break point to be close to shore in relation to the surf beat wave length, the group period should be long and the wind-wave height small, which indicates the wind waves should be of low steepness. This was exactly the case during the NSTS experiment, where the mean deepwater steepness, $H_{rmso}/\bar{L}_o$, was 0.00108 and Thornton and Guza (1983) described the wave climate as very groupy. In general, low steepness waves are likely to be narrow-banded and therefore groupy, making conditions prime for surf beat generation and increased decay in H_{rms} according to mode (d).

Comparisons of the model run in modes (a) and (d) to the NSTS data are displayed in Figure 7.9. With mode (d), the waves shoal more due to the opposing currents, breaking is initiated sooner, and the rate of decay increases in the outer surf zone. However, there still exists a large disparity between model and data. This was especially perplexing

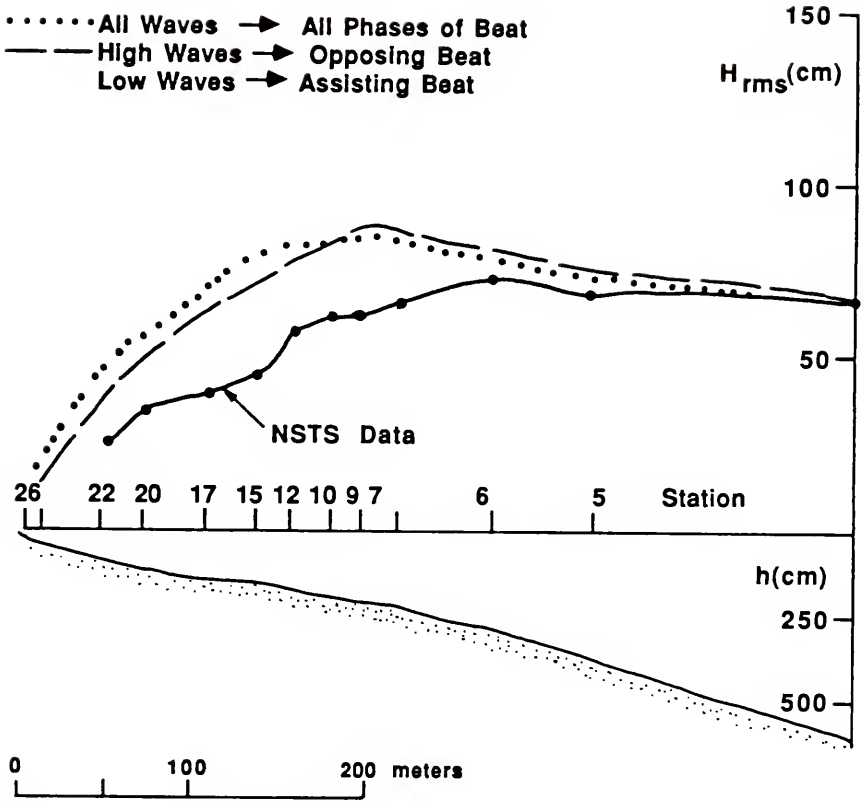

Figure 7.9 Comparison of surf beat model with phase of group independent of phase of beat (mode a) with higher waves encountering opposing beat (mode d) and NSTS data of Thornton and Guza (1983).

in view of the good comparisons to the photopole data of Hotta and Mizuguchi obtained in chapter 5. As is discussed in Appendix F, the original raw data of the NSTS experiment was subject to severe low-pass-filtering which is likely to "clip" the height of the low deepwater steepness, highly non-linear waves present during this study. This is believed to be the source of the remaining disparity between model and data.

The effect of surf beat on the shape of the histogram of wave height is investigated for the Hotta and Mizuguchi (1980) experiment. The standard deviation for the mean water level was calculated at each station using the expression (7.1) of Goda (1975). It can be shown from shallow water linear wave theory that the dimensionless standard deviation for the currents $\hat{\sigma}_u$ given by (7.6b) should be equal to $\hat{\sigma}_h$, and such an assumption is also supported by the measured values for the NSTS data. With the surf beat specified in this manner the model was run in the uncorrelated mode (a) and histograms generated. For the five stations presented in Figure 5.3, improved agreement of the histograms is obtained and is characterized by a smoothing of the peak. Figure 7.10 shows the histograms for the two innermost stations. Note that although still overpredicting the number of waves near the mean value, the peak has been noticeably reduced, with most of the associated probability density transferred to the adjacent bin of lower wave height as desired. Improvement is also noted for the bins of the higher waves of the histograms.

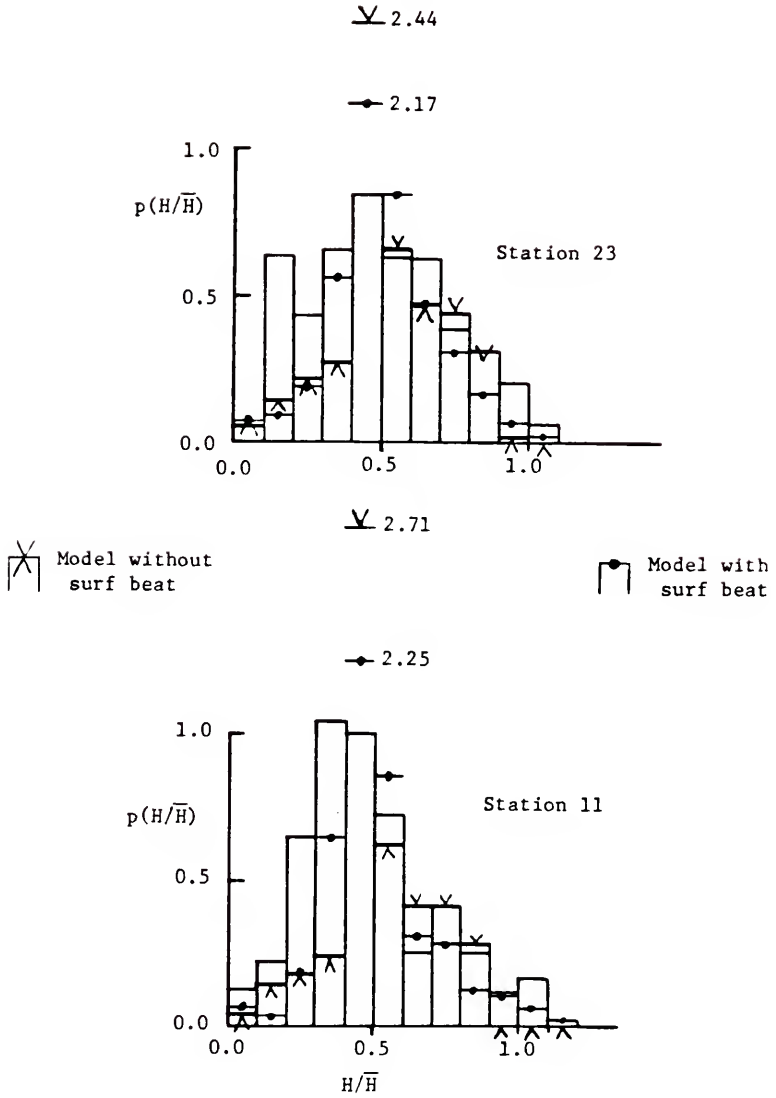

Figure 7.10 Comparison of histograms of wave height for field data of Hotta and Mizuguchi (1980) to model results with and without surf beat effects.

CHAPTER 8

SUMMARY AND CONCLUSIONS

The primary goal of this investigation was to develop and verify a quantitative model for the transformation of random waves in the nearshore region. The processes which most greatly affect this transformation include shoaling, breaking, and reformation. The effect of currents and surf beat on the transformation process, especially pertaining to wave breaking, were also investigated and found to be important in some situations.

Although the dissipation models of others that have appeared in the literature were reviewed and discussed, all the transformation models developed in this study utilized the dissipation function proposed earlier by the author for regular waves (Dally, 1980; Dally, Dean, and Dalrymple, 1984, 1985). The major attributes of this model are its qualitative and quantitative accuracy over a wide range of wave conditions and bottom configurations, its simplicity and ease of application, and the existence of several closed-form solutions for idealized topography. This model for regular waves was further generalized by removing the assumption of shallow water conditions during shoaling, and by predicting the incipient break point using the criterion of Weggel (1972). Although the earlier model had been calibrated and verified using only small-scale laboratory data, the successful verification of the model to three full-scale tests without altering its coefficients is both enlightening and reassuring.

As the review of previous models of random waves in the surf zone indicates, the probability density function for breaking and shoaling waves has received only ad hoc and somewhat contrived treatments, except for that of Mase and Iwagaki (1984). The assumption that wave height is Rayleigh distributed for non-breaking waves seaward of the surf zone is well-supported by laboratory and field data. However, there is almost no support for adopting this shape in the surf zone. Several of the ad hoc treatments of the tail of the Rayleigh pdf fail to distinguish between breaking and non-breaking waves, and none permit study of the effects of beach slope and mean wave steepness on the shape of the pdf or the behavior of statistically representative waves.

Based on the analytical solution for decay of regular waves, the two closed-form solutions for the transformed pdf of shoaling and breaking waves over a planar beach are unique in that the transformation from the initial Rayleigh shape takes place logically and "naturally"; i.e., no ad hoc shape of the pdf is adopted a priori. The effect of beach slope on the shape of the pdf and the behavior of statistically representative waves can be observed directly in the first solution. Although this solution exhibits a sharp truncation at the upper limiting height and a high peak in the breaking portion in the inner surf zone, it is still useful for monitoring statistically representative waves. The second closed form solution removes the sharp truncation by allowing the incipient condition to vary according to any of the available predictive expressions for γ. The sharp peak in the breaking pdf is also removed except for mild slopes, and might possibly be representative of nature were it not for the smoothing induced by surf beat, the variable incipient condition, and the natural variability in the breaking process

present even with regular waves. Because the integration necessary to determine the marginal pdf of wave height must be accomplished numerically, the second closed form solution is slightly more cumbersome.

Extension of the random wave model to beach profiles of more complex shape such as including bar/trough formations requires numerical solution, and is accomplished by transforming representative waves from the intial histogram individually, using the numerical solution for regular waves. The model results compared well to the photopole field data of Hotta Mizuguchi (1980) both in respect to the measured histograms of wave height and the transformation of statistically representative waves (H_{rms}, $H_{1/3}$, $H_{1/10}$). Due to the use of linear wave theory, the shoaling behavior of $H_{1/10}$ and to a lesser degree $H_{1/3}$, was not represented as faithfully as might be desired; but the breaking behavior was predicted well. The incorporation of Cnoidal wave theory to shoal the waves significantly improved this comparison in the outer surf zone, but apparently at slight expense to the comparison in the inner surf zone. Here the linear model predicted quite well, while the Cnoidal model fell a bit below the measurements.

Comparison of the numerical models to the photopole data of Hotta and Mizuguchi (1986) was a severe test because two bar/trough systems were present in the bottom profile and only results for $H_{1/3}$ reported. However, the models compared well in most respects except that they seem to allow too many waves to reform in the troughs. There are potentially several ways to correct this, one being for each wave and at each station to average the depth over the local wave length. In this manner only the shorter waves would respond to the trough and reform.

The investigation of the effects of a collinear current on the breaking of regular waves was an extremely useful "stepping stone" to the problem of random waves encountering surf beat. The results of this study might even relate more directly to waves encountering rip currents or propagating through tidal inlets. The expansion solution to the steady form of the kinematical conservation equation used to calculate properties such as intrinsic frequency and wave number proved quite useful, and is of potential value in situations which preclude numerical solution. Based on conservation of wave action and the author's previous dissipation function, a governing equation for wave decay on collinear currents was proposed and an analytical solution for a bottom of uniform depth derived. The laboratory study of regular breaking waves on steady opposing currents showed that as compared to breaking without a current, the breaker line is moved slightly offshore, dissipation is intensified, and the point where a wave reforms in a uniform depth is moved offshore a significant distance. In short, the surf zone is compressed and displaced seaward. It was also discovered that the stable wave height attained after reformation appears to be relatively independent of current strength, as long as breaking was fully developed initially. Comparisons of the analytical and numerical solutions for waves breaking on currents to the laboratory data generally showed good agreement. However, in those cases where the current was strong and the wave period short, the model underpredicted the rate of decay, while maintaining accuracy in regard to the stable wave height. It is unclear if the predicted rate of decay is less due to inaccuracy in the kinematical treatment or in the proposed dissipation equation. Fortunately, the currents associated with surf beat are generally small and the

period of groupy wind-waves long, so it seems relatively safe to use the proposed dissipation model.

As noted, the only treatment the effect of surf beat on random wave transformation has received previously is the inclusion of a varying mean water level. However, as discovered by examination of the response of the probability density functions of kinematical equivalent water depth and wave action equivalent water depth to surf-beat-induced fluctuation in mean water level and current, the current dominates transformation of the waves due to the beat, especially out near the break point. Surf beat was included in the random wave transformation model by prescribing variances in current and mean water level at each location in the surf zone. The behavior of each representative wave from the initial histogram in response to each stage of surf beat was then used to develop local histograms of wave height and to monitor statistically representative waves. Surf beat tends to smooth the high peak in the histogram and redistribute the area to the neighboring bins. When the phase of the incoming wave group is assumed to be statistically independent of the phase of the surf beat, only a slight increase in decay of H_{rms} is noted, with most of it attributed to the currents and not fluctuations in the mean water level. However, if high waves of the group are prone to encounter the opposing currents and/or low water level of the beat, decay in H_{rms} can increase on the order of 15%. In nature, surf beat effects are potentially significant, but are probably limited to the inner surf zone where the beat is strongest. However, in the laboratory, surf beat effects are expected to be unrealistically amplified if long wave energy is trapped in the tank. The direct application to field situations of random wave transformation models calibrated using laboratory data is therefore questioned.

In comparing the surf beat model to the NSTS data, the increase in decay was still not sufficient to improve agreement significantly. It is believed the deviant behavior of this data is due to low-pass-filter-induced clipping of the waves during the original treatment of the data. Unfortunately, this is the only field experiment for which synchronous measurements of wave transformation and surf beat are available.

In addition to the clipping induced by the low-pass-filtering, the filtered time series becomes more sinusoidal and therefore behaves more like a narrow-banded Gaussian random process. This is believed to be the reason why the NSTS data seems to follow the expression $H_{rms} = \sqrt{8a_0}$ and the Rayleigh pdf in the surf zone as reported by Thornton and Guza (1983), while data not filtered in this manner fail to support these models. Because the model of Battjes and Janssen (1978) assumes that $H_{rms} = \sqrt{8a_0}$, and Battjes and Stive (1985) support this assumption based on the filter-induced results of the Thornton and Guza (1983), the calibration coefficients which dictate decay in this model display a dependence on mean deepwater steepness (i.e., wave peakedness). In conclusion, to avoid the artificial behavior induced by extreme low-pass-filtering it is recommended that filtering be used only to obtain wave periods, and that the original record collected at high frequency ($\geq$ 4 Hz) be used to obtain wave heights.

APPENDIX A

EXPANSION APPROXIMATION FOR THE DISPERSION RELATION INCLUDING CURRENTS

A.1 Introduction

There appear to be many methods available for solving the dispersion relation (6.4) for regular linear waves on steady collinear currents. One is to employ one of several available direct numerical techniques such as repeated substitution or the Newton-Raphson method for determining roots of transcendental equations. Another is to expand the hyperbolic tangent term to the desired order in kh and find the appropriate root of the resulting polynomial using perhaps Müller's Method and Hotteling's deflation. A more direct method which is computationally less time-consuming is to extend the Taylor expansion approach utilized by Nielsen (1984) for the dispersion relation without currents to the case with currents. The only drawback is the method loses accuracy in deeper water or with strong opposing currents.

A.2 Taylor Expansion Approach

The dispersion relation for linear waves on steady currents is restated for convenience

$$\omega = (gk \tanh kh)^{1/2} + kU \tag{6.4}$$

where again ω is the absolute (no current) frequency and is constant for regular waves, g is gravity, k is wave number, h is water depth and U is

collinear current strength. Expressing ω in terms of the deepwater wave number k_o and rearranging slightly

$$(kh \tanh kh)^{1/2} = (k_o h)^{1/2} - kh \frac{U}{\sqrt{gh}} \tag{A.1}$$

In shallow water ($kh \to 0$) this becomes

$$kh = \frac{\sqrt{k_o h}}{1 + \frac{U}{\sqrt{gh}}} \tag{A.2}$$

The shallow water behavior is extracted and we seek a truncated expansion of the form

$$kh \simeq \frac{\sqrt{k_o h}}{1 + \frac{U}{\sqrt{gh}}} [1 + \alpha k_o h + \beta (k_o h)^2] \tag{A.3}$$

Squaring both sides of (A.1) yields

$$k_o h + (kh)^2 \frac{U^2}{gh} - 2(k_o h)^{1/2} kh \frac{U}{\sqrt{gh}} - kh \tanh kh = 0 \tag{A.4}$$

and expanding the tanh to

$$\tanh kh \simeq kh - \frac{1}{3}(kh)^2 + \frac{2}{15}(kh)^5 \tag{A.5}$$

(A.4) becomes

$$k_o h + (kh)^2 \left(\frac{U^2}{\sqrt{gh}} - 1\right) - 2(k_o h)^{1/2} kh \frac{U}{\sqrt{gh}} + \frac{1}{3}(kh)^4 - \frac{2}{15}(kh)^6 = 0 \tag{A.6}$$

The coefficients α and β are determined by substituting (A.3) into (A.6) and equating like powers of $(k_o h)$. The first power is already zero as is expected. Equating the second power produces

$$\alpha = \frac{1}{6(1 + \frac{U}{\sqrt{gh}})^3} \tag{A.7}$$

and for the third power

$$\beta = \frac{1/9 - 1/15(1 + \frac{U}{\sqrt{gh}}) + 1/72(\frac{U}{\sqrt{gh}} - 1)}{(1 + \frac{U}{\sqrt{gh}})^6} \tag{A.8}$$

The expansion solution to second order is then

$$kh \simeq \frac{\sqrt{k_o h}}{\hat{U}} \left\{1 + \frac{1}{6\hat{U}^3}(k_o h) + \left[\frac{1/9 - 1/15\,\hat{U} + 1/72(\hat{U} - 2)}{\hat{U}^6}\right](k_o h)^2\right\} \tag{A.9a}$$

where

$$\hat{U} = (1 + \frac{U}{\sqrt{gh}}) \tag{A.9b}$$

The analysis of Nielsen (1984) indicates that (A.9) is accurate to within 0.5% for $(k_o h/\hat{U}^3) < 2.51$. Because the shallow water behavior has been extracted, (A.9) is exact as $(k_o h/\hat{U}^3) \to 0$.

APPENDIX B

LABORATORY EXPERIMENT OF REGULAR WAVES BREAKING ON OPPOSING CURRENTS

B.1 Introduction

The major purpose of this laboratory investigation was to obtain a data set with which to verify the concepts, governing equations and solutions presented in chapter 6 concerning the effects of collinear currents on the wave breaking process. Although wave-current interaction is by no means a new topic to the literature, the interactions studied to date generally include only shoaling, refraction and diffraction. Not until recently has breaking been examined, e.g., Sakai and Saeki (1984), and abstracts by Huyamizu, Sakai and Saeki (1986) and Lee, Sawaragi and Deguchi (1986). Only a very limited number of measurements are available thus far.

B.2 Apparatus and Procedure

The major goal in designing the apparatus was to devise a system whereby the effect of varying current strength on wave breaking could be examined while holding the offshore wave conditions constant. Such an apparatus is displayed in Figure B.1. The "tilting flume" at the University of Florida Coastal and Oceanographic Engineering Laboratory was used, although its tilting capability was not employed in these experiments. The tank is 15.5 m long, 0.9 m high, and 0.6 m wide. It has one wall of glass panels and is equipped with a mechanical piston-type generator. A false bottom of glass-resin-coated plywood on an

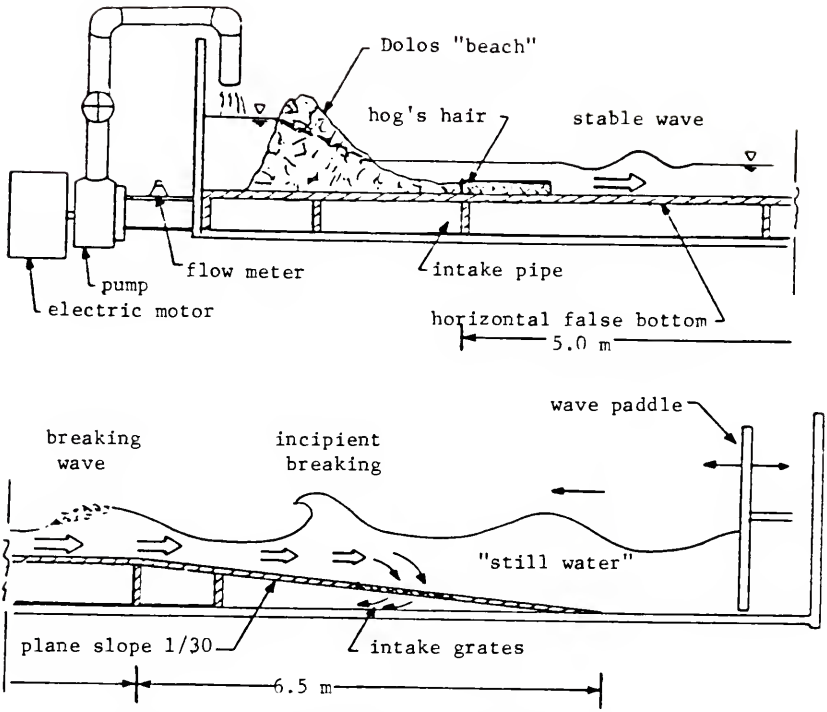

Figure B.1 Apparatus for laboratory experiment of regular waves breaking on opposing currents.

aluminum frame was constructed, which had a horizontal section 5.0 m long fronted by a ramp with a planar slope of 1/30, 6.5 m in length. A pump and electric motor (capacity = 2,072 ℓ/min) were installed outside the tank with an intake pipe which passed through the end wall, underneath the false bottom, and extended down the tank to a point under the sloping section. At this point it was sealed to a plywood partition. Intake vents were installed near the toe of the 1/30 slope, and the entire false bottom was sealed with silicone caulk to the walls of the tank. With this configuration water is drawn through the vents and into the intake pipe, passed through the pipe to the exterior pump, and

discharged up and over the end wall back into the tank. A "beach" constructed of small-scale dolos armor units fronted by hog's hair dissipative material was installed, behind which the discharged water would pond and create a hydraulic head sufficient to drive the constant discharge through the voids in the structure. The water then passes down the tank above the false bottom and through the vents to close the system. The discharge is steady so that currents are steady, at least in a gross sense, and are approximately uniform (in the horizontal) in the uniform depth section and vary as 1/h over most of the plane beach section. The discharge rate of the pump is measured with a rotating-vane flow meter mounted in the intake pipe. The meter was calibrated and displayed good linearity in the range of flow rates used.

Because the intake vents are shoreward of the generator, waves are generated in almost completely still water so the same offshore wave conditions can be run against whatever opposing current is desired. The waves travel down the tank, shoal on the sloping bottom and current, break, and reform somewhere in the uniform depth section. The hog's hair and dolos structure absorb the reformed wave with very little reflection, and also dissipate any waves generated by the discharge of the pump. Wave height was measured visually, and mean water level recorded using a manometer and stilling well. The mean water level in the surf zone displayed only slight wave-induced set-up, in the general range of 1 to 3 mm. Wave period was determined with a stop watch.

In conducting a test, a nominal water depth was selected and stroke and period of the generator set. The pump was started at a chosen discharge and the flow allowed to stabilize for approximately 5 minutes. Because of the storage behind the dolos structure, water was slowly

added to the tank to bring the mean water level back up to the desired elevation. The generator was then started and wave transformation and mean water level variation measured.

In a few tests, the waves and opposing currents interacted in an unstable fashion which caused cross-tank variations, and in one case a temporal oscillation in conditions at the break point. It is interesting to note that small-scale turbulence introduced to the mean flow by the roughness of the dolos structure helped prevent these unstable interactions. In fact, adding hog's hair to dampen this turbulence increased the cross-tank variations. It is suggested that the mixing induced by this turbulence makes the cross-tank distribution of the mean current more uniform, as opposed to parabolic for reduced turbulence. This is analogous to the flow distribution in turbulent versus laminar pipe flow. With reduced turbulence the incoming waves encounter a current that varies considerably across the tank and is subject to meandering, thereby setting up cross-tank variations in wave transformation.

B.3 Results and Model Comparison

Results of the nineteen experiments of wave transformation due to shoaling and breaking on opposing currents and predictions of the numerical model are displayed in Figures B.2-B.5. They are grouped by incident wave condition and nominal water depth to facilitate examination of the effect of current strength on wave breaking. Nominal water depth increases as one proceeds through the set of figures.

Figure B.2 depicts typical effects of increasing opposing current strength on the wave decay process. As the current increases from test

824C through 824A, the break point is pushed offshore only slightly, while the point of wave reformation is moved significantly; i.e., the surf zone is compressed and shifted offshore. The model appears to describe the decay faithfully for the two milder currents but underpredicts the rate of decay in 824A. Measured stable wave height is slightly less than predicted. It is noted that without a current, no breaking would take place for these offshore wave conditions.

The effects of wave period on the decay process with currents can be observed by comparing tests 86A, 810A and 811B, which are for wave periods of 3.0, 1.8 and 1.15 s, respectively. Each figure portrays results of breaking on the sloping section with a current of moderate strength. Decreasing wave period increases both the seaward shift of the break point and the compression of the surf zone, while the stable wave condition remains relatively fixed at $H_s/h = 0.4$. Thus decreasing wave period increases the rate of energy dissipation, and the effects of the opposing current become more apparent. The model includes this wave period effect, at least qualitatively, when calculating the wave number and intrinsic frequency and group velocity. For a given current strength, short waves undergo greater changes than long waves. The model compared well in Figures B.2-B.3 for the cases with no current and for a current with a long period wave, but underpredicts the decay for short waves with a current.

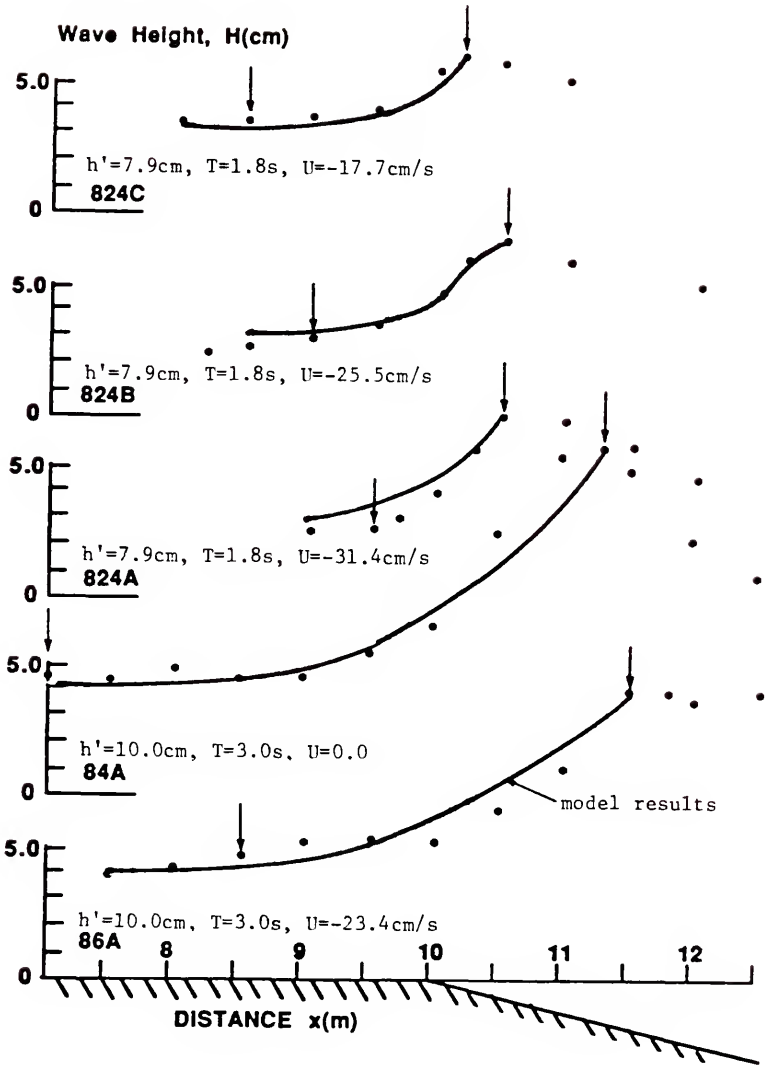

Figure B.2 Results of laboratory tests 824C, 824B, 824A, 84A and 86A for waves breaking on opposing currents.

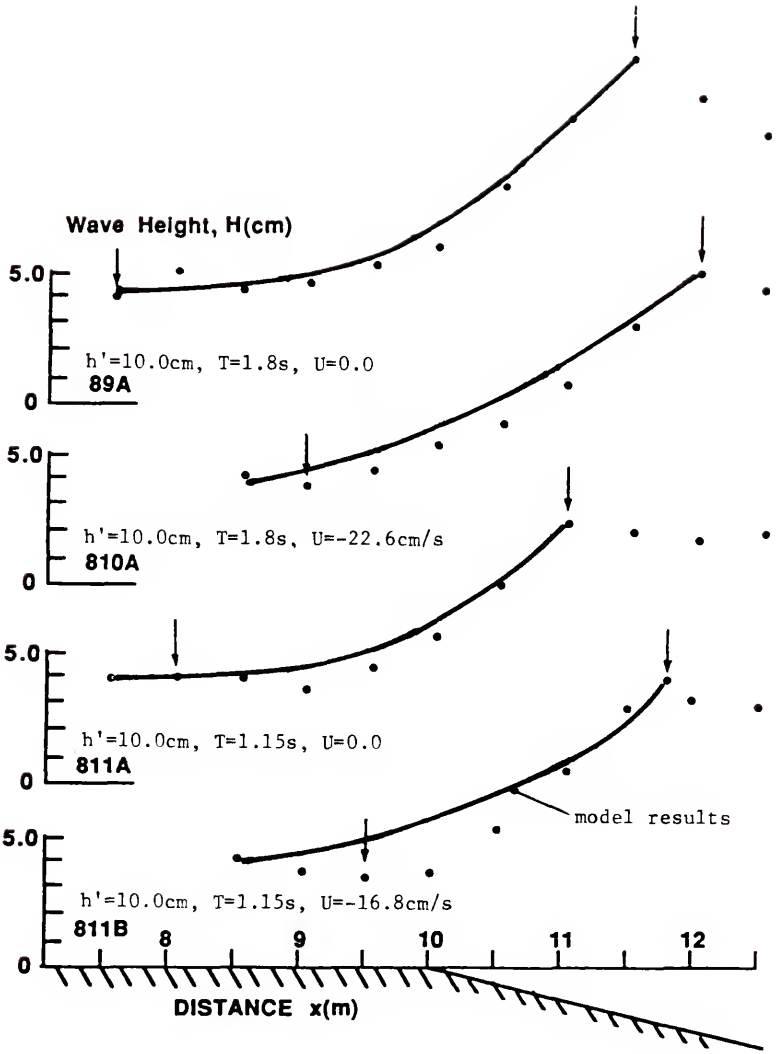

Figure B.3 Results of laboratory tests 89A, 810A, 811A and 811B for waves breaking on opposing currents.

In one series of tests, offshore wave conditions and water depth were contrived such that without an opposing current only a minimal amount of breaking would take place. This "barely break" case (827A*) is shown in Figure B.4, where it is interesting to note that incipient breaking did not occur until the wave had passed a full meter into the uniform depth section and that the wave reformed when $H_s/h = 0.46$. With a relatively mild current (827B), the surf zone moves offshore one meter, the rate of decay increases, and the stable wave drops to $H_s/h = 0.42$. Because the decay increased and the stable wave decreased simultaneously, the length of the surf zone did not change significantly. Increasing the current strength further (827C) did not move the break point but greatly compressed the surf zone and dropped the stable wave to $H_s/h = 0.4$. The model slightly overpredicted decay in 827A and 827B but compared quite well in 827C where breaking in the tank was fully developed.

The comparisons of the model to the results of the laboratory experiment displayed in Figure B.4 are consistent with the findings thus far. The model compared well for breaking initiated at the beginning of the uniform depth section on a moderate current, but again slightly underpredicted the decay for the strong current with breaking initiated on the sloping beach.

Conditions in Figure B.5 were tuned such that without a current, the wave was just below the point of breaking. A very slight current in test 812D* causes a barely break situation, analogous to that of Figure 827A* caused by the sloping bottom. The model predicts the rate of decay well, but the measured stable wave condition was $H_s/h = 0.47$. Increasing the current strength in test 812C decreases the stable

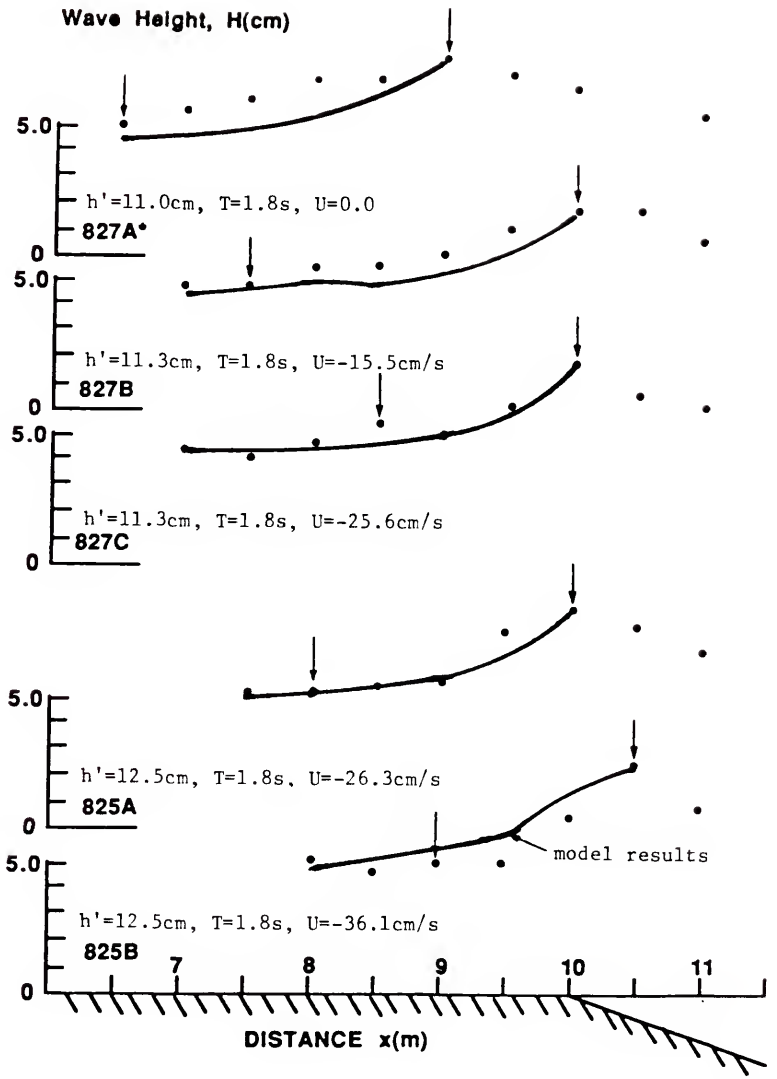

Figure B.4 Results of laboratory tests 827A*, 827B, 827C, 825A and 825B for waves breaking on opposing currents.

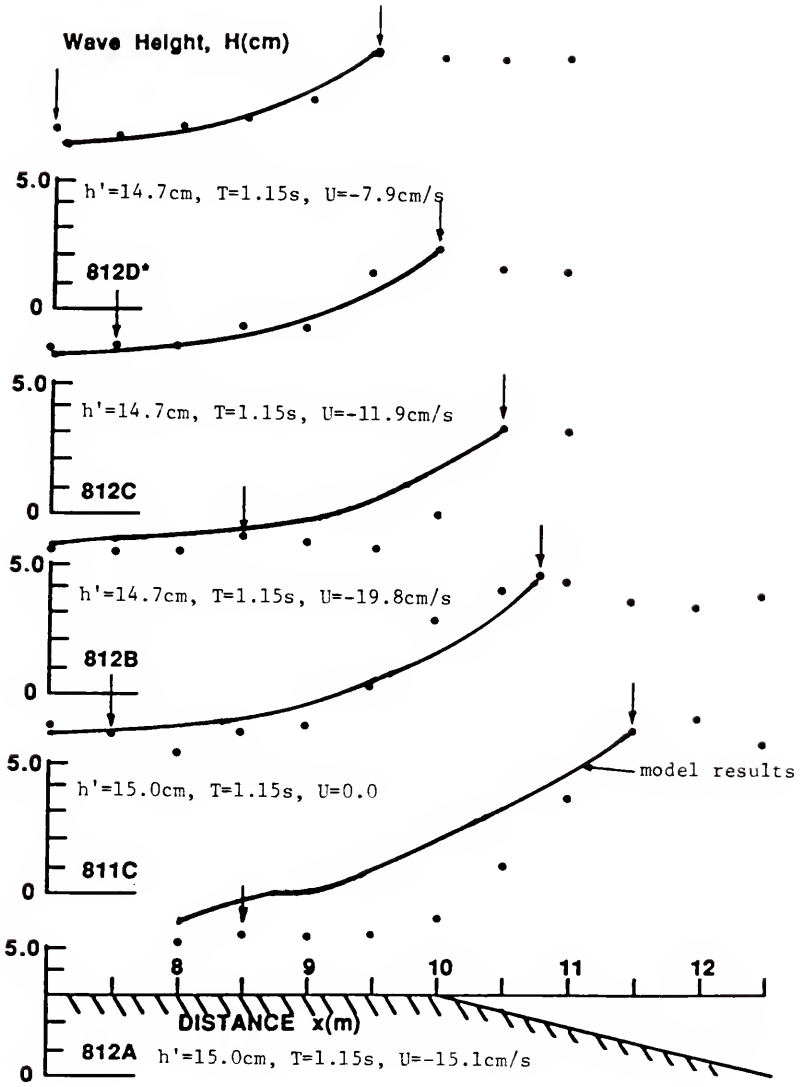

Figure B.5 Results of laboratory tests 812D*, 812C, 812B, 811C and 812A for waves breaking on opposing currents.

condition ($H_s/h = 0.44$) and further improves agreement of the model. However as found previously, stronger currents and a short wave period with breaking initiated in the sloping section (test 812B) show a measured rate of decay greater than the model predicts, although the stable condition ($H_s/h = 0.37$) agrees within reason.

The final set of results are for a short period wave (1.15 s) and breaking initiated on the sloping section, without (811C) and with a current (812A). Again, the model-predicted decay compares well for the no-current case and the stable wave assumption is accurate; however, with a moderate opposing current, the rate of decay is underpredicted and the stable wave condition slightly overpredicted.

In summary, increasing opposing current strength compresses the surf zone and displaces it offshore slightly. A distinct increase in decay for waves of short period is observed, contrary to the no-current situation where decay is almost independent of period (Dally et al., 1985). For situations where breaking is fully developed, due either to the current or the sloping bottom, the stable wave assumption $H_s/h = 0.4$ appears to remain valid and the model compares well to the data for the longer period waves. For short period waves and strong currents, the model underpredicts the rate of decay, and the stable wave criterion decreases slightly.

The reason for the disparity between the measurements and model for the short period waves on strong currents is unclear to the author. Aside from the conclusion that (for some reason) the proposed governing equation (6.15) loses validity for these conditions, the use of linear wave theory to calculate intrinsic frequency, group velocity and energy density in shallow water is of course subject to question. Although

spot comparisons of measured wave length and predictions using the expansion solution (6.15) showed good agreement, the measurements of Sakai and Saeki (1984) show that linear theory underpredicts the wave length on opposing currents especially for short waves (i.e., over-predicts the contracting effect of the current) which would in turn overpredict the intrinsic frequency and underpredict the group velocity. In result, the rate of energy dissipation in the model, i.e., the R.H.S. of (6.15) might be artificially reduced for short waves due to the use of linear wave theory.

Another possible reason for the discrepancy of the model from the measurements in several cases is the assumption that the currents in the sloping section are uniform over depth, and that their magnitudes are calculated by dividing the measured discharge by the cross-sectional area of the tank. To investigate, the flow conditions for the seven experiments in question (824A, 86A, 810A, 811B, 825B, 812B, and 812A) were re-created and the currents measured with an electromagnetic current meter (ball diameter = 1.0 cm). In the uniform depth section, as might be expected, the flow in the upper water column along the centerline was found to be an average of 26% greater than the calculated value, while it was less than calculated along the side walls. Distribution of current with depth was found to be approximately uniform. On the sloping bottom, the flow near the surface decreased in less than a 1/h manner from the value at the beginning of the section but showed significant decay with depth, as might be expected for flow with a diverging bottom. However, when the actual measured flow rates along the centerline near the surface were used in the model comparisons the results changed almost imperceptibly. This is because the intrinsic group velocity is still much greater than the current strength.

APPENDIX C

PROBABILITY DENSITY FUNCTION FOR KINEMATICAL EQUIVALENT WATER DEPTH

As introduced in chapter 7, one approach to expressing the effect of a collinear current on the kinematical properties of waves, specifically wave length, intrinsic frequency and celerity, is by defining an equivalent water depth based on the dispersion relation. This fictitious water depth is defined for a wave with absolute frequency ω and wave number k riding on a current, as the water depth the wave would have to encounter with no current while still retaining the same wave number, i.e.,

$$\omega^2 = \left[(gk \tanh kh)^{1/2} + kU\right]^2 = gk \tanh kh_{ek} \tag{C.1}$$

where h_{ek} is the equivalent water depth and can also be expressed as

$$h_{ek} = \frac{\tanh^{-1} (\omega^2/gk)}{k} \tag{C.2}$$

The assumption is that the current, U (i.e., the water particle velocity), and the mean water level fluctuation, $\bar{n}$, associated with the surf beat are normally distributed and uncorrelated at any location in the surf zone:

$$\text{pdf}(U, h) = \frac{1}{2\pi \sigma_u \sigma_h} \exp\left\{-\frac{1}{2}\left[\left(\frac{U}{\sigma_u}\right)^2 + \left(\frac{h - h'}{\sigma_h}\right)^2\right]\right\} \tag{C.3}$$

where σ_u and σ_h are the specified standard deviations of the current and mean water level respectively and $\bar{\eta}$ has been defined as

$$\bar{\eta} = h - h' \tag{C.4}$$

where h is the mean water level including surf beat and h' is the mean mean water level, i.e., the time-averaged water level over the surf beat period. The procedure to be followed to derive the marginal pdf of kinematical equivalent water depth is shown conceptually by

$$\text{pdf}(U,\ h) \Rightarrow \text{pdf}(kh,h :k_o) \Rightarrow \text{pdf}(h_{ek},h :k_o)$$

$$\text{mpdf}(h_{ek} :k_o) = \int \text{pdf}(h_{ek},h :k_o)\, dh \tag{C.5}$$

In the first step, the dispersion relation (6.4) is reverted for the current strength

$$U = \frac{\omega - (gk \tanh kh)^{1/2}}{k} \tag{C.6}$$

or in terms of the notation of chapter 4

$$U = (gh)^{1/2}\left[\frac{(k_o h)^{1/2} - (D \tanh D)^{1/2}}{D}\right] \tag{C.7}$$

where $D = kh$. Again employing a transformation of random variable, $U \rightarrow D$, which requires

$$\left|\frac{\partial U}{\partial D}\right| = (gh)^{1/2}\left|\frac{-D\left[\frac{\tanh D + D\,\mathrm{sech}^2 D}{2(D\tanh D)^{1/2}}\right] + (D\tanh D)^{1/2} - (k_o h)^{1/2}}{D^2}\right|$$

$$= (gh)^{1/2}\,|F_1(D)| \tag{C.8}$$

we find

$$\mathrm{pdf}(D,h : k_o) = \frac{(gh)^{1/2}|F_1(D)|}{2\pi\,\sigma_u\,\sigma_h}$$

$$\exp -\frac{1}{2}\left\{\frac{gh}{\sigma_u^2}\left[\frac{(k_o h)^{1/2} - (D\tanh D)^{1/2}}{D}\right]^2 + \left(\frac{h - h'}{\sigma_h}\right)^2\right\} \tag{C.9}$$

Hunt's approximate solution to the dispersion relation without currents (2.14) is employed to solve (C.1) for the wave number given the equivalent water depth which yields

$$D = k_o h\left\{1 + \left[D_{oek}\left(1 + \sum_{n=1}^{6} d_n D_{oek}^n\right)\right]^{-1}\right\}^{1/2} \tag{C.10}$$

where $D_{oek} = k_o h_{ek}$. To transform from D to D_{oek} requires

$$\left|\frac{\partial D}{\partial D_{oek}}\right| = \left|\frac{k_o h}{2}\{\ \}^{-1/2}\left[\{\ \} - 1\right]^2\left[1 + \sum_{n=1}^{6}(n+1)d_n D_{oek}^n\right]\right| = |F_2(D_{ek})| \tag{C.11}$$

in which $\{\ \}$ denotes the expression in the braces of (C.10), and finally

$$\mathrm{pdf}(D_{oek},h : k_o) = \frac{(gh)^{1/2}|F_1||F_2|}{2\pi\,\sigma_u\,\sigma_h}$$

$$\exp -\frac{1}{2}\left\{\frac{gh}{\sigma_u^2}\left[\frac{(k_o h)^{1/2} - (D\tanh D)^{1/2}}{D}\right]^2 + \left(\frac{h - h'}{\sigma_h}\right)^2\right\} \tag{C.12}$$

where (C.8), (C.10) and (C.11) are substituted appropriately. Casting (C.12) into completely dimensionless form by defining water depths

$$\hat{h} = h/h' \tag{C.13a}$$

$$\hat{h}_{ek} = h_{ek}/h' \tag{C.13b}$$

produces

$$\text{pdf}(\hat{h}_{ew},\hat{h} : k_o h') = \frac{k_o h' \hat{h}^{1/2} |F_1||F_2|}{2\pi \hat{\sigma}_u \hat{\sigma}_h} \cdot$$

$$\exp -\frac{1}{2}\left\{\frac{\hat{h}}{\hat{\sigma}_u^2}\left[\frac{D_o^{1/2} - (D \tanh D)^{1/2}}{D}\right]^2 + \left[\frac{(\hat{h}-1)}{\hat{\sigma}_h}\right]^2\right\} \tag{C.14}$$

where $\hat{\sigma}_u = \sigma_u/\sqrt{gh'}$ and $\hat{\sigma}_h = \sigma_h/h'$, and it is noted that $D_o = k_o h' \hat{h}$ and $D_{oek} = k_o h' \hat{h}_{ek}$.

The marginal pdf of dimensionless kinematical equivalent water depth is found by integrating (C.14) with respect to $\hat{h}$ over realistic limits. Because negative water depths are physically impossible, the joint pdf is truncated at $\hat{h} = 0$. The volume under the joint pdf is used to normalize. Plots of (C.14) are displayed for various values of $k_o h'$, $\hat{\sigma}_u$ and $\hat{\sigma}_h$ in Figures 7.1 and 7.2.

APPENDIX D

PROBABILITY DENSITY FUNCTION FOR WAVE ACTION
EQUIVALENT WATER DEPTH

An alternative to the kinematical approach of examining the effect of surf beat on wave transformation is to address the problem in terms of group velocity. As explained in chapter 7, the wave action equivalent water depth, h_{ew}, is defined by

$$\frac{\sqrt{gh_{ew}}}{\omega} = \frac{(U + Cg)}{\sigma} \tag{D.1}$$

This expression could be solved for kh as a function of ω and h_{ew} using a numerical technique; however, an explicit function is required if we hope to perform a transformation of random variables for surf beat. A truncated Taylor expansion for kh is derived in Appendix E and is given by

$$kh = (k_o h)^{1/2} \tilde{h}_{ew}^{1/4} \{1 + [\frac{1}{12} \tilde{h}_{ew}^{1/2} - \frac{1}{6} \tilde{h}_{ew}^{3/4}] k_o h +$$

$$[\frac{1}{120} \tilde{h}_{ew} - \frac{7}{360} \tilde{h}_{ew}^{5/4} + \frac{1}{8} \tilde{h}_{ew}^{3/2}](k_o h)^2\} \tag{D.2}$$

where $\tilde{h}_{ew} = h/h_{ew}$. As in Appendix C, the transformation will proceed conceptually as follows:

$$pdf(U,h) \Rightarrow pdf(kh,h : k_o) \Rightarrow pdf(h_{ew},h : k_o)$$

$$mpdf(h_{ew} : k_o) = \int pdf(h_{ew},h : k_o)\, dh \tag{D.3}$$

If it is again assumed that U and h are each normally distributed and uncorrelated, the first transformation is exactly the same as that in Appendix C, i.e.,

$$\text{pdf}\ (D,h : k_o) = \frac{(gh)^{1/2}|F_1(D)|}{2\pi\ \sigma_u\ \sigma_h} \cdot$$

$$\exp - \frac{1}{2}\{\frac{gh}{\sigma_u^2}[\frac{(k_o h)^{1/2} - (D \tanh D)^{1/2}}{D}]^2 + (\frac{h - h'}{\sigma_h})^2\} \qquad (D.4)$$

where $D = kh$ and σ_u and σ_h are the standard deviations of the current and mean water level respectively. The next step requires the Jacobian of (D.2):

$$\left|\frac{\partial D}{\partial\ \tilde{h}_{ew}}\right| = \left|\frac{1}{4}\tilde{h}_{ew}^{-3/4}(k_o h)^{1/2} + [\frac{1}{16}\tilde{h}_{ew}^{-1/4} - \frac{1}{6}]\ (k_o h)^{3/2}\right.$$

$$\left. + [\frac{1}{96}\tilde{h}_{ew}^{1/4} - \frac{7}{240}\tilde{h}_{ew}^{1/2} + \frac{7}{32}\tilde{h}_{ew}^{3/4}]\ (k_o h)^{5/2}\right| = |F_3(\tilde{h}_{ew})| \qquad (D.5)$$

and the pdf becomes

$$\text{pdf}(\tilde{h}_{ew}, h : k_o) = \frac{(gh)^{1/2}|F_1||F_3|}{2\pi\ \sigma_u\ \sigma_h} \cdot$$

$$\exp - \frac{1}{2}\{\frac{gh}{\sigma_u^2}[\frac{(k_o h)^{1/2} - (D \tanh D)^{1/2}}{D}]^2 + (\frac{h - h'}{\sigma_h})^2\} \qquad (D.6)$$

with (D.2) substituted for D. Finally letting

$$\hat{h} = h/h' \qquad (D.7a)$$

$$\hat{h}_{ew} = \frac{h_{ew}}{h'} = \frac{1}{\tilde{h}_{ew}}\frac{h}{h'} \qquad (D.7b)$$

the pdf becomes

$$\text{pdf}(\hat{h}_{ew},\hat{h} : k_o) = \frac{|F_1||F_3|}{2\pi \hat{\sigma}_u \hat{\sigma}_h} \frac{\hat{h}^{3/2}}{\hat{h}_{ew}^2} \cdot$$

$$\exp - \frac{1}{2}\{\frac{\hat{h}}{\hat{\sigma}_u^2}[\frac{D_o^{1/2}-(D \tanh D)^{1/2}}{D}]^2 + [\frac{(\hat{h} - 1)}{\hat{\sigma}_h}]^2\} \qquad (D.8)$$

where again $\hat{\sigma}_u = \sigma_u/\sqrt{gh'}$, $\hat{\sigma}_h = \sigma_h/h'$ and $D_o = k_o h' \hat{h}$.

The marginal pdf of dimensionless wave action equivalent water depth (given k_o) is found by integrating with respect to $\hat{h}$ from zero to infinity, i.e.,

$$\text{mpdf}(\hat{h}_{ew} : k_o) = \int_o^\infty \text{pdf}(\hat{h}_{ew},\hat{h} : k_o)\, d\hat{h} \qquad (D.9)$$

The pdf is again normalized by dividing by the total area. Plots of (D.9) are displayed in Figures 7.3 and 7.4.

APPENDIX E

EXPANSION SOLUTION FOR WAVE ACTION EQUIVALENT WATER DEPTH

As in chapter 7, the equivalent water depth defined for wave action, h_{ew}, is defined by

$$\frac{(gh_{ew})^{1/2}}{\omega} = \frac{(U + Cg)}{\sigma} \tag{E.1}$$

Applying the dispersion realtion in the form of (C.6) and expressing Cg and σ in terms of k yields

$$(gh_{ew})^{1/2} = \omega\left[\frac{\omega}{k^{3/2}\sqrt{g}\ (\tanh kh)^{1/2}} - \frac{1}{2k} + \frac{h}{2}\left(\frac{1 - \tanh^2 kh}{\tanh kh}\right)\right] \tag{E.2}$$

However, to solve this expression for k, the procedure of Appendix A must again be utilized. When kh is small (E.2) reduces to

$$kh = (k_o h)^{1/2}\ \left(\frac{h}{h_{ew}}\right)^{1/4} \tag{E.3}$$

so we will be seeking a truncated expansion of the form

$$kh = (k_o h)^{1/2}\ \left(\frac{h}{h_{ew}}\right)^{1/4}\left[1 + \alpha\, k_o h + \beta\, (k_o h)^2\right] \tag{E.4}$$

Rearranging (E.2) produces

$$(k_o h)^2 \tanh kh = [B]^2 \tanh^2 kh + \frac{k_o h (kh)^3}{4} (1 - \tanh^2 kh)^2$$

$$-2[B]\frac{(k_o h)^{1/2}(kh)^{3/2}}{2} \tanh kh(1 - \tanh^2 kh) \qquad \text{(E.5a)}$$

where $$B = \left[(kh)^{3/2}\left(\frac{h_{ew}}{h}\right)^{1/2} + \frac{(k_o h)^{1/2}(kh)^{1/2}}{2}\right] \qquad \text{E.5b)}$$

Expanding further, inserting the Taylor Series expansions

$$\tanh kh = kh - \frac{1}{3}(kh)^3 + \frac{2}{15}(kh)^5 + \ldots \qquad \text{(E.6a)}$$

$$\tanh^2 kh = (kh)^2 - \frac{2}{3}(kh)^4 + \frac{17}{45}(kh)^6 + \ldots \qquad \text{(E.6b)}$$

$$\tanh^3 kh = (kh)^3 - (kh)^5 + \ldots \qquad \text{(E.6c)}$$

$$\tanh^4 kh = (kh)^4 - \frac{4}{3}(kh)^6 + \ldots \qquad \text{(E.6d)}$$

applying (E.4), and equating terms of like power in $(k_o h)$ yields after much tedium

$$\alpha = \frac{1}{12}\left(\frac{h}{h_{ew}}\right)^{1/2} - \frac{1}{6}\left(\frac{h}{h_{ew}}\right)^{3/4} \qquad \text{(E.7a)}$$

$$\beta = \frac{1}{120}\left(\frac{h}{h_{ew}}\right) - \frac{7}{360}\left(\frac{h}{h_{ew}}\right)^{5/4} + \frac{1}{8}\left(\frac{h}{h_{ew}}\right)^{3/2} \qquad \text{(E.7b)}$$

Finally, (E.4) becomes

$$kh = (k_o h)^{1/2}\, \tilde{h}_{ew}^{1/4}\{1 + [\tfrac{1}{12}\, \tilde{h}_{ew}^{1/2} - \tfrac{1}{6}\, \tilde{h}_{ew}^{3/4}]\, k_o h +$$

$$[\tfrac{1}{120}\, \tilde{h}_{ew} - \tfrac{7}{360}\, \tilde{h}_{ew}^{5/4} + \tfrac{1}{8}\, \tilde{h}_{ew}^{3/2}](k_o h)^2\} \qquad \text{(E.8a)}$$

where $\tilde{h}_{ew}$ is the dimensionless water depth given by

$$\tilde{h}_{ew} = \frac{h}{h_{ew}} \qquad \text{(E.8b)}$$

APPENDIX F

FILTERING-INDUCED "CLIPPING" OF WAVE HEIGHT

As mentioned in chapter 7, the unusual behavior of the NSTS data of Thornton and Guza (1983) as compared to other data sets and the model predictions, was the original impetus for investigating the possible effects of surf beat on random wave transformation. These data (see Figure 7.5) began their decay at the point where the ratio H_{rms}/h was equal to 0.26. This is slightly less than half that for the Hotta and Mizuguchi (1980) data of Figure 5.2, which had an "incipient" ratio of 0.54. This is exactly opposite to what should be expected because NSTS conditions were of very low steepness and, according to every investigation of the incipient condition appearing in the literature, low steepness waves have higher incipient conditions. To quote the visual observations of Thornton and Guza (1983, page 5929):

> The groupiness was exhibited by the waves at breaking going every several minutes from 2-m heights to essentially calm conditions and back again to 2-m waves at the arrival of another group of waves.

However, in the histograms of wave height generated using low-pass-filtered data and presented in their paper, the largest wave occurring anywhere on the transect was a 1.5 m wave in 3.5 m of water. The highest wave occurring at a depth of 1.5 m was only 1.0 m in height, i.e., γ was only 0.67. What happened to the wave heights? The author believes the manner in which the data were filtered during the original field experiment is responsible.

Application of the zero-up-crossing technique for analyzing wave records often involves first low-pass filtering the signal to remove higher frequency oscillations from the free surface. This high frequency "noise" increases the number of waves counted in a record by the up-crossing technique, and results in lower calculated values for statistically representative waves, such as H_{rms}. The original data for NSTS-Torrey Pines was taken at 64 Hz, block averaged which reduced the sampling rate to 8 Hz, deglitched, then low-pass-filtered "to substantially reduce energy between 0.5 and 1 Hz," and finally output to tape at 2 Hz (Gable, 1979). Thornton and Guza (1983) treated these time series further by Fourier Transforming the filtered record and zeroing the amplitude coefficients above 0.5 Hz (for gages where $h < 3$ m). The time series was then reconstructed and wave heights and periods determined using the up-crossing technique. However, if the original waves are either very peaked (as they are when approaching the break point) or have sudden discontinuities (as is the case at the front face of a wave at incipient breaking, or the face of a bore), filtering in the above manner can significantly "clip" the wave height. As noted, wave conditions during NSTS were characterized by long-period, low deepwater steepness swell, which become very peaked in shallow water. For the peak frequency of 0.055 Hz, significant deepwater height of 79 cm, and local water depth equal 279 cm (i.e., where the data begin decay), and assuming Stream Function Theory is valid (Dean, 1974), the free surface before and after filtering above 0.5 Hz (the ninth harmonic in this instance) is shown in Figure F.1. Note that the wave height was clipped by almost 25%.

It seems the clipping artifice was induced more by the original filtering of the raw data, as one of these records from the inner surf zone was analyzed with and without the additional filtering of Thornton and Guza, and only a 6% drop in H_{rms} was found (Thornton - personal communication). This artifice is also believed by the author to be responsible for the apparent agreement between the Rayleigh pdf and histograms of wave height in the surf zone as reported by Thornton and Guza (1983). Filtering the waves makes them appear more sinusoidal and narrow-banded, so assuming a Gaussian sea becomes, artificially, more valid. This would also appear to be why Thornton and Guza found $H_{rms} = \sqrt{8a_0}$ to be relatively valid in the surf zone.

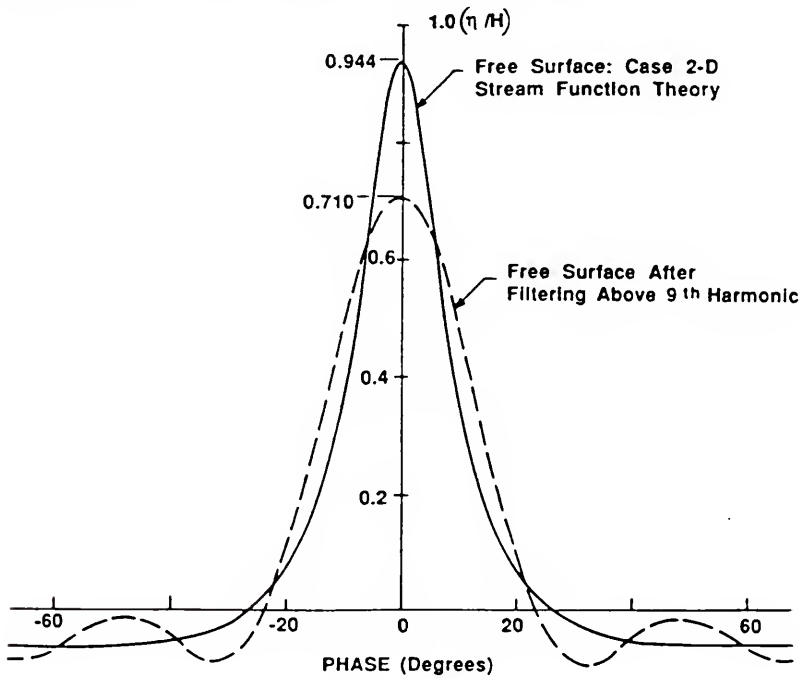

Figure F.1 "Clipping" of wave height of peaked waves due to low-pass-filtering. Conditions are analogous to those of NSTS data of Thornton and Guza (1983).

APPENDIX G

MEAN WAVE STEEPNESS EFFECTS ON RANDOM WAVE TRANSFORMATION

A few previous investigations have noted an apparent dependence of random wave decay on mean wave steepness. For example, Battjes and Stive (1985) increase the decay in wave height for low deepwater steepness waves by varying empirical coefficients. A figure from their paper is presented in Figure G.1. Mean deepwater steepness is plotted versus $\hat{\gamma}$, an empirical breaker height parameter that is somewhat analogous to γ for regular breaking waves, and was determined for 16 laboratory and 4 field data sets of H_{rms} transformation. The trend of increased decay with decreasing steepness is somewhat slight, but clearly evident. No explanation for this behavior has been given. The models which display this behavior are all "energy models" rather than "wave height models", and are based on the assumption of a Gaussian sea in the surf zone, i.e., that $H_{rms} = \sqrt{8a_0}$ where a_0 is the area under the spectral density function. This assumption is refuted for surf zone conditions by nearly all laboratory and field data sets except that of Thornton and Guza (1983), which supported this assumption only because of the low-pass-filtering-induced clipping of wave height discussed in Appendix F.

The author believes the majority of the behavior in Figure G.1 is an artifice of assuming a Gaussian sea in the surf zone. A low steepness wave becomes peaked in shallow water and even though it may have the same actual height as a higher steepness wave, it contains less energy. (Steepness was found by Dally et al. (1984, 1985) to have

little effect on wave height decay after breaking is initiated.) Therefore, if energy is used to calculate H_{rms} rather than the actual free surface displacement between trough and crest, a lower value for wave height is produced. As a result, for the transformation of H_{rms} as defined by $\sqrt{8a_0}$, the heights of the breaking waves in the model must be artificially suppressed to obtain good fit if the measured waves were of low steepness.

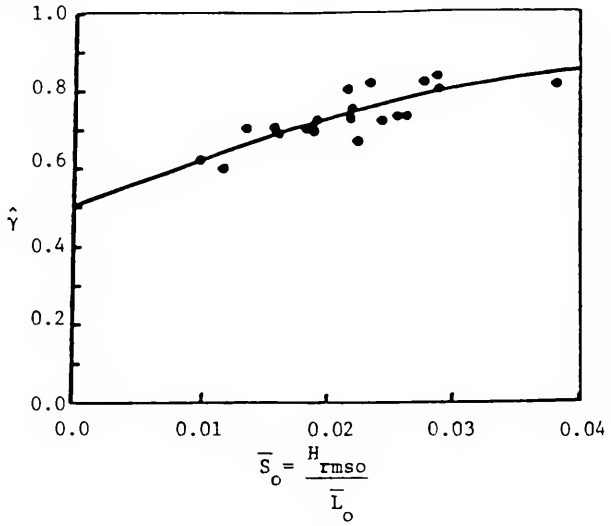

Figure G.1 Dependence of decay coefficient $\hat{\gamma}$ of model of Battjes and Janssen (1978) on mean deepwater steepness $\bar{S}_o$ reported by (and figure adapted from) Battjes and Stive (1985).

Finally, part of the increased decay with decreasing steepness may be due to the interaction with surf beat detailed in chapter 7. Low steepness waves are more likely to be groupy, drive energetic surf beat, and therefore enhance the mechanisms which increase decay in the surf zone.

REFERENCES

Abdelrahman, S. M. and Thornton, E. B., 1986, "Modification of Sea Swell by Long Waves Within the Surf Zone," Abstracts 20th Conf. Coastal Eng., ASCE, 245.

Battjes, J. A. and Janssen, J. P. F. M., 1978, "Energy Loss and Set-up Due to Breaking of Random Waves," Proc. 16th Conf. Coastal Eng., ASCE, Vol. 1, 569-587.

Battjes, J. A. and Stive, M. J. F., 1985, "Calibration and Verification of a Dissipation Model for Random Breaking Waves," J. Geophys. Res., Vol. 90, No. C5, 9159-9167.

Bretherton, F. P. and Garrett, C. J. R., 1969, "Wave Trains in Inhomogeneous Moving Media," Proc. Roy. Soc., A, No. 302, 529.

Collins, J. I., 1970, "Probabilities of Breaking Wave Characteristics," Proc. 12th Conf. Coast. Eng., ASCE, Vol. 1, 399-412.

Dally, W. R., 1980, "A Numerical Model for Beach Profile Evolution," Master's thesis, Dept. Civil Eng., Univ. of Delaware, Newark.

Dally, W. R., Dean, R. G., and Dalrymple, R. A., 1984, "A Model for Breaker Decay on Beaches", Proc. 19th Conf. Coastal Engr., ASCE, Vol. 1, 82-98.

Dally, W. R., Dean, R. G., and Dalrymple, R. A., 1985, "Wave Height Variation Across Beaches of Arbitrary Profile", J. Geophys. Res., Vol. 90, No. C6, 11,917-11,927.

Dalrymple, R. A. and Dean, R. G., 1975, "Waves of Maximum Height on Uniform Currents," J. Wtrwys., Hrbrs. and Coast. Eng. Div., ASCE, Vol 3, No. WW3, 259-268.

Dean, R. G., 1974, "Evaluation and Development of Water Wave Theories for Engineering Application," U.S. Army Coast. Eng. Res. Cent., Special Report No. 1, U.S. Govt Print. Off., Wash. D.C.

Dean, R. G., 1977, "Equilibrium Beach Profiles: U.S. Atlantic and Gulf Coasts," Ocean Eng. Rep. 12, Dep. of Civ. Eng., Univ. of Del., Newark.

Divoky, D., LeMéhauté, B. and Lin, A., 1970, "Breaking Waves on Gentle Slopes," J. Geophys. Res., Vol. 75, No. 9, 1681-1692.

Galvin, C. J., 1968, "Breaker Type Classification on Three Laboratory Beaches," J. Geophys. Res., 73, No. 12, 3651-3659.

Goda, Y., 1975, "Irregular Wave Deformation in the Surf Zone," Coast. Eng. in Japan, Vol. 18, 13-26.

Goodknight, R. C. and Russell, T. L., 1963, "Investigation of the Statistics of Wave Heights," Proc. Wtrwys. Hrbrs. Div., ASCE, Vol. 89, No.WW2, 29-54.

Guza, R. T. and Thornton, E. B., 1985, "Observations of Surf Beat," J. Geophys. Res., Vol. 90, No. C2, 3161-3172.

Hizamizu, K., Sakai, S. and Saeki, H., 1986, "Irregular Wave Transformation Affected by Opposing Current," Abstracts 20th Conf. Coastal Eng., ASCE, 155-156.

Horikawa, K. and Kuo, C. T., 1966, "A Study of Wave Transformation Inside Surf Zone," Proc. 10th Conf. Coastal Eng., ASCE, Vol. 1, 217-233.

Hotta, S. and Mizuguchi, M., 1980, "A Field Study of Waves in the Surf Zone," Coastal Engr. Japan, JSCE, Vol. 23, 79-89.

Hotta, S. and Mizuguchi, M., 1986, "Wave Statistics in the Surf Zone," Abstracts 20th Conf. Coastal Eng., ASCE, 342-343.

Hunt, J. N., 1979, "Direct Solution of Wave Dispersion Equation," J. Wtrwy., Port, Coast and Ocean Div., ASCE, Vol. 105, No.WW4, 457-459.

Hwang, L. S. and Divoky, D., 1970, "Breaking Wave Set-Up and Decay on Gentle Slopes," Proc. 12th Conf. Coastal Engr., ASCE, 377-389.

Komar, P. D. and Gaughan, M. K., 1972, "Airy Wave Theory and Breaker Height Prediction," Proc. 13th Conf. Coastal Engr., ASCE, 405-418.

Kuo, C. T. and Kuo, S. T., 1975, "Effect of Wave Breaking on Statistical Distribution of Wave Heights," Proc. Civil Eng. in the Oceans/3, ASCE, Vol. 2, 1211-1231.

Lamb, H., 1945, Hydrodynamics, 6th ed., Dover, New York.

Lee, J. S., Sawaragi, T. and Deguchi, I., 1986, "Numerical Model of Breaking Wave Around Rivermouth," Abstracts 20th Conf. Coastal Eng., ASCE, 432-433.

LeMéhauté, B., 1962, "On Non-Saturated Breakers and the Wave Run-up," Proc. 8th Conf. Coastal Eng., ASCE, 77-92.

Lin, S. C. and Hwang, J. S., 1986, "Wave Transformation and Mean Sea Level Variation," Abstracts 20th Conf. Coastal Eng., ASCE, 302-303.

Lo, J-M., 1981, "Surf Beat: Numerical and Theoretical Analyses," Ph.D. dissertation, Dep. Civil Eng., Univ. of Delaware, Newark.

Longuet-Higgins, M. S., 1983, "On the Joint Distribution of Wave Periods and Amplitudes in a Random Wave Field," Proc. Roy. Soc. Lond., A389, 241-258.

Longuet-Higgins, M. S. and Stewart, R. W., 1962, "Radiation Stress and Mass Transport in Gravity Waves, with Applications to Surf Beats," J. Fluid Mech., Vol. 13, 481-504.

Longuet-Higgins, M. S. and Stewart, R. W., 1963, "A Note on Wave Set-Up," J. of Mar. Res., Vol. 21, 4-10.

Maruyama, K., Sakakiyama, T., Kajima, R., Saito, S., and Shimizu, T., 1983, "Experimental Study of Wave Height and Water Particle Velocity Near the Surf Zone Using a Large Wave Flume," Civil Eng. Lab. Rep. #382034, Cent. Res. Inst. Elec. Powr. Ind., Chiba, Japan (in Japanese).

Mase, H. and Iwagaki, M., 1982, "Wave Height Distributions and Wave Grouping in Surf Zone", Proc. 18th Conf. Coast. Eng., ASCE, Vol. 1, 58-76.

Mizuguchi, M., 1981, "An Heuristic Model of Wave Height Distribution in Surf Zone," Proc. 17th Conf. Coastal Eng., ASCE, Vol. 1, 278-289.

Moore, B. D., 1982, "Beach Profile Evolution in Response to Changes in Water Level and Wave Height," Master's thesis, Dept. Civil Engr., Univ. of Delaware, Newark.

Nakamura, M., Shiraishi, H., and Sasaki, Y., 1966, "Wave Decaying Due to Breaking," Proc. 10th Conf. Coastal Eng., ASCE, Vol. 1, 234-253.

Nielsen, P., 1984, "Explicit Solutions to Practical Wave Problems," Proc. 19th Conf. Coastal Engr., ASCE, Vol. 1, 968-982.

Ochi, M. K. and Wang, W.-C., 1984, "Non-Gaussian Characteristics of Coastal Waves," Proc. 19th Conf. Coastal Engr., ASCE, 516-531.

Peregrine, D. H. and Svendsen, I. A., 1978, "Spilling Breakers, Bores, and Hydraulic Jumps," Proc. 16th Conf. Coastal Eng., ASCE, Vol. 1, 540-550.

Phillips, O. M., 1977, The Dynamics of the Upper Ocean, Camb. Univ. Press, Cambridge, 2nd edition.

Sakai, S., Hiyamizu, K. and Saeki, H., 1986, "Wave Height Decay Model Within a Surf Zone," Abstracts 20th Conf. Coastal Eng., ASCE, 106-107.

Sakai, S. and Saeki, H., 1984, "Effects of Opposing Current on Wave Transformation on a Sloping Sea Bed," Proc. 19th Conf. Coastal Eng., ASCE, 1132-1148.

Sallenger, A. H. and Holman, R. A., 1985, "Wave Energy Saturation on a Natural Beach of Variable Slope," J. Geophys. Res., Vol. 90, No. C6, 11939-11944.

Singamsetti, S. R. and Wind, H. G., 1980, "Characteristics of Shoaling and Breaking Periodic Waves Normally Incident to Plane Beaches of Constant Slope," Report M1371, Foegepast Onderzock Waterstaat, The Netherlands.

Stive, M. J. F., 1985, "A Scale Comparison of Waves Breaking on a Beach," Coastal Eng., Vol. 9, 151-158.

Suhayda, J. N. and Pettigrew, N. R., 1977, "Observations of Wave Height and Wave Celerity in the Surf Zone," J. Geophys. Res., Vol. 82, No. 9, 1419-1424.

Svendsen, I. A., 1984, "Wave Heights and Set-up in a Surf Zone," Coastal Engr., Vol. 8, 303-329.

Svendsen, I. A. and Buhr Hansen, J., 1977, "The Wave Height Variation for Regular Waves in Shoaling Water," Coast. Eng., Vol. 1, 261-84.

Svendsen, I. A., Madsen, P. A., and Buhr Hansen, J. B., 1978, "Wave Characteristics in the Surf Zone," Proc.16th Conf. Coastal Eng., ASCE, Vol. 1, 520-539.

Symonds, G., Huntley, D. A., and Bowen A. J., 1982, "Two Dimensional Surf Beat: Long Wave Generation by a Time-Varying Breakpoint," J. Geophys. Res., Vol. 87, No. C1, 492-498.

Thornton, E. B. and Guza, R. T., July 1983, "Transformation of Wave Height Distribution," J. of Geophys. Res., Vol. 88, No. C10, 5925-5938.

Thornton, E. B., Wu, C.-S. and Guza, 1984, "Breaking Wave Design Criteria," Proc. 19th Conf. Coastal Eng., ASCE, 31-41.

Weggel, J. R., 1972, "Maximum Breaker Height," J. of Wtrwys, Hrbrs, Coast. Eng. Div., ASCE, Vol. 98, No. WW4, 529-548.

Williams, J. W. J., 1964, "Heap Sort (Algorithm 232)," Communications ACM, Vol. 7, No. 6, 200-205.

Yu, Y.-Y., 1952, "Breaking of Waves by an Opposing Current," Transactions, Am. Geophys. Union, Vol. 33, No. 1, 39-41.

BIOGRAPHICAL SKETCH

William R. (Bill) Dally was born November 30, 1955, in Wilmington, Delaware, to Louise D. Dally, loving full-time homemaker, and William J. Dally, an architect of most honorable timbre. His early childhood was spent climbing trees in Duncan woods (now a housing development), attending meetings of the "Indian Guides" with his father (pals forever!), and being encouraged by his mother to spend as much time at the neighborhood swimming pool as possible. Although an Eagle Scout and avid backpacker, summer vacations on the beach at Cape Cod with his "not too bad" sisters Kathleen, Ellen and Janette, and thrilling T.V. episodes of "Sea Hunt" enamored him to the ocean, and he was a certified scuba diver by the age of 16. Graduating from Thomas McKean High School, William entered the University of Delaware as a member of the springboard diving team, with dreams of some day designing, building and living in an underwater habitat. However, somewhere amidst the calculus, structural analysis, and reinforced concrete of the civil engineering curriculum, the dream slipped away. It was not until his senior year, when he met Dr. Robert G. Dean, that he "got wet" again (also sunburnt, frozen, and bitten by horseflies) on a field study of the inlet at Ocean City, Maryland. William graduated with a Bachelor of Civil Engineering degree and a member of Tau Beta Pi and spent a summer working at the Coastal Engineering Research Center (CERC) before returning to Delaware for a Master of Civil Engineering degree in Coastal/Ocean Engineering. After a year with the U.S. Army Corps of

Engineers district office in Wilmington, North Carolina, and three years back at CERC, William followed Dr. Dean to the University of Florida to pursue his doctorate. Although he has devoted many years to his education, the diploma William is most proud of was awarded him by Mr. Tsutomu Ohshima, as a black belt in Shotokan Karate of America.

I certify that I have read this study and that in my opinion it conforms to acceptable standards of scholarly presentation and is fully adequate, in scope and quality, as a dissertation for the degree of Doctor of Philosophy.

Robert G. Dean, Chairman
Graduate Research Professor of
Engineering Sciences

I certify that I have read this study and that in my opinion it conforms to acceptable standards of scholarly presentation and is fully adequate, in scope and quality, as a dissertation for the degree of Doctor of Philosophy.

Joseph L. Hammack
Professor of Engineering Sciences

I certify that I have read this study and that in my opinion it conforms to acceptable standards of scholarly presentation and is fully adequate, in scope and quality, as a dissertation for the degree of Doctor of Philosophy.

Lawrence E. Malvern
Professor of Engineering Sciences

I certify that I have read this study and that in my opinion it conforms to acceptable standards of scholarly presentation and is fully adequate, in scope and quality, as a dissertation for the degree of Doctor of Philosophy.

Michel K. Ochi
Professor of Coastal and
Oceanographic Engineering

I certify that I have read this study and that in my opinion it conforms to acceptable standards of scholarly presentation and is fully adequate, in scope and quality, as a dissertation for the degree of Doctor of Philosophy.

Andrew J. Vince
Associate Professor of Mathematics

This dissertation was submitted to the Graduate Faculty of the College of Engineering and to the Graduate School and was accepted as partial fulfillment of the requirements for the degree of Doctor of Philosophy.

May 1987

Dean, College of Engineering

Dean, Graduate School